Synthesis of Electrophilic Rhodium and Iridium Complexes and Investigation of Reactivity for C-H Bond Activation and Functionalization

Kate E. Allen

A dissertation submitted in partial fulfillment of the requirements for the degree of

Doctor of Philosophy

University of Washington

2013

Reading Committee:

Karen I. Goldberg, Chair

D. Michael Heinekey

Julie A. Kovacs

Program Authorized to Offer Degree:

Chemistry

University of Washington

Abstract

Synthesis of Electrophilic Rhodium and Iridium Complexes and Investigation of Reactivity for C-H Bond Activation and Functionalization

Kate E. Allen

Chair of the Supervisory Committee:
Professor Karen I. Goldberg
Department of Chemistry

Direct methods for the transformation of alkanes into alcohols, alkenes, amines and other functionalized products would have a great impact on industrial processes. In this thesis the work described is aimed at developing electrophilic Rh and Ir systems to promote C-H bond activation and functionalization of alkanes and arenes. Several approaches have been taken to prepare the target complex $[Tp^*Ir(OH_2)_3]^+$ (Tp^* = hydridotris(3,5-dimethylpyrazoyl)borate). While this species has not been synthesized, C-N coupling between ethylene and N-iodosuccinimide has been observed during the course of this study and is promoted by $Tp^*Ir(C_2H_4)_2$. Electrophilic Rh and Ir complexes bearing dimethylbutadiene (DMB) ligands have been found to be poor species for C-H activation due to low stability at elevated temperatures. Interestingly, formation of the unique five-coordinate $[(DMB)Ir(COE)Cl]_2$ dimer has been observed. Alkane dehydrogenation using (^{dm}Phebox)Ir(OAc)$_2$(OH$_2$) (^{dm}Phebox = 2,6-bis(4,4-dimethyloxazolinyl)-3,5-dimethylphenyl) is promoted at 200 °C and results in quantitative formation of olefin and (^{dm}Phebox)Ir(OAc)H. At early reaction times 1-octene is the

major product, supporting terminal C-H activation by the Ir center. Oxygen can be utilized in this system as a hydrogen acceptor to promote regeneration of the Ir bisacetate species at room temperature. This is the first example of regeneration of a complex for dehydrogenation using oxygen. Unfortunately, the system is not catalytic as the reaction with oxygen is not compatible with the high temperatures required for C-H bond activation. In order to expand the number of examples of alkane dehydrogenation at Ir^{III} centers, a second system utilizing the ^{tBu}NOCON (^{tBu}NOCON = 4,6-di-*tert*-butyl-(1,3-bis(2-pyridyloxy)benzene)) pincer ligand has been developed. Complexes (^{tBu}NOCON)M$(OAc)_2OH_2$ (M = Rh or Ir) were synthesized and explored for C-H bond functionalization. The Ir analogue promotes alkane dehydrogenation at 200 °C, but is not stable under the reaction conditions. Arene functionalization has also been explored using Ir-aryl complexes. The product of benzene C-H activation, (Phebox)Ir(OAc)Ph has been investigated for arene functionalization using hypervalent iodide reagents and CO. Reactions utilizing $C_6F_5I(TFA)_2$ are promising and may potentially yield functionalized arene. Coordination of CO to the Ir center has been observed and isomerization of the *trans* product, (^{dm}Phebox)Ir(CO)(OAc)Ph, occurs at room temperature to yield the *cis* isomer (^{dm}Phebox)Ir(OAc)(CO)Ph.

Table of Contents

List of Figures

List of Schemes

Scheme Number Page

List of Equations

List of Tables

Glossary

Common Abbreviations:

bpym: bipyrimidine

CMD: concerted metalation deprotonation

COA: cyclooctane

COD: 1,5-cyclooctadiene

COE: *cis*-cyclooctene

m-CPBA: *meta*-chloroperoxybenzoic acid

Cp^*: pentamethylcyclopentadienyl

DMB: 2,3-dimethyl-1,3-butadiene

NBD: norbornene

NIS: N-iodosuccinimide

NNC^{tBu}: 6-phenyl-4,4′-di-*tert*-butyl-2,2′-bipyridine

NOCON: 1,3-bis(2-pyridyloxy)benzene

^{tBu}NOCON: 4,6-di-*tert*-butyl-(1,3-bis(2-pyridyloxy)benzene)

OAc: acetate

OBz: benzoate

OTF: triflate (trifluoromethanesulfonate)

PCP: 1,3-bis-(di-alkyl-phosphinomethyl)benzene

^{iPr}Phebox: 2,6-bis(4,4-*iso*propyloxazolinyl)-3,5-dimethylphenyl

^{dm}Phebox: 2,6-bis(4,4-dimethyloxazolinyl)-3,5-dimethylphenyl

PNP: 1,3-bis-(di-alkyl-phosphinomethyl)pyridine

^{tBu}POCOP: $[1,3\text{-}(OP^tBu_2)_2C_6H_4]$

TBE: *tert*-butylethylene

TFA: trifluoroacetate

Tp^*: hydridotris(3,5-dimethylpyrazoyl)borate

Compound Numbering Scheme

Chapter 2

1: $[Tp^{*}Ir(OH_2)_3]^{2+}$

2: $(Tp^{*}IrCl_2)_2$

3: $Tp^{*}Ir(C_2H_4)_2$

4: $(Tp^{*}IrI_2)_2$

5: $Tp^{*}Ir(TFA)_2$

6: $Tp^{*}IrI(C_2H_4NO)$

7: $Tp^{*}IrI_2(CH_2Cl_2)$

8-X: $[(DMB)Rh(OH_2)_2][X]$ (X = BF_4, OAc, or TFA)

9: $[(\eta^6\text{-indenyl})Rh(DMB)][BF_4]$

10: $[(\eta^3\text{-indenyl})Rh(DMB)]$

11: $[(DMB)IrCl]_2$

12: $(DMB)_2IrCl$

13: $[(DMB)Ir(COE)Cl]_2$

14: $(DMB)_2IrCH_3$

Chapter 3

1a: $(^{dm}Phebox)Rh(OAc)_2(H_2O)$

1b: $(^{iPr}Phebox)Rh(OAc)_2(OH_2)$

2a: $(^{dm}Phebox)Ir(OAc)_2(OH_2)$

2b: $(^{iPr}Phebox)Ir(OAc)_2(OH_2)$

3b: $[(^{iPr}Phebox)RhOAc]_2$

4b: $(^{iPr}Phebox)Rh_2(OAc)_3$

5a: $(^{dm}Phebox)Ir(OAc)(Ph)$

5b: $(^{iPr}Phebox)Ir(OAc)(Ph)$

5a-d_5: (^{dm}Phebox)Ir(OAc)(Ph-d_5)

6a: (^{dm}Phebox)Ir(OAc)(H)

7a: (^{dm}Phebox)Ir(OAc)(*n*-octyl)

Chapter 4

1a: (^{dm}Phebox)Ir(OAc)$_2$(OH$_2$)

1b: (^{dm}Phebox)Ir(OBz)$_2$(OH$_2$)

1c: (^{dm}Phebox)Ir(OPiv)$_2$(OH$_2$)

2a: (^{dm}Phebox)Ir(OAc)H

2b: (^{dm}Phebox)Ir(OBz)H

2c: (^{dm}Phebox)Ir(OPiv)H

3a: intermediate observed during the reaction of **2a**, acetic acid, and oxygen

3b: intermediate observed during the reaction of **2b**, acetic acid, and oxygen

3c: intermediate observed during the reaction of **2c**, acetic acid, and oxygen

4a: [(^{dm}Phebox)Ir(HOAc)(OH$_2$)][BF$_4$]

5a: (^{dm}Phebox)Ir(OAc)OOH

6a: (^{dm}Phebox)Ir(OAc)OH

7a: (^{dm}Phebox)IrCl$_2$(OH$_2$)

8a: (^{dm}Phebox)Ir(TFA)(OH$_2$)Cl

9a: (^{dm}Phebox)Ir(OAc)(C$_2$H$_3$)

10a: (^{dm}Phebox)Ir(OAc)CH^3

11a: (^{dm}Phebox)Ir(OAc)Cl

Chapter 5

1a: (^{iPr}Phebox)Ir(OAc)Ph

1b: (^{dm}Phebox)Ir(OAc)Ph

1b-d_5: (^{dm}Phebox)Ir(OAc)Ph-d_5

2a: symmetrical product obtained from reaction of **1a** and $C_6F_5I(TFA)_2$

3a: asymmetrical product obtained from reaction of **1a** and $C_6F_5I(TFA)_2$

***trans*-4b**: (^{dm}Phebox)Ir(CO)(OAc)Ph

***cis*-4b**: (^{dm}Phebox)Ir(OAc)(CO)Ph

***trans*-4b-d_5**: (^{dm}Phebox)Ir(CO)(OAc)Ph-d_5

***cis*-4b-d_5**: (^{dm}Phebox)Ir(OAc)(CO)Ph-d_5

5b: (^{dm}Phebox)Ir(OAc)H

Chapter 6

1a: (NOCON)$RhCl_2(OH_2)$

1b: (^{tBu}NOCON)$RhCl_2(OH_2)$

2a: (NOCON)$Rh(OAc)_2(OH_2)$

2b: (^{tBu}NOCON)$Rh(OAc)_2(OH_2)$

3a: (NOCON)$IrCl_2(OH_2)$

3b: (^{tBu}NOCON)$IrCl_2(OH_2)$

4b: (^{tBu}NOCON)Rh(OAc)Ph

5b: (^{tBu}NOCON)$Ir(OAc)_2(OH_2)$

6b: (^{tBu}NOCON)$Ir(OH_2)$(OAc)(Ph)

6b-d_5: (^{tBu}NOCON)$Ir(OH_2)$(OAc)(Ph-d_5)

7b: (^{tBu}NOCON)Ir(OAc)H

8b: (^{tBu}NOCON)Ir(OAc)(CO)Ph

Acknowledgements

Thank you, Karen for your encouragement and guidance. I greatly appreciate the motivation and help that you have given me over the last 5 years. I'm also glad that we were able to share golden retriever stories. I have to thank all of the Goldberg group members that I have had the opportunity to work with. Specifically, thank you to the current members for all of your suggestions and all the time spent together inside and outside of the lab. To Prof. Luc Boisvert I owe a huge thank you for getting me started in the group and for your willingness to answer questions. Thank you Wilson for your help with TOCs and compiling PDFs, and an extra big thank you for pranking Tyler with me.

I owe my family a huge thank you for all of your support throughout this process. It has felt like such a long journey and I would not have finished if not for your support. To my beautiful goldens, Zoe and Brodie, you have no idea how much your happy faces have kept me from losing my mind. Thank you Michael for your tons of help, understanding, and support. It made it much easier to go through graduate school with you and share our dislike of the rain. I'm very appreciative that we were able to do this together and I'm so excited to start at UNC with you.

Chapter 1: Introduction to Alkane Functionalization

Functionalization of alkanes obtained from petroleum has widespread importance as the majority of products used around the world are derived from this dwindling supply of fossil fuels. The current methods used to industrially transform alkanes are generally inefficient; requiring multiple steps and high temperatures to obtain value added products. Processes that selectively transform alkanes to functionalized products are difficult to develop due to the relative inertness of the C-C and C-H bonds.[1] In general the functionalized products are more reactive than alkanes under the conditions employed which can result in overfunctionalization.[2]

As an alternative to crude oil, alkanes derived from natural gas are an abundant and inexpensive potential feedstock for fuels and commodity chemicals. Methane, which makes up the largest fraction of natural gas, could serve as a C-1 source for value-added chemicals or fuels.[1b] Commercial utilization of methane is challenging because transportation from the remote locations where natural gas reserves originate is expensive, but conversion of methane to methanol, a liquid, would decrease the transportation costs. Current industrial methods for methanol production utilize syngas (CO and H_2) and operate at high temperatures (730-845 °C).[3] The harsh conditions required for this process are a result of the energy required for the generation of syngas. In contrast, the formation of methanol from CO and H_2 is relatively easy. The syngas process accounts for the production of 40 million tons annually of methanol.[4] Alkenes are another valuable feedstock obtained from syngas using Fischer-Tropsch technology. Another method to obtaining light alkenes is thermal cracking of alkane feedstocks. This process requires high temperatures, 800-880 °C and depending upon the feedstock used, ethylene and propylene are obtained.[5] The ratio of ethylene to propylene produced is not easily controlled, which is important as propylene has higher value than ethylene.[6] Methods for the

conversion of alkanes directly to alcohols, alkenes, amines and other valuable products would have far-reaching applications in the production of fuels and commodity chemicals.

The need for the development of direct, selective alkane functionalization methods has led to the exploration of homogeneous late transition metal complexes for C-H functionalization. The hallmark example for catalytic methane oxidation was reported by Shilov and coworkers in 1972. In this system, Pt^{II} was demonstrated to be a competent catalyst for the transformation of methane to methanol, albeit in low yields (Scheme 1.1).[7] Competitive with methanol formation, methyl chloride was also a product of this reaction. In order to obtain the alcohol or chloride products a stoichiometric amount of a Pt^{IV} oxidant was utilized. In addition to the use of an expensive oxidant the Shilov system suffers from catalyst decomposition to Pt^0, and these drawbacks have prevented this process from being utilized on an industrial scale.

Scheme 1.1

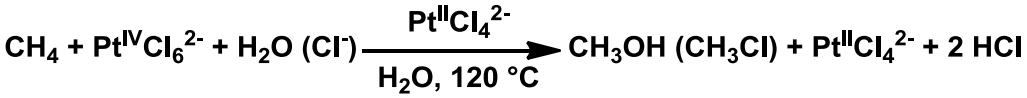

A second successful example of methane functionalization was reported in 1995 by Periana and coworkers. Using a (bpym)$Pt^{II}Cl_2$ (bpym = bipyrimidine) catalyst precursor in neat H_2SO_4 at 220 °C, methyl bisulfate was obtained from methane with 81% selectivity for the ester product in 73% one pass yield (Scheme 1.2).[8] By using a bidentate ligand the lifetime of the Pt^{II} catalyst was increased, the ester product was obtained in higher yield and selectivity in comparison to the Shilov system. Unfortunately, this system cannot be applied on an industrial scale as the catalyst is inhibited by water (a byproduct of the reaction) and separation of methyl bisulfate from the H_2SO_4 medium has proven difficult.

Scheme 1.2

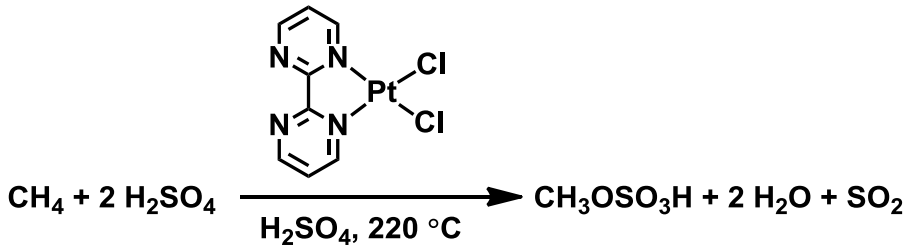

Stoichiometric dehydrogenation of alkanes was demonstrated by Crabtree and coworkers using $[(H)_2Ir(acetone)_2(PPh_3)_2][BF4]$.[9] In this system, cyclopentane and cyclooctane were dehydrogenated to cyclopentadiene and cyclooctadiene using tert-butylethylene (TBE) as a hydrogen acceptor. An acceptor is required to make dehydrogenation thermodynamically favorable. Alkane dehydrogenation has been most effectively demonstrated using (PCP)Ir catalysts by Jensen, Goldman and Brookhart. In the initial report Jensen and coworkers demonstrated transfer dehydrogenation from cyclooctane (COA) to TBE using a $(^{tBu}PCP)Ir(H)_2$ catalyst at 200 °C.[10,11] When catalysis was performed at 200 °C, a TOF of 12 min^{-1} was observed. At temperatures as low as 100 °C, catalytic dehydrogenation was still observed although with a lower turnover frequency. Brookhart and coworkers found that $(^{tBu}POCOP)Ir$ catalysts exhibited higher TONs and initial TOFs for COA/TBE transfer dehydrogenation.[12] The $^{tBu}POCOP$ catalyst achieved 1580 TONs after 40 h at 200 °C in contrast to the ^{tBu}PCP analogue which only produced 227 TONs.[12] The greater activity of the $^{tBu}POCOP$ catalyst has been suggested to be a result of the less sterically demanding POCOP ligand.[13] The Rh complex, $(^{tBu}PCP)Rh(H)_2$, was also found to be a catalyst for COA dehydrogenation at 150 °C, but at 200 °C significant catalyst decomposition was observed.[11] Decomposition of the Rh catalyst in this

initial report reflected the greater stability of Ir at the high temperatures that would become standard for homogeneous dehydrogenation of alkanes.

Scheme 1.3

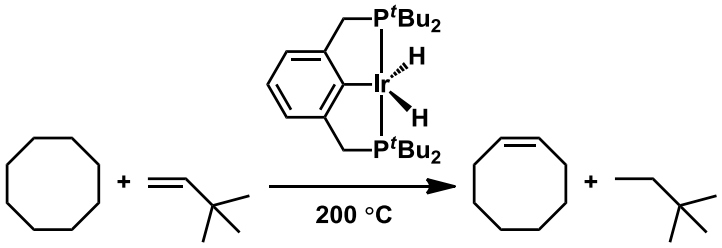

TOF = 12 min^{-1}

Acceptorless dehydrogenation has also been observed by Crabtree, Goldman, and Jensen. In this method hydrogen is removed from the system at high temperatures, shifting the equilibrium of dehydrogenation towards product. Crabtree and coworkers first reported acceptorless dehydrogenation of COA using $Ir(H)_2(TFA)(PCy_3)_2$ at 150 °C.[14] Catalyst deactivation was observed under these conditions, which was attributed to decomposition of the PCy_3 ligands. Greater catalyst stability was observed in the PCP pincer systems. Using (^{tBu}PCP)Ir$(H)_2$ COA and cyclodecane could be catalytically dehydrogenated to COE and cyclodecene without any observable catalyst decomposition.[15] Acceptorless dehydrogenation of linear alkanes could be observed when the *tert*-butyl substituents of the phosphine ligands were exchanged for *iso*-propyl groups.[16] The high temperatures required for dehydrogenation coupled with the need to release hydrogen limits the practicality of this process. New methods for alkane dehydrogenation that could use inexpensive hydrogen acceptors, such as oxygen, would result in milder processes.

There is a need to find catalysts that promote sp^3 C-H bond functionalization in the presence of water. Industrially, catalysts that are insensitive to water are of great interest as removing water from a process is costly. In addition, if oxygen could be utilized as a hydrogen acceptor for alkane dehydrogenation water would be generated as a byproduct. For C-H activation to occur at a metal center, an open site is required to coordinate alkane. In many cases water or the alcohol product (in the case of Shilov chemistry) can bind more effectively to a metal center than alkanes or arenes and block the desired reactivity.[17] Bergman and coworkers have observed catalytic C-H activation of Et_2O with $(\eta^5{:}\eta^1\text{-}Me_2PCH_2SiMe_2C_5Me_4)Ir(OSO_2CF_3)_2$ and $[(\eta^5{:}\eta^1\text{-}Me_2PCH_2SiMe_2C_5Me_4)Ir(OH_2)_2](SO_4)$ complexes in D_2O solutions.[18] Decomposition of the catalysts was observed in these reactions, but this study demonstrated that C-H activation in the presence of water could be achieved. Our group has also developed a system that is not inhibited by water that uses (^{tBu}PNP)Rh complexes to promote arene C-H activation.[19] In this study, catalytic H/D exchange between benzene and D_2O was observed at 100 °C without catalyst decomposition. Surprisingly, added alcohol accelerated the C-H activation reaction. Under these conditions the catalyst, (^{tBu}PNP)Rh(OR) (R = C_6H_5, $C_6H_4NO_2$), interacts with phenol to release the OR ligand and provide an open site for C-H cleavage. These results are promising and support that functionalization systems can be developed that are insensitive to water.

Utilizing oxygen as an oxidant in catalytic C-H functionalization processes is desirable as this would result in a "greener" system, produce less waste, and may avoid the harsh conditions that are sometimes needed with alternative oxidants. Alkane oxidation using oxygen via an autoxidation process has been observed to proceed at high temperatures by a radical chain mechanism.[1d,20] The autoxidation process is generally unselective and is most efficient when

organic substrates that contain benzylic or tertiary C-H bonds are used. There is a need for a selective oxidation process that is compatible with a wide variety of C-H bonds, most particularly with sp^3 C-H bonds of alkanes. Utilizing late transition metal catalysts and oxygen for this transformation may result in increased selectivity and a milder process. An issue to consider is that C-H cleavage by late transition metals is typically inhibited in the presence of oxygen as a result of oxidative catalyst decomposition.[21] While the compatibility of C-H activation and oxygen still needs to be resolved, there are examples of metal complexes that react productively with oxygen. Oxygen insertion into late transition metal alkyl and hydride bonds to generate M-OOR (R = CH_3 or H) species has been observed in several systems.[22] Insertion of oxygen into metal alkyl and hydride bonds represents a potential pathway to selectively incorporate oxygen into C-H bonds.

The work discussed in this thesis has focused on exploring electrophilic Rh and Ir complexes for alkane and arene functionalization. Chapter 2 explores the synthesis of an octahedral Ir^{III} aqua complex that would utilize the Ir^{III}/Ir^{V} couple to promote oxidative transformations of alkanes and arenes. Diene Rh^{I} and Ir^{I} aqua complexes were also explored for the transformation of C-H bonds. In Chapter 3, (Phebox)Rh^{III} and Ir^{III} complexes were found to promote alkane dehydrogenation. The Ir analogue exhibited greater stability at the high temperature required to obtain functionalization. Chapter 4 explores regeneration of the (Phebox)Ir complex discussed in Chapter 3 using oxygen and olefins. In this system, hydrogen peroxide evolution has been observed from the Ir^{III} center. Chapter 5 describes work aimed at functionalization of a (Phebox)Ir-aryl bond using hypervalent iodide reagents and CO. The work in Chapter 6 explores the synthesis of (NOCON)Rh^{III} and Ir^{III} complexes in order to expand on the examples of alkane dehydrogenation at Ir^{III}.

Exploration of Electrophilic Ir^{III}, Rh^{I}, and Ir^{I} Complexes for C-H Functionalization

Three different steps have been proposed in the methane functionalization system described by Shilov (Scheme 1.4).[1d,23] Alkane activation at the Pt^{II} center occurs in the first step to generate a Pt^{II}-CH_3 complex. Oxidation to Pt^{IV} occurs in the second step, followed by functionalization of the alkyl ligand to generate methanol. C-H cleavage in this system has been proposed to proceed by two different mechanisms (Scheme 1.5). In both mechanisms, initial coordination of C-H bond to the metal center occurs with no change in the oxidation state to form a σ complex. In Path A, oxidative addition of the C-H bond occurs, concomitantly with an increase in oxidation state at the metal center. Deprotonation of the M-hydride bond yields the M-alkyl product. Electrophilic activation, Path B, does not involve any change in oxidation state at the metal center, instead deprotonation of the σ complex results in the M-alkyl species. This mechanism is different from oxidative addition, which occurs at electron rich metal centers (Path A, Scheme 1.5). Theoretical studies on this system and the Periana system strongly suggest that C-H activation proceeds through an electrophilic activation mechanism.[24]

Scheme 1.4

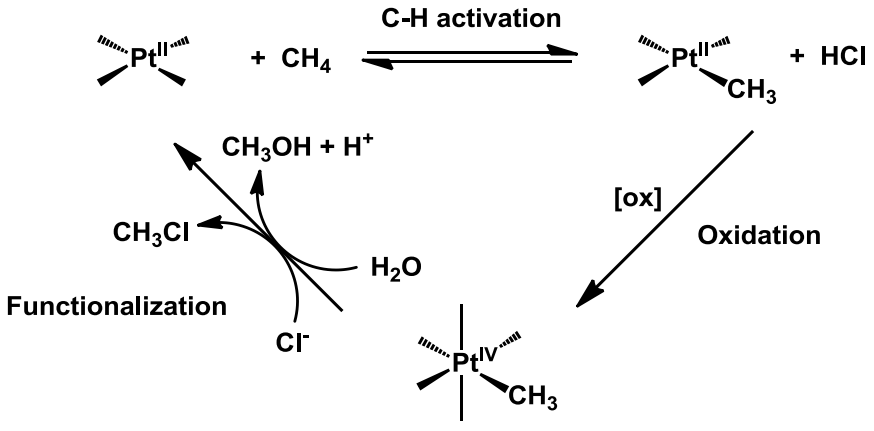

Scheme 1.5

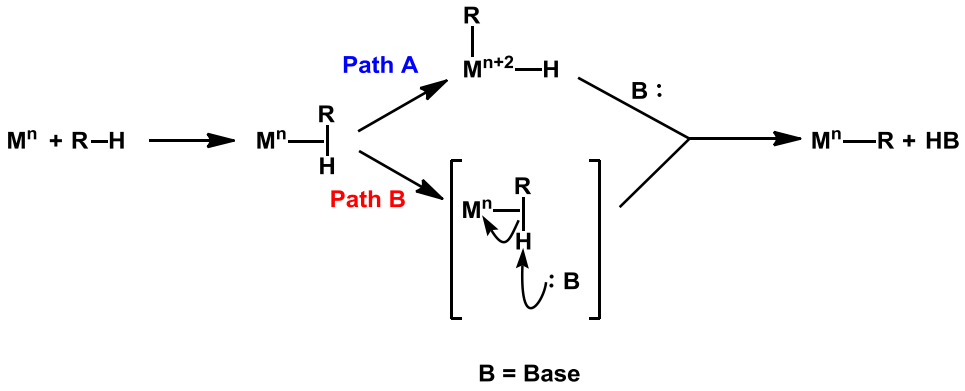

The drawbacks associated with the Pt^{II} systems discussed above provide a need for improvement on this technology. To this end electron poor Rh and Ir complexes have been explored as models for the Shilov system. In Chapter 2 of this thesis, Ir and Rh complexes with Tp^* or diene ligands have been explored for electrophilic C-H activation. The target complexes in these studies possess water ligands, which have the potential to provide an open site for coordination of C-H bonds. The water ligands may also serve as a nucleophile for oxidation of alkanes and arenes. While C-H activation was ultimately not observed in these systems, formation of a Tp^*Ir metallocycle using ethylene has been observed, and a unique five coordinate olefin dimer supported by diene ligands at an Ir^{III} center has been characterized.

Alkane Dehydrogenation by Rh^{III} and Ir^{III} Acetate Complexes Containing Pincer Ligands

The mechanism of alkane dehydrogenation by $(PCP)Ir^{I}$ catalysts has been shown to occur through a reactive 14-electron Ir^{I} species (Scheme 1.6).[25] Loss of hydrogen from the Ir^{III} center was promoted by insertion of olefin (typically TBE) into the Ir-hydride bond followed by reductive elimination to generate alkane and the three coordinate $(PCP)Ir^{I}$ species. This species promotes cleavage of C-H bonds to generate an Ir^{III}-alkyl hydride complex, which undergoes β-

hydride elimination. The kinetic product of dehydrogenation is 1-alkene, which is isomerized under the reaction conditions by the (PCP)Ir^{I} species to generate a distribution of internal alkene isomers.[26] Significant inhibition of the reactivity of the (PCP)Ir^{I} species by alkene, nitrogen and water has been observed.[10,27] Roddick and workers reported that substitution of the alkyl substituents on the phosphine arms by CF_3 groups resulted in a dehydrogenation system that was insensitive to nitrogen and water, but was still inhibited by alkene.[28] There is a need to develop dehydrogenation systems that are insensitive to these reagents.

Scheme 1.6

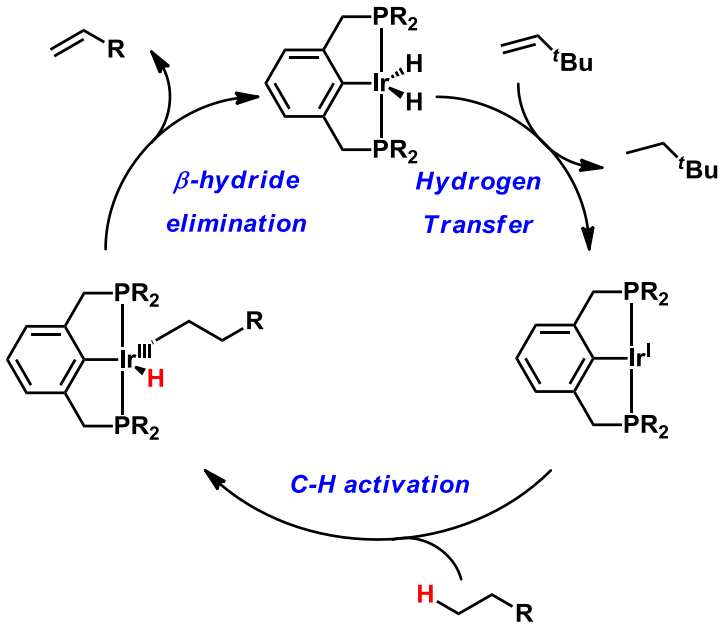

Our work focused on developing a dehydrogenation system where C-H activation is promoted at an Ir^{III} center which should be less reactive towards nitrogen, water, and alkene. To this end we examined pincer Ir^{III} acetate systems for dehydrogenation of alkanes. Recently, reports of carboxylate assisted C-H activation have been disclosed using Ru^{II}, Rh^{III}, and Ir^{III} complexes.[29] Additionally, a variety of Pd systems that promote sp^2 or activated sp^3 C-H

functionalization have been proposed to proceed through a concerted metalation deprotonation (CMD) mechanism.[30] The difference between a CMD mechanism and electrophilic activation is that an internal base is present to assist in C-H cleavage (Scheme 1.7). In contrast, electrophilic activation involves external deprotonation of a C-H σ complex. Work on alkane dehydrogenation with (Phebox)Ir^{III} complexes in Chapter 3 has demonstrated that utilizing Ir^{III} instead of Ir^{I} centers resulted in a system that is insensitive to nitrogen, alkene, and water. In this work C-H cleavage is proposed to occur by a CMD mechanism. The Ir^{III} analogue is stable at high temperatures and promotes C-H cleavage of the terminal C-H bonds of alkanes. In Chapter 6, we extended our studies of alkane dehydrogenation at Ir^{III} centers by exploring (NOCON)M^{III} acetate complexes (M = Rh, Ir). Using (NOCON)Ir acetate complexes, C-H activation of arenes and alkane dehydrogenation of *n*-octane were observed.

Scheme 1.7

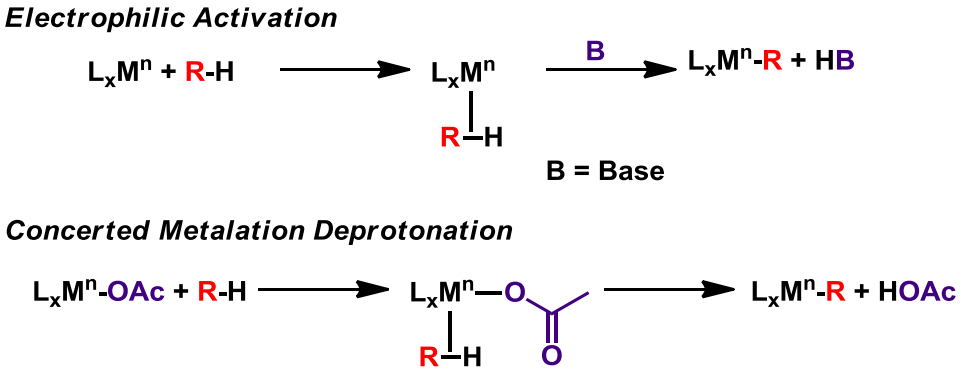

Generation of (^{dm}Phebox)$Ir(OAc)_2(OH_2)$ Using Oxygen as a Hydrogen Acceptor

In order to make alkane dehydrogenation thermodynamically favorable, sacrificial hydrogen acceptors have been utilized to remove H_2 from the reaction.[25] Using a hydrogen acceptor, such as TBE, increases the cost of the process. An alternative to using an acceptor is to

drive the generated hydrogen out of the reaction vessel. A challenge associated with acceptorless dehydrogenation is that hydrogen must be vented from the reaction vessel, which is difficult at the high temperatures required for this reaction.

Scheme 1.8

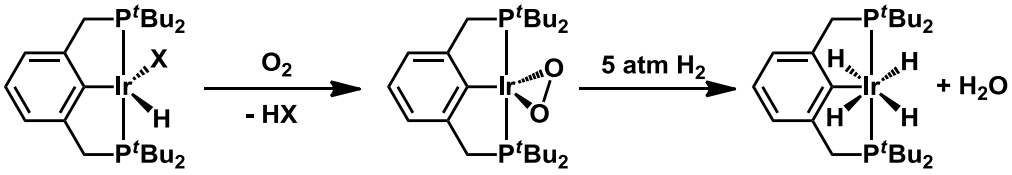

X = H, Ph, CCPh

An alternative to using olefins as hydrogen acceptors would be to utilize oxygen. Oxygen is abundant, inexpensive and would result in a more atom economical process. The dehydrogenation systems discussed above are incompatible with oxygen at elevated temperatures. Studies within our group have demonstrated that oxygen induced reductive elimination from (^{tBu}PCP)Ir(H)(X) (X = H, Ph, CCPh) occurred when benzene solutions were subjected to 5 atm of oxygen.[31] Coordination of oxygen to form (^{tBu}PCP)Ir(η^2-O_2)$_n$ (n = 1 or 2) complexes was observed depending on the amount of oxygen present. Under catalytic conditions this would prevent formation of the active catalyst (^{tBu}PCP)Ir^I. Interestingly, when hydrogen was added to (^{tBu}PCP)Ir(η^2-O_2), the formation of water and (^{tBu}PCP)Ir(H)$_4$ was observed (Scheme 1.8). While insertion into the Ir-H bond was not observed under these conditions, hydrogenation of oxygen was observed, which represents a new method for the regeneration of alkane dehydrogenation catalysts. In Chapter 4, regeneration of (Phebox)Ir(OAc)$_2$(OH$_2$) from the product of alkane dehydrogenation, (Phebox)Ir(OAc)H, has

been explored using alkenes and oxygen. Efficient regeneration is achieved using oxygen and the formation of hydrogen peroxide has been observed.

Exploration of (Phebox)Ir Phenyl Complex for Arene Functionalization

The functionalization of arenes represents a major route to the production of value added chemicals. Oxidation of arene C-H bonds to produce phenols is an important process in the production of plastics and pharmaceuticals.[5] Transition metal catalysts utilizing Pd have been shown to be effective for directed arene C-H oxidation using oxygen or air.[32] Recent work from the Sanford group has demonstrated that non-directed acetoxylation of benzene can be performed using Pd pyridine complexes and hypervalent iodide oxidants (Scheme 1.9).[33] The mechanisms for arene oxidation using either air or iodide oxidants are still under investigation. While examples of oxidative arene functionalization utilizing Ir complexes have not been widely reported, arene borylation has been described by Hartwig and coworkers.[34] Insertion of CO into Ir-aryl bonds has been also been reported by Jones and coworkers using neutral Cp^*Ir complexes. In order to better understand what governs oxidation and insertion of molecules into Ir-aryl bonds we explored (Phebox)Ir(OAc)Ph for arene functionalization in Chapter 5.

Scheme 1.9

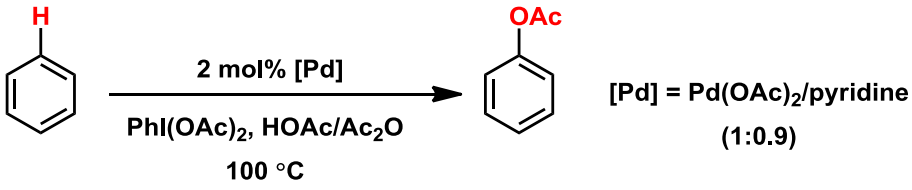

Summary

The work described in this thesis explores the reactivity of electrophilic M^{I} and M^{III} (M = Rh, Ir) complexes for C-H bond functionalization. Attempts to develop diene Ir^{I} and Rh^{I} complexes for electrophilic C-H functionalization resulted in species that were not stable at elevated temperatures. These studies suggested that the utilization of L_3 ligands may result in systems that exhibit greater thermal stability. High valent Rh^{III} and Ir^{III} complexes utilizing Phebox and NOCON ligands were found to promote arene and alkane C-H activation. Alkane dehydrogenation was most effectively promoted using a (Phebox)Ir complex, which exhibited higher thermal stability than both the analogous (Phebox)Rh^{III} and (NOCON)Ir^{III} species. Dehydrogenation of *n*-octane by (Phebox)Ir was not inhibited by nitrogen, water, or alkene supporting the hypothesis that Ir^{III} centers may be less sensitive than Ir^{I} species. At room temperature the active complex for C-H activation in the (Phebox)Ir system can be efficiently regenerated using oxygen and alkane. Using oxygen as the hydrogen acceptor in this system represents the first example of regeneration of a potential dehydrogenation catalyst using oxygen. These studies provide new directions for the utilization of Ir^{III} complexes as alkane dehydrogenation catalysts and the use of oxygen as a hydrogen acceptor for catalyst regeneration.

Notes to Chapter 1

1. (a) Arndtsen, B. A.; Bergman, R. G.; Mobley, T. A.; Peterson, T. H. *Acc*. *Chem*. *Res*. **1995**, *28*, 154. (b) Labinger, J. A.; Bercaw, J. E. *Nature* **2002**, *417*, 507. (c) Conley, B. L.; Tenn, W. J., III; Young, K. J.; Ganesh, S. K.; Meier, S. K.; Ziatdinov, V. R.; Mironov, O.; Oxgaard, J.; Goddard, W. A., III; Periana, R. A. *J*. *Mol*. *Cat*. *A: Chem*. **2006**, *251*, 8. (d) Shilov, A. E.; Shul'pin, G. B. *Chem*. *Rev*. **1997**, *97*, 2879.

2. (a) Stahl, S. S.; Labinger, J. A.; Bercaw, J. E. *Angew*. *Chem*. *Int*. *Ed*. **1998**, *37*, 2180. (b) Labinger, J. A. *J*. *Mol Catal*. *A* **2004**, *220*, 27.

3. *Handbook of Alternative Fuel Technologies*; Lee, S.; Speight, J. G.; Loyalka, S.; CRC Press: Boca Raton, FL, 2007; pp 158-159.

4. Olah, G. A.; Goeppert, A.; Prakash, G. K. S. *J*. *Org*. *Chem*. **2009**, *74*, 487.

5. *Industrial Organic Chemistry*; Weissermel, K.; Arpe, H.-J.; Wiley-VCH: Weinheim, Germany, 2003; pp 59-75.

6. (a) van Goethem, M. W. M.; Barendregt, S.; Grievink, J.; Moulijn, J. A.; Verheijen, P. J. T. *Ind*. *Eng*. *Chem*. *Res*. **2007**, *46*, 4045. (b) Rahimi, N.; Karimzadeh, R. *Appl*. *Catal*. *A-Gen*. **2011**, *398*, 1.

7. Gol'dshleger, N. F.;Es'kova, V. V.; Shilov, A. E.; Shteinman, A. A. *Zh*. *Fiz*. *Khim*. **1972**, *46*, 1353.

8. Periana, R. A.; Taube, D. J.; Gamble, S.; Taube, H.; Satoh, T.; Fujii, H. *Science*, **1998**, *280*, 560.

9. Crabtree, R. H.; Mihelcic, J. M.; Quirk, J. M. *J*. *Am*. *Chem*. *Soc*. **1979**, *101*, 7738.

10. Gupta, M.; Hagen, C.; Flesher, R. J.; Kaska, W. C.; Jensen, C. M. *Chem*. *Commun*. **1996**, 2083.

11. Gupta, M.; Hagen, C.; Kaska, W. C.; Cramer, R. E.; Jensen, C. M. *J. Am. Chem. Soc. 1997*, *119*, 840.

12. Gottker, I.; White, P.; Brookhart, M. *J. Am. Chem. Soc.* **2004**, *126*, 1804.

13. Biswas, S.; Huang, Z.; Choliy, Y.; Wang, D. Y.; Brookhart, M.; Krogh-Jespersen, K.; Goldman, A. S. *J. Am. Chem. Soc.* **2012**, 134, 13726.

14. Aoki, T.; Crabtree, R. H. *Organometallics* **1993**, *12*, 294.

15. Xu, X.; Rosini, G. P.; Gupta, M.; Jensen, C. M.; Kaska, W. C.; Krogh-Jespersen, K.; Goldman, A. S. *Chem. Commun.* **1997**, 2273.

16. Liu, F.; Goldman, A. S. *Chem. Commun.* **1999**, 655.

17. (a) Periana, R. A.; Bhalla, G.; Tenn, W. J., III; Young, K. J. H.; Liu, X. Y.; Mironov, O.; Jones, C. J.; Ziatdinov, V. R. *J. Mol. Catal. A* **2004**, *220*, 8. (b) Conley, B. L.; Tenn, W. J., III; Young, K. J. H.; Ganesh, S. K.; Meier, S. K.; Ziatdinov, V. R.; Mironov, O.; Oxgaard, J.; Gonzales, J.; Goddard, W. A., III; Periana, R. A. *J. Mol. Catal. A* **2006**, *251*, 8.

18. Klei, S. R.; Tilley, T. D.; Bergman, R. G. *Organometallics* **2002**, *21*, 4905.

19. Hanson, S. K.; Heinekey, D. M.; Goldberg, K. I. *Organometallics* **2008**, *27*, 1454.

20. Sheldon, R. A.; Kochi, J. K. *Metal-Catalyzed Oxidations of Organic Compounds: Mechanistic Principals and Synthetic Methodology Including Biochemical Processes*; Academic Press: New York, 1981.

21. Arndtsen, B. A.; Bergman, R. G. *Science* **1995**, *270*, 1970.

22. (a) Wick, D. D.; Goldberg, K. I. *J. Am. Chem. Soc.* **1999**, *121*, 11900. (b) Denney, M. C.; Smythe, N. A.; Cetto, K. L.; Kemp, R. A.; Goldberg, K. I. *J. Am. Chem. Soc.* **2006**, *128*, 2508. (c) Keith, J. M.; Muller, R. P.; Kemp, R. A.; Goldberg, K. I.; Goddard, W. A., III: Oxgaard, J. *Inorg. Chem.* **2006**, *45*, 9631. (d) Konnick, M. M.; Gandhi, B. A.; Guzei, I. A.; Stahl, S. S.

Angew. *Chem*. *Int*. *Ed*. **2006**, 45, 2904. (e) Heiden, Z. M.; Rauchfuss, T. B. *J*. *Am*. *Chem*. *Soc*. **2007**, *129*, 14303. (f) Look, J. L.; Wick, D. D.; Mayer, J. M.; Goldberg, K. I. *Inorg*. *Chem*. **2009**, *48*, 1356. (g) Grice, K. A.; Goldberg, K. I. *Organometallics* **2009**, *28*, 953. (h) Taylor, R. A.; Law, D. J.; Sunely, G. J.; White, A. J. P.; Britovsek, G. J. P. *Angew*. *Chem*. *Int*. *Ed*. **2009**, *48*, 5900. (i) Boisvert, L.; Denney, M. C.; Hanson, S. K.; Goldberg, K. I. *J*. *Am*. *Chem*. *Soc*. **2009**, *131*, 15802. (j) Szajha-Fuller, E.; Bakac, A. *Inorg*. *Chem*. **2010**, *49*, 781. (k) Teets, T. S.; Nocera, D. G. *J*. *Am*. *Chem*. *Soc*. **2011**, *133*, 17796. (l) Teets, T. S.; Cook, T. R.; McCarthy, B. D.; Nocera, D. G. *J*. *Am*. *Chem*. *Soc*. **2011**, *133*, 8114.

23. *Activation and Functionalization of C-H Bonds*; Goldberg, K. I., Goldman, A. S., Eds.; ACS Symposium Series 885; American Chemical Society: Washington, DC, 2004.

24 (a) Kua, J.; Xu, X.; Periana, R. A.; Goddard, W. A., III. *Organometallics* **2002**, *21*, 511. (b) Ess, D. H.; Goddard, W. A., III; Periana, R. A. *Organometallics* **2010**, *29*, 6459. (c) Da Silva, J. C. S.; Rocha, W. R. *J*. *Comput*. *Chem*. **2011**, *32*, 3383.

25. Choi, J.; MacArthur, A. H. R.; Brookhart, M.; Goldman, A. S. *Chem*. *Rev*. **2011**, *111*, 1761.

26. Liu, F.; Pak, E. B.; Singh, B.; Jensen, C. M.; Goldman, A. S. *J*. *Am*. *Chem*. *Soc*. **1999**, *121*, 4086.

27. Morales-Morales, D.; Lee, D. W.; Wang, Z.; Jensen, C. M. *Organometallics* **2001**, *20*, 1144.

28. Adams, J. J.; Arulsamy, N.; Roddick, D. M. *Organometallics* **2012**, *31*, 1439.

29. (a) Davies, D. L.; Al-Duaij, O.; Fawcett, J.; Giardiello, M.; Hilton, S. T.; Russell, D. R. *Dalton Trans*. **2003**, 4132. (b) Davies, D. L.; Donald, S. M. A.; Al-Duaij, O.; Macgregor, S. A.; Polleth, M. *J*. *Am*. *Chem*. *Soc*. **2006**, *128*, 4210. (c) Li, L.; Brennessel, W. W.; Jones, W. D. *Organometallics* **2009**, *28*, 3492. (d) Rhinehart, J. L.; Manbeck, K. A.; Buzak, S. K.; Lippa, G.

M.; Brennessel, W. W.; Goldberg, K. I.; Jones, W. D. *Organometallics* **2012**, *31*, 1943. (e) Allen, K. E.; Heinekey, D. M.; Goldman, A. S.; Goldberg, K. I. *Organometallics* **2013**, *32*, 1579.

30. (a) Ryabov, A. D.; Sakodinskaya, I. K.; Yatsmirsky, A. K. *J*. *Am*. *Chem*. *Soc*., *Dalton Trans*. **1985**, 2629. (b) Davies, D. L.; Donald, S. M. A.; Macgregor, S. A. *J*. *Am*. *Chem*. *Soc*. **2005**, *127*, 13754. (c) Garcia-Cuadrado, D. D.; Braga, A. A. C.; Maseras, F.; Echavarren, A. M. *J*. *Am*. *Chem*. *Soc*. **2006**, *128*, 1066. (d) Gorelsky, S. I.; Lapointe, D.; Fagnou, K. *J*. *Am*. *Chem*. *Soc*. **2008**, *130*, 10648. (e) Gunay, M. E.; Ilyashenko, G.; Richards, C. J. *Tetrahedron: Asymmetry* **2010**, *21*, 2782. (f) Li, H.; Li, B.; Shi, Z. *Catal*. *Sci*. *Technol*. **2011**, *1*, 191, and references within. (g) Gorelsky, S. I.; Stuart, D. R.; Campeau, L.-C.; Fagnou, K. *J*. *Org*. *Chem*. **2010**, *75*, 8180. (h) Gorelsky, S. I.; Lapointe, D.; Fagnou, K. *J*. *Org*. *Chem*. **2012**, *77*, 658.

31. Williams, D. B.; Kaminsky, W.; Mayer, J. M.; Goldberg, K. I. *Chem*. *Commun*. **2008**, 4195.

32. Lyons, T. W.; Sanford, M. S. *Chem*. *Rev*. **2010**, *110*, 1147.

33. (a) Emmert, M. H.; Gary, J. B.; Villalobos, J. M.; Sanford, M. S. *Angew*. *Chem*. *Int*. *Ed*. **2010**, *49*, 5884. (b) Emmert, M. H.; Cook, A. K.; Xie, Y. J.; Sanford, M. S. *Angew*. *Chem*. *Int*. *Ed*. **2011**, *50*, 9409.

34. (a) Hartwig, J. F. *Chem*. *Soc*. *Rev*. **2011**, *40*, 1992. (b) Hartwig, J. F. *Acc*. *Chem*. *Res*. **2012**, *45*, 864.

Chapter 2: Exploration of Electrophilic Ir^{III}, Rh^{I}, and Ir^{I} Complexes for C-H Bond Functionalization

Introduction

Many platinum-based model systems have been investigated in efforts to reproduce the steps of the Shilov system.[1] Alternative late transition metal systems that have been investigated for C-H functionalization include complexes of rhodium and iridium.[1g,2] The Rh^{I}/Rh^{III} and Ir^{I}/Ir^{III} redox couples are isoelectronic to the Pt^{II}/Pt^{IV} oxidation states found in Shilov-type chemistry. Additionally, Ir^{III}/Ir^{V} and $Rh^{III/}Rh^{V}$ couples could be developed to promote electrophilic C-H functionalization. Examples of Ir^{V} and Rh^{V} complexes bearing Cp^{*} ancillary ligands and hydride, methyl, or silyl ligands have been reported, and in general these complexes exist as seven coordinate species.[3] Intermediates with Ir^{V} or Rh^{V} oxidation states have been proposed in a variety of reactions, but there are only a few examples of isolated complexes. The isolated $Cp^{*}Ir^{V}$ complexes reported by Bergman and coworkers are stable at -80 °C, but decompose at higher temperatures, demonstrating the instability of many of these high valent species.[3d] The instability of Ir^{V} and Rh^{V} complexes would be useful in catalysis as this oxidation state needs only to be accessible. Examples of catalytic cycles invoking Ir^{V} or Rh^{V} intermediates are limited.[4] The observation of Ir^{V} species suggests that a system utilizing the Ir^{III}/Ir^{V} couple could be developed to reproduce the chemistry observed in the Shilov cycle.

C-H cleavage in the Shilov system has been proposed to proceed via an electrophilic activation mechanism.[1c] In this mechanism, the oxidation state at the metal center is unchanged during the reaction. Coordination of a C-H bond to the metal center via a σ complex occurs, followed by deprotonation of the bond by a base to generate a metal alkyl species. In order to develop systems for electrophilic C-H activation two approaches have been exploited involving

electron poor Ir^{III} complexes or cationic Rh^{I} and Ir^{I} complexes with poor donor ligands. In the first approach, Ir complexes utilizing the Tp^* ligand were targeted, specifically $[Tp^*Ir(OH_2)_3]^{2+}$. This ligand was chosen because of the decreased electron donor ability in comparison to the commonly employed Cp^* ligand.[5,6] The reported carbonyl stretching frequencies for $Tp^*Ir(CO)_2$ (2039 and 1960 cm^{-1}) suggest that in comparison to the values for $Cp^*Ir(CO)_2$ (2020 and 1953 cm^{-1}), Tp^* is a less electron donating ligand, thus making it a better choice for promoting electrophilic activation.[7]

For the second approach wherein the lower oxidation state Ir^{I} and Rh^{I} species were sought, diene ligands were chosen because they are relatively poor electron donors, are commerically available, and are inexpensive. The first complex chosen for investigation was $[(DMB)Rh(OH_2)_2][BF_4]$ (DMB = 2,3-dimethyl-1,2-butadiene) because the complex is readily synthesized and contains an electrophilic Rh center.[8] The CO stretching frequency for a similar complex, $[(DMB)Rh(CO)(OH_2)][BF_4]$, has been reported at 2049 cm^{-1}, confirming that the cationic rhodium center is rather electrophilic.[8] Both of these approaches towards developing electrophilic C-H cleavage systems utilize complexes that possess water ligands, which may provide several advantages. The weak coordinating ability of water could result in labile ligands which would provide the open site required for C-H activation. Water could also serve as an internal base for alkane functionalization analogous to the Shilov system.

Results and Discussion

Investigation of Tp^*Ir Complexes for C-H Activation

Synthesis of the target complex, $[Tp^*Ir(OH_2)_3]^{2+}$ (**1**), was explored using two different methods. In the first method, synthesis of **1** was attempted starting from $(Tp^*IrCl_2)_2$ (**2**)[9], which is analogous to the synthesis of the known complex, $[Cp^*Ir(OH_2)_3][OTf_2]$ (eq 2.1).[10] The second

method that was explored involved the synthesis of **1** through the proposed route described in Scheme 2.1. In this route, the first step would involve oxidation of the known compound, $Tp^*Ir(C_2H_4)_2$ (**3**)[11], with various iodide reagents to generate $(Tp^*IrI_2)_2$ (**4**). In the second step, complex **1** could be synthesized from complex **4** in the presence of water via a silver salt metathesis reaction.

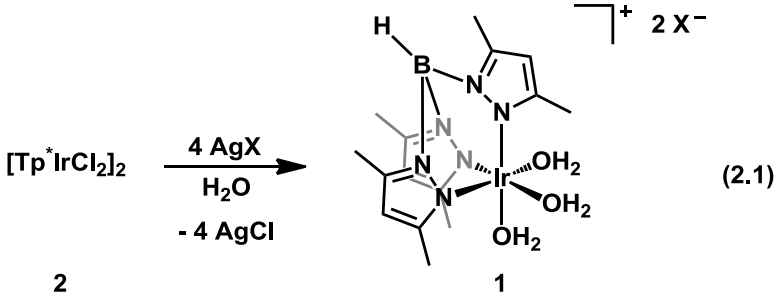

Scheme 2.1

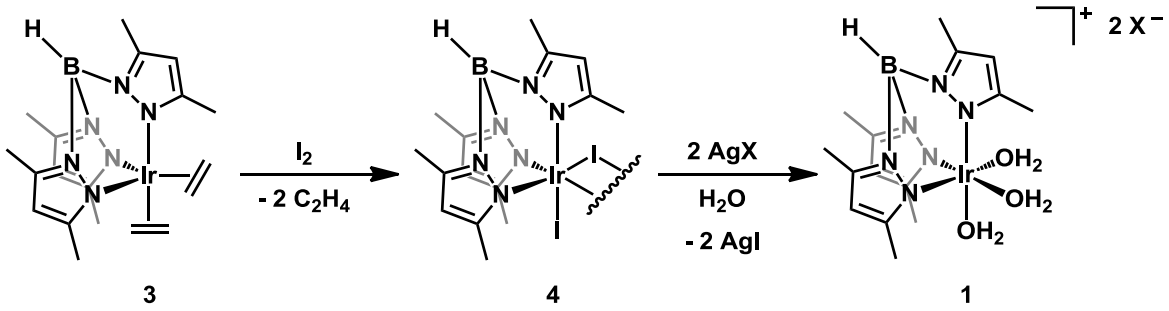

In the literature procedure, complex **2** can be synthesized from $NaTp^*$ and H_2IrCl_6 hydrate after refluxing in 95% EtOH for 24 h. Difficulty in reproducing the synthesis of **2** has been reported by Carmona and co-workers.[6] In our hands, the synthesis of complex **2** also proved to be challenging, as the reaction did not consistently yield the desired product.[6,12] Halide abstraction from **2** to generate **1** was attempted using various silver salts. When the appropriate

amount of Ag_2SO_4, $AgBF_4$, AgOTF, or $AgNO_3$ (2 or 4 equiv. of Ag^+ depending on the counterion) was added to wet THF or CH_2Cl_2 solutions of **2,** no reaction was observed at room temperature in all cases over 24 h. When halide abstraction using 4 equiv. of $AgBF_4$ or AgOTf was attempted at room temperature, complex **2** was recovered. When **2** and Ag_2SO_4 (2 equiv.) were heated at 100 °C in H_2O, starting material was recovered after 24 h along with an intractable product.

Powell and coworkers reported halide abstraction from **2** using 5 equiv. of AgTFA to give $Tp^*Ir(TFA)_2$ (**5**).[9] Synthesis of **5** was successfully reproduced after heating a mixture of AgTFA and **2** in toluene at reflux for 1 week (in contrast to the Powell report, which required only 24 h at reflux to reach completion). This synthesis also proved to be inconsistent and resulted in low yields of **5** (up to 27% isolated yield in comparison to the literature isolated yield of 58%). In order to try to obtain compound **1**, exchange of the TFA ligands of **5** for H_2O ligands was explored. When a wet CD_2Cl_2 solution of 2 equiv. of HOTf and **5** was heated at 100 °C for 15 h, a new product was obtained. In the ^1H NMR spectrum two singlets were observed at 2.44 and 6.25 ppm suggestive of complex **1**, which would be expected to be a symmetrical compound. Only one singlet was observed for the two unique methyl substituents of the Tp^* ligand, which integrated in a 6:1 ratio against the pyrazolyl singlet at 6.25 ppm. The protons of the water ligands of **1** may not be observed in the presence of wet solutions and so only the signals for the Tp^* ligand should be observed. Notably, this new product was insoluble in water, which was unexpected as the analogous complex $[Cp^*Ir(OH_2)_3][OTf_2]$ is water soluble.[10] To confirm if decomposition of the Tp^* ligand had occurred, the product was spiked with an authentic sample of 3,5-dimethylpyrazole. In the ^1H NMR spectrum, the intensity of the signals

at 2.44 and 6.26 ppm increased and confirmed that indeed the product was free pyrazole. Based on the results discussed above the synthesis of **1** following this route was abandoned.

Following the route proposed in Scheme 2.1, complex **3** was prepared using a literature procedure in order to explore generation of **4**.[11] The reaction of **3** with I_2 was explored in CH_2Cl_2 and toluene at room temperature. When 1 equiv. of a 1 M I_2 solution (CH_2Cl_2 or toluene) was added to a solution of **3** in the appropriate solvent at room temperature, a dark brown solid was obtained after removal of the volatiles. This reaction resulted in the formation of multiple Tp^*Ir products as multiple signals were observed for the methyl substituents of the Tp^* ligand by ^1H NMR spectroscopy. Performing the reaction at -78 °C gave similar results. The only identifiable product was the reported complex, $Tp^*IrH(C_2H_3)(C_2H_4)$, which was also the major product of the reaction.[13] The Ir-hydride complex results from oxidative addition of one ethylene ligand to the Ir^I center. The addition of a second equivalent of I_2 solution to the vinyl C-H activation product resulted in the formation of multiple intractable products as observed by ^1H NMR spectroscopy. The desired complex **4** was not obtained from this reaction and so alternative iodide sources were explored for this transformation.

The reaction of **3** and NIS (NIS = N-iodosuccinimide) was explored in order to obtain diiodide complex **4**. The addition of 2 equiv. of NIS to a solution of **3** in CH_2Cl_2 at -78 °C afforded a new complex. When NIS was added to a solution of **4** at -78 °C, the lime green colored solution became distinctly yellow in color. Slowly raising the temperature of the reaction to 22 °C resulted in a brown solid after removal of the volatiles. This product was also obtained using 1 equiv. of NIS at -78 °C or room temperature. Analysis of the reaction mixture by ^1H NMR spectroscopy revealed free ethylene and the presence of a new Tp^*Ir product. In the ^1H NMR spectrum of the new product three methine singlets at 5.8 ppm and a set of six distinct

methyl singlets at 2.5 ppm were observed, which is suggestive of an asymmetrical complex. The two Tp^* methyl signals at 2.47 and 2.69 ppm each integrated to four protons (expected 3H each) and one Tp^* pyrazolyl signal at 5.91 ppm integrated to more than one proton. The higher than expected integration of these signals supported the presence of a second product in the reaction mixture.

Additional evidence in the ^1H NMR spectrum of the new product suggested that an ethylene fragment remained at the Ir center. Four multiplets were observed at 3.04, 3.63, 3.81, and 4.39 ppm, each integrating to one proton, indicative of a coordinated ethylene or CH_2CH_2 fragment. X-ray quality crystals of the new Tp^*Ir product were grown from a CH_2Cl_2 solution layered with pentane. The X-ray crystallographic data confirmed the identity of this product as $Tp^*IrI(C_2H_4NO)$ (**6**) ($C_2H_4NO = C_2H_4NC_2O_2C_2H_4$) (Scheme 2.2, Figure 2.1). This structure is consistent with the ^1H NMR data discussed above for the major product. The four multiplets at 3.04, 3.63, 3.81, and 4.39 ppm in the ^1H NMR spectrum correspond to the Ir-C_2H_4-N moiety present in the crystal structure. Additionally, the multiplet from 2.72 to 2.92 ppm corresponds to the ethyl backbone of the succinimido metalocycle.

Scheme 2.2

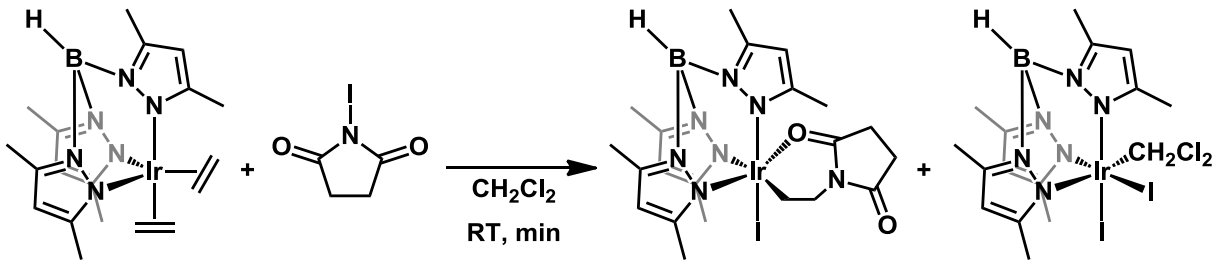

3 **6** **7**

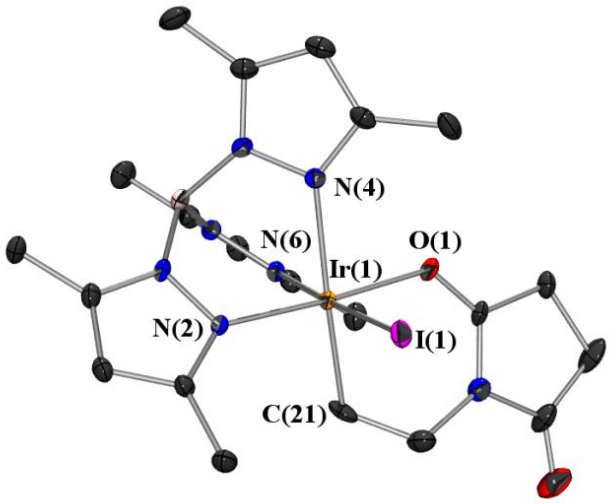

Figure 2.1. ORTEP diagram of complex $Tp^*IrI(C_2H_4NO)$ (**6**) (thermal ellipsoids at 50% probability, H atoms omitted for clarity). Selected bond lengths (Å) and angles (deg): N(2)-Ir(1) = 2.035(3), N(4)-Ir(1) = 2.166(3), N(6)-Ir(1) = 2.067(3), O(1)-Ir(1) = 2.061(4), C(21)-Ir(1) = 2.094(4), I(1)-Ir(1) = 2.6881(4), O(1)-C(16) = 1.274(5), O(2)-C(19) = 1.194(5), N(2)-Ir(1)-O(1) = 176.12(14), N(2)-Ir(1)-N(6) = 88.91(11), O(1)-Ir(1)-N(6) = 88.33(14), O(1)-Ir(1)-C(21) = 89.94(17), N(6)-Ir(1)-C(21) = 90.68(15).

A second compound was crystallized from the reaction mixture along with **6**. Analysis of these pink crystals by X-ray crystallography revealed the identity of the second product as $Tp^*IrI_2(CH_2Cl_2)$ (**7**) (Figure 2.2), which is consistent with the ^1H NMR data. A plausible mechanism for the formation of complex **6** is shown in Scheme 2.3. Initial iodide transfer to **3** could occur to generate $[Tp^*IrI(C_2H_4)]^+$ (**A**). This species could then undergo nucleophilic attack at the ethylene ligand to generate **6**, where coordination of an oxygen substituent of the NIS moiety has occurred. Oxidative addition of NBS has been observed previously at a $Pd^0(PPh_3)_2$ species to generate the corresponding $(PPh_3)_2Pd^{II}Br$(succinimido) complex.[14] Nucleophilic attack at the ethylene ligand of **A** most likely occurs because of the increased electrophilicity of the alkene due to backbonding with the electron poor Ir^{III} center.

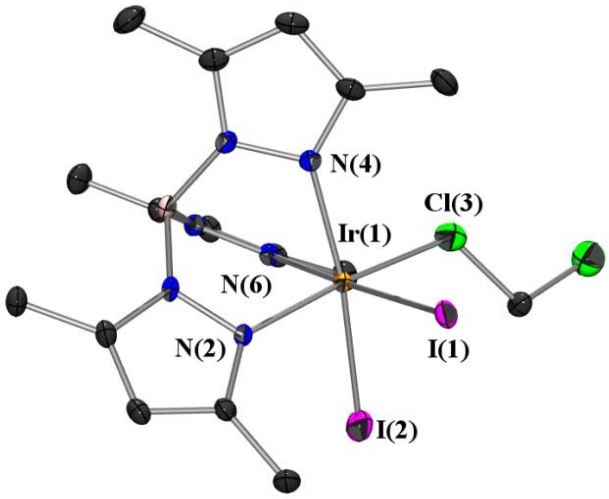

Figure 2.2. ORTEP diagram of complex $Tp^*IrI_2(CH_2Cl_2)$ (**7**) (thermal ellipsoids at 50% probability, H atoms omitted for clarity). Selected bond lengths (Å) and angles (deg): N(2)-Ir(1) = 2.035(3), N(4)-Ir(1) = 2.166(3), N(6)-Ir(1) = 2.067(3), I(1)-Ir(1) = 2.6881(4), I(2)-Ir(1) = 2.727(8), Cl(3)-Ir(1) = 2.29(3), N(2)-Ir(1)-N(6) = 88.91(11), N(2)-Ir(1)-Cl(3) = 174.5(10), Cl(3)-Ir(1)-I(2) = 88.8(10).

Scheme 2.3

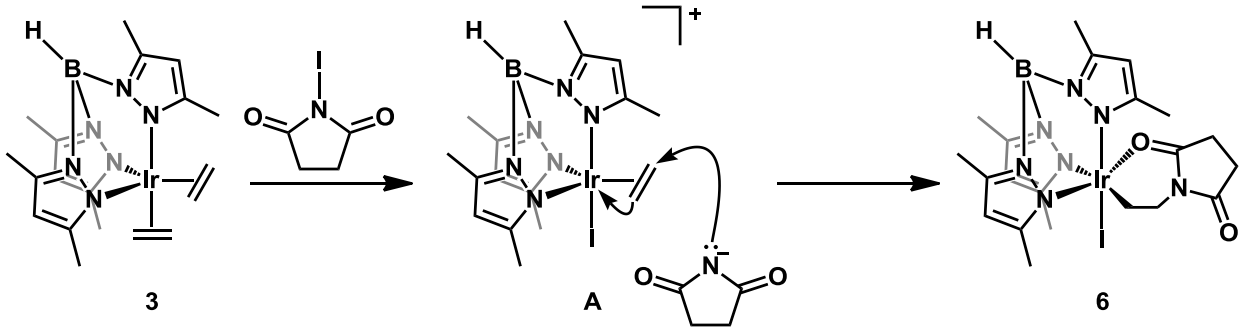

Dimethylbutadiene Rh^I and Ir^I chemistry

The target complex $[(DMB)Rh(OH_2)_2][BF_4]$ (**8-BF_4**) was synthesized using a literature procedure (Scheme 2.4).[8] Many of the Rh and Ir complexes that undergo C-H activation possess good donor ligands, in contrast to DMB. The η^4-DMB and the η^2-DMB species of complex **8-**

BF_4 have been reported to exist in equilibrium in solution at 95 °C (Scheme 2.4).[8] Bercaw and coworkers recently reported the stoichiometric activation of indene using $[(COD)Rh(OH_2)_2][BF_4]$, which was generated from $[(COD)RhOH]_2$ and acid.[15] The bis-aqua complex coordinated indene in an η^6-fashion, and upon addition of an external base C-H cleavage occurred to generate the activated η^3-indenyl Rh product. No activation of benzene was observed using this system. The lability of one arm of the DMB ligand in **8-BF_4** could provide an advantage over the Bercaw system because of the additional open site available for C-H activation.

Scheme 2.4

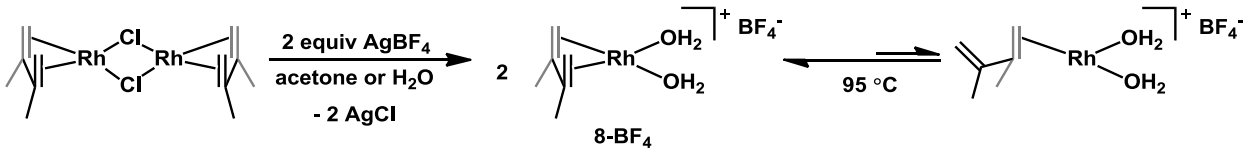

Complex **8-BF_4** was examined for indene activation under similar conditions used in the Bercaw system. When 2 equiv. of indene were added to **8-BF_4** in CD_2Cl_2 an immediate reaction occurred. The asymmetrical product was characterized as the η^6-indenyl Rh^I compound, $[(\eta^6$-indenyl)Rh(DMB)][BF_4] (**9**) by ^1H and ^{13}C NMR spectroscopy (Scheme 2.5).[16] Addition of 1 equiv. of 2,6-lutidine to **9** resulted in the formation of $[(\eta^3$-indenyl)Rh(DMB)] (**10**), which was also characterized using ^1H and ^{13}C NMR spectroscopy (Scheme 2.5). Bercaw and coworkers accessed an indenyl species similar to **10** starting directly from $[(COD)Rh(OH)]_2$. C-H cleavage of indene was proposed to occur via deprotonation by the hydroxide ligand.[15]

Scheme 2.5

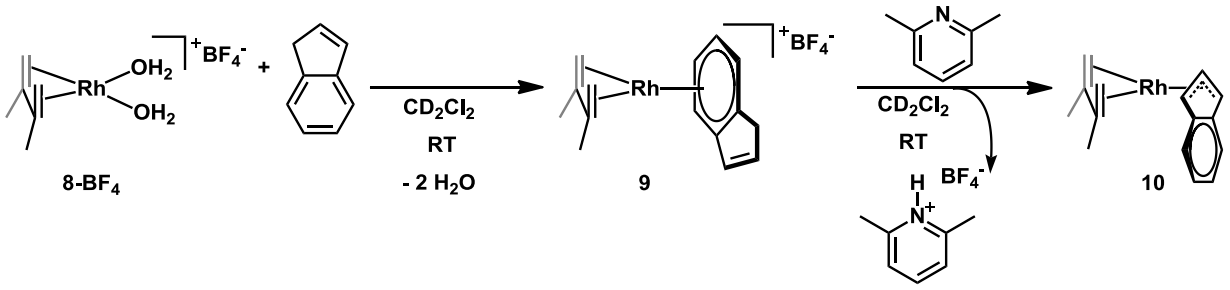

Since **8-BF$_4$** was found to promote C-H cleavage of indene, we wanted to explore activation of stronger C-H bonds such as those found in arenes. Complex **8-X** (X = OAc, TFA, BF_4) was tested as a catalyst for H/D exchange between benzene and various deuterium sources. As complex **8-BF$_4$** is insoluble in a variety of organic solvents, experiments were performed in CD_3OD, D_2O, and TFA-*d*. In these reactions, complex **8-X** was prepared *in situ* in a vessel equipped with a resealable Teflon stopcock containing 2 equiv. of AgOAc, AgTFA, or $AgBF_4$, and the deuterium source. Ten equivalents of benzene were added to the mixture and the reaction vessel was sealed under N_2. After heating for 48 h at 80 °C, the reaction mixtures were cooled to room temperature, filtered through Celite to remove metal black, and then analyzed by GC/MS. No deuterium incorporation into benzene or free DMB was detected in any of these reactions by GC/MS analysis.[17] When isolated **8-BF$_4$** was heated at 80 °C in a CD_3OD/benzene mixture, loss of the DMB ligand was observed after 17 h. In the ^{1}H NMR spectrum the signals at -0.16 and 1.85 ppm, corresponding to coordinated DMB, disappeared concomitantly with the appearance of signals indicative of free ligand. Loss of the DMB ligand was also accompanied by the formation of Rh black supporting that decomposition of **8-BF$_4$** had occurred.

Complexes with bidentate diene ligands similar to **8-BF$_4$**, such as COD, have been reported to coordinate arenes.[18] Coordination of benzene was not observed under the conditions

used in the H/D exchange reactions. Therefore, we were interested in determining if the water ligands of complex **8-BF$_4$** were labile. Complex **8-BF$_4$** does react with anisole, toluene, and benzene in dry CD_2Cl_2 to form the corresponding η^6-arene rhodium cation as observed by ^{1}H and ^{13}C NMR spectroscopy (eq. 2.2). In the presence of 1,3-bis(trifluoromethyl)benzene no reaction occurred, which can be attributed to the electron-deficient arene being an even poorer ligand than water. These experiments demonstrated that the water ligands of complex **8-BF$_4$** can be displaced by arenes.

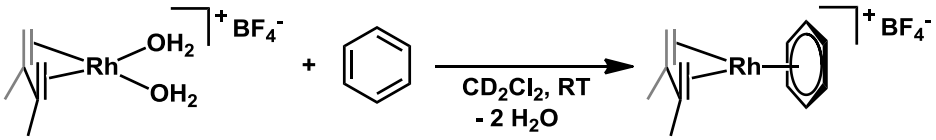

(2.2)

Since **8-BF$_4$** is insoluble in benzene, attempts were made to synthesize and isolate an analogue that would allow for increased solubility in non-coordinating solvents. A (DMB)Rh-acetate complex was synthesized, which was anticipated to have an added benefit because the acetate ligand might assist in C-H activation. Acetate-assisted C-H activation has been observed previously in the literature using different systems.[19] Halide abstraction from $[(DMB)RhCl]_2$ was accomplished by treating a wet acetone solution of the dimer with 2 equiv. of AgOAc. An immediate color change was observed and removal of the volatiles yielded a purple solid (Scheme 2.6). Coordinated DMB was identified in the ^{1}H NMR spectrum (acetone-d_6) as two broad signals at 0.49 and 2.43 ppm (olefinic protons) and a singlet at 2.08 ppm (methyl protons). The bound acetate was observed as a singlet at 1.79 ppm integrating to three protons. In the ^{13}C NMR spectrum the two carbon signals for bound acetate were observed at 180.70 and 22.29 ppm. This purple solid was soluble in benzene at room temperature. Thermolysis of the isolated

complex in a 4% H_2O/benzene-d_6 solution at 80 °C resulted in decomposition to Rh black and free DMB after 24 h. No H/D exchange between benzene-d_6 and H_2O was detected by ^{1}H NMR spectroscopy.

Scheme 2.6

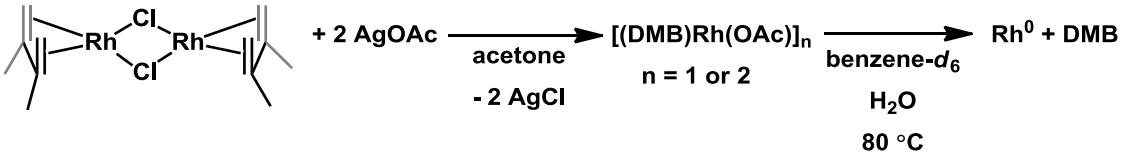

The instability of complex **8-X** at elevated temperatures resulted in the pursuit of the analogous Ir complex as a potentially more robust compound for C-H activation. Initial attempts to synthesize the unreported complex, $[(DMB)IrCl]_2$ (**11**), using $[Ir(COE)_2Cl]_2$ and 2 equiv. of DMB in Et_2O at 60 °C resulted in the formation of multiple species as detected by ^{1}H NMR spectroscopy (Scheme 2.7a). One species was identified by ^{1}H NMR spectroscopy as the known monomeric complex $(DMB)_2IrCl$ (**12**) and confirmed by independent synthesis.[20] In another attempt to make **11**, ethylene was bubbled through an ether solution of $[Ir(COE)_2Cl]_2$ at 0 °C to generate $[Ir(C_2H_4)_2Cl]_2$[21] and then 2 equiv. of DMB was added. The product of this reaction was identified as the previously unreported $[(DMB)Ir(COE)Cl]_2$ (**13**) (Scheme 2.7b) using ^{1}H NMR spectroscopy and X-ray crystallography (Figure 2.3). Complex **13** was obtained in 56% isolated yield. In the ^{1}H NMR spectrum of **13**, a multiplet at 4.4 ppm corresponded to the olefinic protons of the COE ligands. This signal was shifted upfield relative to free COE. Three signals were observed corresponding to the olefinic and methyl protons of the symmetrical DMB ligand. The low solubility of **13** in all solvents precluded the use of ^{13}C NMR spectroscopy as a tool for identification. Repeating this procedure and removing COE during the synthesis in order

to avoid formation of **13** only resulted in the formation of multiple species, one of which was identified as the monomeric complex **12** (Scheme 2.7c).

Scheme 2.7

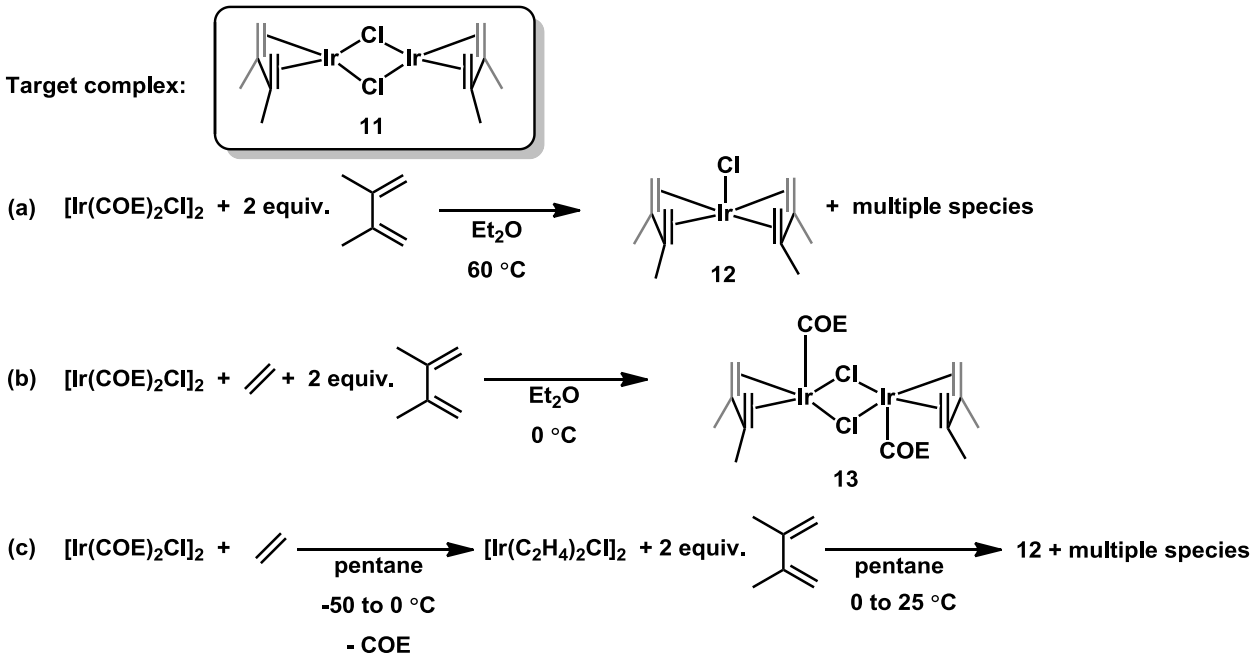

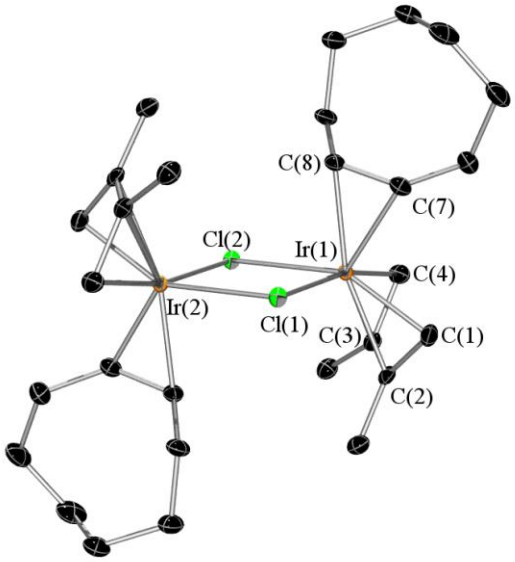

Figure 2.3. ORTEP diagram of complex $[(DMB)Ir(COE)Cl]_2$ (**13**) (thermal ellipsoids at 50% probability, H atoms omitted for clarity). Selected bond lengths (Å) and angles (deg): Ir(1)–C(1) = 2.079(3), Ir(1)-C(2) = 2.203(2), Ir(1)-C(3) = 2.192(2), Ir(1)-C(4) = 2.080(3), Ir(1)-C(7) = 2.162(2), Ir(1)-C(8) = 2.177(2), Ir(1)-Cl(1) = 2.4870(6), C(1)-Ir(1)-C(4) = 79.31(11), C(1)-Ir(1)-C(7) = 98.44(10), C(7)-Ir(1)-C(2) = 125.38(10), C(8)-Ir(1)-Cl(1) = 84.91(7), C(1)-Ir(1)-Cl(1) = 93.08(8), C(2)-Ir(1)-Cl(1) = 111.18(7). The metrical parameters for the two halves of the dimer are equivalent.

Complex **13** is the first example of a structurally characterized five-coordinate iridium olefin dimer. The only other known example of a dimer of this formulation is a rhodium complex where two butadiene ligands are each coordinated to a rhodium center, and a third butadiene ligand bridges the two metal centers (Scheme 2.8).[21] The identity of this structure was confirmed using only IR and ^{1}H NMR spectroscopy.[21] In complex **13** each Ir^I center is coordinated to an η^4-DMB ligand and an η^2-COE ligand, which was surprising given that chloride bridged dimers of Ir and Rh are typically four-coordinate. These four-coordinate complexes are generally used as starting materials in metal complex syntheses. For example, $[M(NBD)_2Cl]_2$ and $[M(olefin)_nCl]_2$ (M = Rh or Ir; NBD = norbornadiene; olefin = COD, COE; n = 1 or 2) exist as four coordinate dimers and do not coordinate an additional olefin ligand to the

metal center.[22] The coordination of a fifth ligand to the Ir center of **13** suggests a more electrophilic metal center relative to the four coordinate dimers, which is consistent with our goal of developing an electrophilic complex.

Scheme 2.8

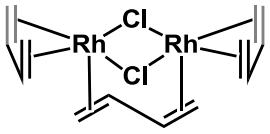

After confirming the identity of complex **13**, the ability to promote C-H activation was explored. Initial H/D exchange experiments between benzene and CD_3OD using **13** and 2 equiv. of AgOAc or AgOTf were unsuccessful, and resulted in decomposition of **13** to iridium black and free ligand. Attempts to isolate the product of silver salt metathesis of **13** with AgOAc, AgOTf, or $AgBF_4$ in CD_3OD, CD_2Cl_2, or acetone were unsuccessful. Heating mixtures of **13** with or without silver salts present at 60 °C also resulted in decomposition to Ir black. The electrophilic nature of the iridium center may contribute to the lack of stability observed at elevated temperatures and alternative complexes were pursued for C-H activation.

The known complex $(DMB)_2IrCl$ (**12**), first obtained as a byproduct in attempts to synthesize $[(DMB)IrCl]_2$ (**11**), was explored for C-H activation. Interestingly, the bis-diene Rh analogue cannot be prepared, only the dimeric compound $[(DMB)RhCl]_2$ has been obtained.[23] Air stable complex **12** was of interest because the corresponding methyl complex $(DMB)_2IrCH_3$ (**14**) could be synthesized from **12** using CH_3Li.[24] Complex **14** was of interest as it contains an Ir-alkyl moiety. Functionalization of the alkyl ligand of **14** using dioxygen or water could result in the formation a new C-O bond. Complex **14** was found to be stable in the presence of water

and oxygen in benzene solutions at room temperature. At 100 °C, benzene solutions of **14** decomposed to free DMB and Ir black in the presence of oxygen. When oxidants such as *m*-CPBA, $PhI(OAc)_2$, or PhIO were added to solutions of **14** in CD_2Cl_2 or CD_3CN consumption of the Ir material was observed by ^1H NMR spectroscopy. Formation of free DMB and Ir black were observed in these reactions. Attempts to observe sp^2 C-H activation using complex **14** in benzene-d_6 at 100 °C did not yield any C-H cleavage products, instead decomposition of **14** to Ir black and free ligand was observed.

Conclusions

Two different methods were followed to try to synthesize the electrophilic Ir^{III} complex, $[Tp^*Ir(OH_2)_3]^{2+}$ (**1**). Synthesis of the dimeric precursor, $(Tp^*IrCl_2)_2$ (**2**), using the literature procedure proved difficult. Halide abstraction from **2** in the presence of water did not yield the desired product **1**. Interestingly, attempts to oxidize $Tp^*Ir(C_2H_4)_2$ (**3**) using NIS resulted in the novel Ir metallocycle $Tp^*IrI(C_2H_4NO)$ (**6**). This complex likely resulted from oxidation the Ir^I center of **3** by NIS followed by nucleophilic attack at the remaining ethylene ligand by succinimide. Ultimately, we abandoned our plans to prepare complex **1** and moved on to prepare and investigate electrophilic Rh^I and Ir^I complexes.

The reactivity of $(DMB)Rh^I$ and Ir^I complexes towards C-H bonds was explored at elevated temperatures. Coordination of arenes to the (DMB)Rh center demonstrated that the aqua ligands of **8-BF$_4$** can be displaced by arenes. Additionally, the unusual five-coordinate Ir dimer $[(DMB)Ir(COE)Cl]_2$ (**13**) was synthesized using DMB and $[Ir(C_2H_4)_2Cl]_2$. A series of (DMB)M (M = Rh or Ir) complexes **8-X**, **13**, **14**, and **15** were tested for H/D exchange between benzene and various deuterium sources, but these reactions only resulted in decomposition of the

metal complexes suggesting that more strongly coordinating ligands are required in order to achieve C-H activation.

Experimental

General Considerations. Unless specified otherwise, all reactions were carried out under a dry nitrogen atmosphere using standard glovebox, Schlenk, or vacuum-line techniques. Dimethylbutadiene, cyclooctene, indene, AgOAc, AgTFA, Ag_2SO_4, AgOTf, $AgBF_4$, $AgNO_3$ and N-iodosuccinimide was used as received from Aldrich. Solvents were purified before use: benzene, ether and pentane were purified by passage through columns of activated alumina and molecular sieves. Deuterated solvents were purchased from Cambridge Isotope Laboratories. Benzene-d_6, toluene-d_8 were dried over sodium/benzophenone and dichloromethane-d_2, chloroform-d_1 were dried over CaH_2. NMR spectra were obtained on Bruker AV300 or AV500 MHZ spectrometers with chemical shifts (δ) reported in ppm downfield of tetramethylsilane. $^{19}F\{^1H\}$ NMR spectra were referenced externally to neat CF_3COOH. H/D exchange reactions were analyzed using an Agilent 5975 mass spectrometer with a 30 m x 0.32 mm Agilent HP-5MS capillary column. KTp^*,[25] $(Tp^*IrCl_2)_2$ (**2**),[9] $Tp^*Ir(C_2H_4)_2$ (**3**),[10] $(Tp^*Ir(TFA)_2$ (**5**),[9] $[(DMB)Rh(OH_2)_2][BF_4]$ (**8-BF_4**),[8] $(DMB)_2IrCl$ (**12**),[20] and $(DMB)_2IrCH_3$ (**14**)[24] were prepared according to literature procedures.

Synthesis and Characterization of Complexes

$Tp^*IrI(C_2H_4NO)$ (6) and $Tp^*IrI_2(CH_2Cl_2)$ (7). A vial was charged with a stir bar, **3** (40 mg, 0.073 mmol), and 1 mL of CH_2Cl_2 and then NIS (17 mg, 0.073 mmol) was added to the solution at room temperature. After 15 min the volatiles were removed in vacuo to give a yellow/tan solid. X-ray quality crystals of **6** and **7** were co-crystallized at room temperature from a saturated CH_2Cl_2 solution layered with pentane. **Complex 6.** ^1H NMR (CD_2Cl_2, 500 MHz): δ

5.91 (s, 1H, Tp*CH), 5.82 (s, 1H, Tp*CH), 5.79 (s, 1H, Tp*CH), 4.39 (CH_2CH_2), 3.79 (CH_2CH_2), 3.64 (CH_2CH_2), 3.04 (CH_2CH_2), 2.91-2.96 (m, 4H, succinimido), 2.69 (s, 3H, Tp*CH_3), 2.54 (s, 3H, Tp*CH_3), 2.47 (s, 3H, Tp*CH_3), 2.43 (s, 3H, Tp*CH_3), 2.38 (s, 3H, Tp*CH_3), 2.08 (s, 3H, Tp*CH_3). ESI-MS (*m*/*z*): 744 (M^+), 646 (M^+- $C_4H_4NO_2$). **Complex 7.** ^{1}H NMR (CD_2Cl_2, 500 MHz): δ 5.91 (s, 1H Tp*CH), 2.69 (s, 3H, Tp*CH_3), 2.47 (s, 3H, Tp*CH_3).

[(η^6-indenyl)Rh(DMB)][BF_4] (9). Formation of **9** was accomplished following the reported procedure for the reaction of [(COD)Rh(OH_2)$_2$][BF_4] with indene.[15] Complex **8-BF_4** was generated in situ from [(DMB)RhCl]$_2$ (14 mg, 0.032 mmol) and $AgBF_4$ (13 mg, 0.065 mmol) in wet acetone. After filtration and removal of the volatiles, **8-BF_4** (yellow) was dissolved in 500 μL of wet CD_2Cl_2 and indene was added (7.6 μL, 0.065 mmol) to generate an orange colored solution. ^{1}H NMR (CD_2Cl_2, 500 MHz): δ 7.25 (m, 1H, H_d), 7.07 (m, 1H, H_g), 6.98 (dt, 1H, H_b), 6.83 (m, 2H, H_e and H_f), 6.77 (m, 1H, H_a), 3.54 (d, 1H, $^1J_{HH}$ = 24.3 Hz, H_c), 3.29 (d, 1H, H_c, $^1J_{HH}$ = 24.3 Hz), 2.98 (br s, 1H, H_h), 2.86 (br s, 1H, H_j), 1.95 (s, 3H, H_l), 1.93 (s, 3H, H_m), 1.18 (1H, Hi), 1.17 (1H, H_k). ^{13}C NMR (CD_2Cl_2, 500 MHz): δ 142.2 (indenyl CH_2), 127.24 (indenyl CH_2), 125.19 (indene aryl, $^1J_{RhC}$ = 2.5 Hz), 122.13 (indene aryl, $^1J_{RhC}$ = 2.9 Hz), 103.07 (DMB *C*=CH_2, $^1J_{RhC}$ = 6.7 Hz), 103.01 (DMB *C*=CH_2, $^1J_{RhC}$ = 6.7 Hz), 100.54 (indene aryl, $^1J_{RhC}$ = 3.5 Hz), 100.05 (indene aryl, $^1J_{RhC}$ = 4.3 Hz), 98.17 (indene aryl, $^1J_{RhC}$ = 4.5 Hz), 97.71 (indene aryl, $^1J_{RhC}$ = 3.3 Hz), 49.29 (DMB CH_2, $^1J_{RhC}$ = 15.6 Hz), 48.98 (DMB CH_2, $^1J_{RhC}$ = 15.4 Hz), 39.31 (indenyl CH_2), 18.21 (DMB CH_3), 17.86 (DMB CH_3).

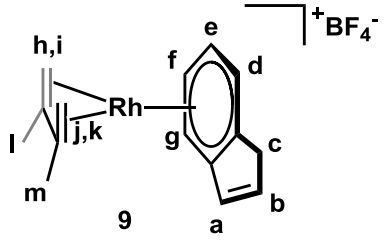

[(η^3-indenyl)Rh(DMB)] (10). To a solution of **9** (25 mg, 0.064 mmol) in CH_2Cl_2, 2,6-lutidine (8 μL, 0.070 mmol) was added. After 2.5 h the volatiles were removed *in vacuo*. The yellow solid was washed with pentane 4x1mL and then dried. ^{1}H NMR (CD_2Cl_2, 500 MHz): δ 6.93 (m, 4H, H_c and H_d), 6.10 (dd, 1H, $^1J_{HH}$ = 5.4 Hz, $^1J_{RhH}$ = 2.7 Hz, H_a), 5.91 (br d, 2H, $^1J_{RhH}$ = 2.7 Hz, H_b), 2.50 (br s, 2H, H_e), 1.31 (s, 6H, H_g), 0.99 (dd, 2H, $^1J_{HH}$ = 0.99 Hz, $^1J_{RhH}$ = 2.5 Hz, H_f). ^{13}C NMR (CD_2Cl_2, 500 MHz): δ 122.26 (s, indene aryl), 119.57 (s, indene aryl), 108.00 (d, $^1J_{RhC}$ = 2.8 Hz, indene aryl), 91.04 (d, $^1J_{RhC}$ = 7.5 Hz, C_a), 88.65 (d, $^1J_{RhC}$ = 7.2 Hz, DMB *C*=CH_2), 75.97 (d, $^1J_{RhC}$ = 5.3 Hz, C_b), 38.45 (d, $^1J_{RhC}$ = 17.4 Hz, DMB *C*H_2) 17.84 (s, DMB CH_3).

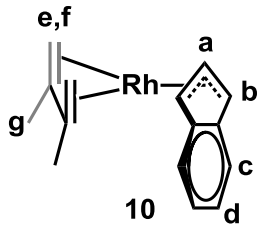

General Procedure for Formation of (DMB)Rh arene complexes. Complex **8-BF_4** was prepared in situ from $[(DMB)RhCl]_2$ and $AgBF_4$ in wet acetone (500 μL). The volatiles were removed and **8-BF_4** was dissolved in CD_2Cl_2 (450 μL). To this solution 1 equiv. of arene was added via microsyringe to cleanly generate the corresponding (DMB)Rh arene complex.

[(DMB)Rh(C_6H_6)][BF_4]. Following the general procedure, C_6H_6 (2 μL, 0.02 mmol) was added to a solution of $[(DMB)RhCl]_2$ (5.0 mg, 0.011 mmol) and $AgBF_4$ (4.4 mg, 0.023 mmol). ^{1}H NMR (CD_2Cl_2, 500 MHz): δ 6.86 (s, 6H, C_6H_6), 3.37 (d, 2H, $^1J_{HH}$ = 1.8 Hz, DMB CH_2), 2.22 (s, 6H, DMB CH_3), 1.26 (t, 2H, $^1J_{HH}$ = 2.5 Hz, $^1J_{RhH}$ = 2.2 Hz, DMB CH_2). ^{13}C NMR (CD_2Cl_2, 500 MHz): δ 105.78 (d, $^1J_{RhC}$ = 7.4 Hz, DMB *C*=CH_2), 103.15 (d, $^1J_{RhC}$ = 3.6 Hz, C_6H_6), 48.60 (d, $^1J_{RhC}$ = 15.3 Hz, DMB CH_2), 19.39 (s, DMB CH_3). ^{19}F NMR (CD_2Cl_2, 300 MHz): -153.1 (BF_4).

[(DMB)Rh(toluene)][BF_4]. Following the general procedure, toluene (2 μL, 0.02 mmol) was added to a solution of $[(DMB)RhCl]_2$ (4.5 mg, 0.010 mmol) and $AgBF_4$ (4.0 mg, 0.020 mmol).

^{1}H NMR (CD_2Cl_2, 500 MHz): δ 6.82 (t, 2H, 3-tolyl), 6.74 (t, 1H, 4-tolyl), 6.68 (d, 2H, 2-tolyl), 3.21 (br s, 2H, DMB CH_2), 2.39 (s, 3H, toluene CH_3), 2.18 (s, 6H, DMB CH_3), 1.27 (br s, 2H, DMB CH_2). ^{19}F NMR (CD_2Cl_2, 300 MHz): -152.7 (BF_4).

[(DMB)Rh(anisole)][BF_4]. Following the general procedure, anisole (2 μL, 0.02 mmol) was added to a solution of [(DMB)RhCl]$_2$ (4.8 mg, 0.011 mmol) and $AgBF_4$ (4.2 mg, 0.022 mmol). ^{1}H NMR (CD_2Cl_2, 500 MHz): δ 688 (t, 2H, 3-anisolyl), 6.59 (d, 2H, 2-anisolyl), 6.47 (t, 1H, 4-anisolyl), 3.90 (s, 3H, anisole CH_3), 3.22 (d, 2H, $^1J_{HH}$ = 1.6 Hz, DMB CH_2), 2.21 (s, 6H, DMB CH_3), 1.27 (t, 2H, $^1J_{HH}$ = 2.4 Hz, $^1J_{RhH}$ = 2.0 Hz, DMB CH_2). ^{19}F NMR (CD_2Cl_2, 300 MHz): -153.3 (BF_4).

[(DMB)Rh(OAc)]n (n = 1 or 2). A 25 mL flask was charged with [(DMB)RhCl]$_2$ (24 mg, 0.055 mmol) and 1.5 mL of acetone to give an orange colored solution. AgOAc (18 mg, 0.11 mmol) was added and the mixture was stirred at room temperature for 5 min. The purple solution was filtered through a syringe filter and the volatiles were removed in vacuo to give a dark purple solid (20 mg). ^{1}H NMR (acetone-d_6, 500 MHz): δ 2.43 (br s, 2H, DMB CH_2), 2.08 (s, 6H, DMB CH_3), 1.79 (s, 3H, OAc), 0.49 (br s, 2H, DMB CH_2). ^{13}C NMR (acetone-d_6, 500 MHz): δ 179.70 (OAc), 94.15 (DMB *C*=CH_2), 40.01 (DMB CH_2), 22.29 (OAc), 17.82 (DMB CH_3).

[(DMB)Ir(COE)Cl]$_2$ (13). A 50 mL Teflon stoppered reaction vessel was charged with [Ir(COE)$_2$Cl]$_2$ (300 mg, 0.34 mmol) and 30 mL of Et_2O. Ethylene was bubbled through the orange suspension at 0 °C until the solution became grey in color. This mixture was stirred under an ethylene atmosphere for 20 min and then DMB (76 μL, 0.67 mmol) was added. The vessel was closed and stirred at 40 min. After allowing the mixture to warm to room temperature, the volatiles were removed in vacuo to give an orange solid, which was washed with pentane 3x5 mL. Complex **13** was isolated as a yellow powder (156 mg, 56%). ^{1}H NMR

($CDCl_3$, 500 MHz): δ 4.34 (m, 4H, COE CH_2), 2.24 (d, 4H, DMB CH_2, $^1J_{HH}$ = 3.1 Hz), 2.17 (s, 12H, DMB CH_3), 1.83 (m, 12H, COE), 1.59 (m 12H, COE), 0.42 (d, 4H, DMB CH_2, $^1J_{HH}$ = 3.1 Hz).

Details of Solid State Structure Determination of 6 and 7.

A yellow piece, measuring 0.15 x 0.09 x 0.03 mm^3 was mounted on a loop with oil. Data was collected at -163 °C on a Bruker APEX II single crystal X-ray diffractometer, Mo-radiation. Crystal-to-detector distance was 40 mm and exposure time was 10 seconds per frame for all sets. The scan width was 0.5^o. Data collection was 100% complete to 25^o in ϑ. A total of 279723 reflections were collected covering the indices, h = -23 to 22, k = -21 to 21, l = -27 to 27. 7128 reflections were symmetry independent and the R_{int} = 0.0677 indicated that the data was of slightly less than average quality (0.07). Indexing and unit cell refinement indicated a primitive monoclinic lattice. The space group was found to be P b c a (No.61). The data was integrated and scaled using SAINT, SADABS within the APEX2 software package by Bruker.[26]

Solution by direct methods (SHELXS, SIR97[27]) produced a complete heavy atom phasing model consistent with the proposed structure. The structure was completed by difference Fourier synthesis with SHELXL97.[28,29] Scattering factors are from Waasmair and Kirfel.[30] Hydrogen atoms were placed in geometrically idealized positions and constrained to ride on their parent atoms with C---H distances in the range 0.95-1.00 Angstrom. Isotropic thermal parameters U_{eq} were fixed such that they were $1.2U_{eq}$ of their parent atom Ueq for CH's and $1.5U_{eq}$ of their parent atom U_{eq} in case of methyl groups. All non-hydrogen atoms were refined anisotropically by full-matrix least-squares. The structure exhibits chemical disorder of 95% of the major compound (complex **6**) and 5% of an impurity (complex **7**). Restraints to bond distances and thermal parameters were required for the CH_2Cl_2 binding to Ir.

Table 2.1. Crystal data and structure refinement for **6** and **7**.

Empirical formula	$C_{21} H_{30} B I Ir N_7 O_2$, $0.05(C_{16} H_{24} B Cl_2 I_2 Ir)$	
Formula weight	831.64	
Temperature	110(2) K	
Wavelength	0.71073 Å	
Crystal system	Orthorhombic	
Space group	P b c a	
Unit cell dimensions	a = 17.220(3) Å	α = 90°.
	b = 16.014(2) Å	β = 90°.
	c = 20.716(3) Å	γ = 90°.
Volume	5712.7(14) $Å^3$	
Z	8	
Density (calculated)	1.934 Mg/m^3	
Absorption coefficient	6.038 mm^{-1}	
F(000)	3195	
Crystal size	0.15 x 0.09 x 0.03 mm^3	
Theta range for data collection	1.97 to 28.37°.	
Index ranges	-23<=h<=22, -21<=k<=21, -27<=l<=27	
Reflections collected	279723	
Independent reflections	7128 [R(int) = 0.0677]	
Completeness to theta = 25.00°	100.0 %	
Max. and min. transmission	0.8396 and 0.4645	
Refinement method	Full-matrix least-squares on F^2	
Data / restraints / parameters	7128 / 31 / 367	
Goodness-of-fit on F^2	1.090	
Final R indices [I>2sigma(I)]	R1 = 0.0229, wR2 = 0.0453	
R indices (all data)	R1 = 0.0374, wR2 = 0.0509	
Largest diff. peak and hole	1.011 and -0.861 $e.Å^{-3}$	

Details of Solid State Structure Determination of 13.

A yellow-green needle, measuring 0.17 x 0.02 x 0.02 mm^3 was mounted on a glass capillary with oil. Data was collected at -173 °C on a Bruker APEX II single crystal X-ray diffractometer, Mo-radiation. Crystal-to-detector distance was 40 mm and exposure time was 10 seconds per degree for all sets. The scan width was 0.5^o. Data collection was 100% complete to 25^o in ϑ. A total of 53947 (merged) reflections were collected covering the indices, h = -9 to 9, k = -29 to 29, l = -14 to 14. 4267 reflections were symmetry independent and the R_{int} = 0.0337 indicated that the data was brilliant (average quality 0.07). Indexing and unit cell refinement

indicated a primitive monoclinic lattice. The space group was found to be P 2_1/n (No.14). The data was integrated and scaled using SAINT, SADABS within the APEX2 software package by Bruker.[26]

Solution by direct methods (SHELXS, SIR97[27]) produced a complete heavy atom phasing model consistent with the proposed structure. The structure was completed by difference Fourier synthesis with SHELXL97.[28,29] Scattering factors are from Waasmair and Kirfel.[30] Hydrogen atoms were placed in geometrically idealized positions and constrained to ride on their parent atoms with C---H distances in the range 0.95-1.00 Angstrom. Isotropic thermal parameters U_{eq} were fixed such that they were $1.2U_{eq}$ of their parent atom Ueq for CH's and $1.5U_{eq}$ of their parent atom U_{eq} in case of methyl groups. All non-hydrogen atoms were refined anisotropically by full-matrix least-squares. Hydrogen atom positions on double bonded carbon were refined with isotropic thermal parameters. The dimer exhibits centro-symmetry with two dimers per monoclinic unit cell.

Table 2.2. Crystal data and structure refinement for **13**.

Empirical formula	$C_{28}H_{48}Cl_2Ir_2$	
Formula weight	839.96	
Temperature	100(2) K	
Wavelength	0.71073 Å	
Crystal system	Monoclinic	
Space group	P 2_1/n	
Unit cell dimensions	a = 6.7988(2) Å	α = 90°.
	b = 20.5391(7) Å	β = 105.7250(10)°.
	c = 10.2299(3) Å	γ = 90°.
Volume	1375.05(7) Å^3	
Z	2	
Density (calculated)	2.029 Mg/m^3	
Absorption coefficient	9.877 mm^{-1}	
F(000)	808	
Crystal size	0.17 x 0.02 x 0.02 mm^3	
Theta range for data collection	1.98 to 30.75°.	
Index ranges	-9<=h<=9, -29<=k<=29, -14<=l<=14	
Reflections collected	53947	
Independent reflections	4267 [R(int) = 0.0337]	
Completeness to theta = 25.00°	100.0 %	
Max. and min. transmission	0.8269 and 0.2845	
Refinement method	Full-matrix least-squares on F^2	
Data / restraints / parameters	4267 / 0 / 147	
Goodness-of-fit on F^2	1.157	
Final R indices [I>2sigma(I)]	R1 = 0.0197, wR2 = 0.0338	
R indices (all data)	R1 = 0.0248, wR2 = 0.0348	
Largest diff. peak and hole	1.704 and -0.916 e.Å^{-3}	

Notes to Chapter 2

---

1. (a) Shilov, A. E.; Shul'pin, G. B. *Chem*. *Rev*. **1997**, *97*, 2879. (b) Fekl, U.; Goldberg, K. I. *Adv*. *Inorg*. *Chem*. **2003**, *54*, 259. (c) *Activation and Functionalization of C-H Bonds*; Goldberg, K. I.; Goldman, A. S., Eds.; ACS Symposium Series 885; American Chemical Society: Washington, DC, 2004. (d) Lersch, M; Tilset, M. *Chem*. *Rev*. **2005**, *105*, 2471. (e) West, N. M.; Templeton, J. L. *Can*. *J*. *Chem*. **2009**, *87*, 288. (f) Labinger, J. A.; Bercaw, J. E. *Top*. *Organomet*. *Chem*. **2011**, *35*, 29. (g) Hashiguchi, B. G.; Bischof, S. M.; Konnick, M. M.; Periana, R. A. *Acc*. *Chem*. *Res*. **2012**, *45*, 885.

2. (a) Janowicz, A. H.; Bergman, R. G. *J*. *Am*. *Chem*. *Soc*. **1982**, *104*, 352. (b) Periana, R. A.; Bergman, R. G. *J*. *Am*. *Chem*. *Soc*. **1986**, *108*, 7332. (c) Arndtsen, B. A.; Bergman, R. G. *Science* **1995**, *270*, 1970. (d) Jones, W. D. *Science* **2000**, *287*, 1942. (e) Labinger, J. A.; Bercaw, J. E. *Nature* **2002**, *417*, 507. (f) Hartwig, J. F. *Chem*. *Soc*. *Rev*. **2011**, *40*, 1992. (g) Choi, J.; MacArthur, A. H. R.; Brookhart, M.; Goldman, A. S. *Chem*. *Rev*. **2011**, *111*, 1761.

3. (a) Heinekey, D. M.; Millar, J. M.; Koetzle, T. F.; Zilm, K. W. *J*. *Am*. *Chem*. *Soc*. **1990**, *112*, 909. (b) Tanke, R. S.; Crabtree, R. H. *Organometallics* **1991**, *10*, 415. (c) Gutierrez-Puebla, E.; Monge, A.; Paneque, M.; Poveda, M. L.; Toboada, S.; Trujillo, M.; Carmona, E. *J*. *Am*. *Chem*. *Soc*. **1999**, *121*, 346. (d) Alaimo, P. J.; Bergman, R. G. *Organometallics* **1999**, *18*, 2707. (e) Klei, S. R.; Tilley, T. D.; Bergman, R. G. *J*. *Am*. *Chem*. *Soc*. **2000**, *122*, 1816. (f) Webster, C. E.; Hall, M. B. *Coord*. *Chem*. *Rev*. **2003**, *238-239*, 315 and references within. (h) Hartwig, J. F.; Cook, K. S.; Hapke, M.; Incarvito, C. D.; Fan, Y.; Webster, C. E.; Hall, M. B. *J*. *Am*. *Chem*. *Soc*. **2004**, *127*, 2538.

4. (a) Park, S.; Brookhart, M. *J*. *Am*. *Chem*. *Soc*. **2012**, *134*, 640. (b) Karshtedt, D.; Bell, A. T.; Tilley, T. D. *Organometallics*, **2006**, *25*, 4471.

5. Pettinari, C. *Scorptionates II: Chelating Borate Ligands*; Imperial College Press: London, 2008.

6. Slugovc, C.; Padilla-Martinez, I.; Sirol, S.; Carmona, E. *Coord*. *Chem*. *Rev*. **2001**, *213*,129.

7. Tellers, D. M.; Skoog, S. J.; Bergman, R. G.; Gunnoe, T. B.; Harman, W. D. *Organometallics* **2000**, *19*, 2428.

8. Wagner, T.; Kolle, U. *Chem*. *Ber*. **1995**, *128*, 911.

9. May, S.; Reinsalu, P.; Powell, J. *Inorg*. *Chem*. **1980**, *19*, 1582.

10. Ogo, S.; Makihara, N.; Watanabe, Y. *Organometallics* **1999**, *18*, 5470.

11. Fernandez, M. J.; Rodriquez, M. J.; Oro, L. A.; Lahoz, F. J. *J*. *Chem*. *Soc*., *Dalton Trans*. **1989**, *10*, 2073.

12. Dr. Lisa Park-Gerke previously synthesized complex **2** using the reported procedure and provided 300 mg for this work.

13. (a) Tanke, R. S.; Crabtree, R. H. *Inorg*. *Chem*. **1989**, *28*, 3444. (b) Alvarado, Y.; Boutry, O.; Gutierrez, A. M.; Nicasio, M. C.; Poveda, M. L.; Perez, P. J.; Ruiz, C.; Bianchini, C.; Carmona, E. *Chem*. *Eur*. *J*. **1997**, *3*, 860.

14. Crawforth, C. M.; Burling, S.; Fairlamb, I.; Kapdi, A. R.; Taylor, R.; Whitwood, A. C. *Tetrahedron* **2005**, *61*, 9736.

15. Bercaw, J. E.; Hazari, N.; Labinger, J. A. *Organometallics* **2009**, *28*, 5489.

16. Cationic Rh complexes of this type have been reported in the literature previously using COD: Clark, D. T.; Miekuz, M.; Sayer, B. G.; McCarry, B. E.; McGlinchey, M. J. *Organometallics* **1987**, *6*, 2201.

17. All raw GC MS data was deconvoluted using a benzene H/D exchange worksheet reported by Periana and coworkers: Young, K. J. H.; Meier, S. K.; Gonzales, J. M.; Oxgaard, J.; Goddard III, W. A.; Periana, R. A. *Organometallics* **2006**, *25*, 4734.

18. Similar η^6-arene complexes have been reported previously in the literature: (a) Bennett, M. A.; McMahon, I. J.; Pelling, S.; Brookhart, M.; Lincoln, D. M. *Organometallics* **1992**, *11*, 127. (b) Green, M.; Kuc, T. A. *J. Chem. Soc., Dalton Trans*. **1972**, *7*, 832.

19. (a) Ryabov, A. D. *Chem. Rev*. **1990**, *90*, 403. (b) Davies, D. L.; Donald, S. M. A.; Macgregor, S. A. *J. Am. Chem. Soc*. **2005**, *127*, 13754. (c) Davies, D. L.; Donald, S. M. A.; Al-Duaij, O.; Macgregor, S. A.; Polleth, M. *J. Am. Chem. Soc*. **2006**, *128*, 4210. (d) Garcia-Cuadrado, D.; Braga, A. A. C.; Maseras, F.; Echavarren, A. M. *J. Am. Chem. Soc*. **2006**, *128*, 1066. (e) Lafrance, M.; Rowley, C. N.; Woo, T. K.; Fagnou, K. *J. Am. Chem. Soc*. **2006**, *128*, 8754. (f) Ito, J.; Nishiyama, H. *Eur. J. Inorg. Chem*. **2007**, 1114. (g) Ess, D. H.; Bischof, S. M.; Periana, R. A.; Goddard III, W. A. G. *Organometallics* **2008**, *27*, 6440. (h) Li, L.; Brennessel, W. W.; Jones, W. D. *Organometallics* **2009**, *28*, 3492. (i) Boutadla, Y.; Al-Duaij, O.; Davies, D. L.; Griffith, G. A.; Singh, K. *Organometallics* **2009**, *28*, 433. (j) Young, K. J. H.; Oxgaard, J.; Ess, D. H.; Meier, S. K.; Stewart, T.; Goddard III, W. A. G.; Periana, R. A. *Chem. Commun*. **2009**, 3270. (k) Bischof, S. M.; Ess, D. H.; Meier, S. K.; Oxgaard, J.; Nielsen, R. J.; Bhalla, G.; Goddard III, W. A. G.; Periana, R. A. *Organometallics* **2010**, *29*, 742. (l) Ito, J.; Kaneda, T.; Nishiyama, H. *Organometallics* **2012**, *31*, 4442. (m) Allen, K. E.; Heinekey, D. M.; Goldman, A. S.; Goldberg, K. I. *Organometallics* **2013**, *32*, 1579.

20. Winkhaus, G.; Singer, H. *Chem. Ber*. **1966**, *99*, 3619.

21. Onderdelinden, A. L.; van der Ent, A. *Inorg. Chim. Acta* **1972**, *6*, 420.

22. (a) Abel, E. W.; Bennett, M. A.; Wilkinson, G. *J*. *Chem*. *Soc*. **1959**, 3178. (b) Giordano, G.; Crabtree, R. H. *Inorg*. *Synth*. **1979**, *19*, 218. (c) Cotton, F. A.; Lahuerta, P.; Sanau, M.; Schwotzer, W. *Inorg*. *Chim*. *Acta* **1986**, *120*, 153. (d) van der Ent, A.; Onderdelinden, A. L.; Schunn, R. A. *Inorg*. *Synth*. **1990**, *28*, 90. (e) Yamagata, T.; Najakima, K.; Arimitsu, K.; Iseki, A.; Tani, K. *Acta Cryst*. **2008**, *64*, 579.

23. Nelson, S. M.; Sloan, M.; Drew, M. G. B. *J*. *Chem*. *Soc*., *Dalton Trans*. **1973**, 2195.

24. Muller, J.; Hahnlein, W.; Passon, B. *Z*. *Naturforsch*. *Pt*. *B* **1982**, *12*, 1573.

25. Trofimenko, S. *J*. *Am*. *Chem*. *Soc*. **1967**, *89*, 6288.

26. Bruker (**2007**) APEX2 (Version 2.1-4), SAINT (version 7.34A), SADABS (version 2007/4), BrukerAXS Inc, Madison, Wisconsin, USA.

27. (a) Altomare, A.; Burla, C.; Camalli, M.; Cascarano, L.; Giacovazzo, C.; Guagliardi, A.; Moliterni, A. G. G.; Polidori, G.; Spagna, R. *J*. *Appl*. *Cryst*. **1999**, *32***,** 115-119. (b) Altomare, A.; Cascarano, G.; Giacovazzo, C.; Guagliardi, A. *J*. *Appl*. *Cryst*. **1993**, *26*, 343.

28. Sheldrick GM. **(1997)** SHELXL-97, Program for the Refinement of Crystal Structures. University of Göttingen, Germany.

29. Mackay, S.; Edwards, C.; Henderson, A.; Gilmore, C.; Stewart, N.; Shankland, K.; Donald, A. *MaXus: a computer program for the solution and refinement of crystal structures from diffraction data*. University of Glasgow, Scotland, **1997**.

30. Waasmaier, D.; Kirfel, A. *Acta Crystallogr*. A. **1995**, *51*, 416.

Chapter 3: Alkane Dehydrogenation by (Phebox)Rh^{III} and Ir^{III} Complexes

Introduction

Methods for the conversion of alkanes directly to alkenes, alcohols, amines and other valuable products would have far-reaching applications in the production of fuels and chemicals. To this end, there has been intensive study of transition metal complexes that can selectively activate and functionalize alkane C-H bonds.[1] A particular challenge is to discover metal species that can remain active in the presence of the functionalized products and water. The active site needed for C-H bond activation is often inhibited by coordination of the oxidized product or water.[2]

Several years ago, Nishiyama reported that the Rh^{III} complex (^{dm}Phebox)$Rh(OAc)_2(H_2O)$ (**1a**) (^{dm}Phebox = 2,6-bis(4,4-dimethyloxazolinyl)-3,5-dimethylphenyl) activated C-H bonds of substituted arenes (C_6H_5X; X = H, CH_3, CF_3, OCH_3, $COCH_3$, Cl) to form Rh^{III}-aryl complexes and acetic acid.[3] We have examined the reactivity of the closely related (^{iPr}Phebox)$Rh(OAc)_2(OH_2)$ (**1b**) (^{iPr}Phebox = 2,6-bis(4,4-isopropyloxazolinyl)-3,5-dimethylphenyl) towards alkanes. We have also examined the reactivity of the analogous complex, (^{dm}Phebox)$Ir(OAc)_2(OH_2)$ (**2a**),[4] towards arenes and alkanes to provide a comparison to the C-H activation studies with the Rh analogue. During our study of the Ir^{III} system, Nishiyama and coworkers also reported on the reactivity of (**2a**) towards arene and alkane C-H bonds.[5] Similar to the Nishiyama group, we found that benzene activation yields the Ir-phenyl complex, but in contrast to their results we observed alkane functionalization rather than simply alkane activation. In the absence of added potassium carbonate and at higher temperatures alkane dehydrogenation occurred, thus resulting in a novel Ir^{III}-hydride complex and free alkene.

The differences between our system and that of Nishiyama have been investigated and provide valuable insight into the mechanism of C-H bond activation and functionalization by (Phebox)Ir complexes. Alkane functionalization by **2a** differs significantly from the previous reports of alkane dehydrogenation reactions at Ir and Pt centers, wherein metal centers in low-valent oxidation states are proposed to activate the C-H bonds.[6]

Results and Discussion

Complex **1b** was reported previously to undergo C-H activation of benzene over the course of 6 days at 90 °C.[3] Alkane activation by **1b** has not been previously reported. Initially, we examined the ability of **1b** to activate the C-H bonds of cyclohexane and *n*-octane. Cyclohexane was chosen as a substrate as all of the C-H bonds are the same, while *n*-octane contains terminal and internal C-H bonds. Heating a cyclohexane-d_{12} solution of **1b** at 150 °C for 10 days resulted in the formation of multiple (^{iPr}Phebox)Rh containing species and free ^{iPr}Phebox ligand precursor by ^{1}H NMR spectroscopy along with a significant amount of Rh black (Scheme 3.1). When the reaction was performed in *n*-octane, octene was obtained in 22% yield via GC analysis. The formation of alkene suggested that C-H activation followed by *β*–hydride elimination had occurred. When the reaction was monitored by ^{1}H NMR spectroscopy, a hydride signal corresponding to the formation of a Rh hydride complex was not observed. The ^{1}H NMR spectrum obtained at the end of the reaction demonstrated the formation of the same two Rh containing products. Two different singlets were observed for the ^{iPr}Phebox-aryl protons of the two different pincer ligands. Additionally, free ^{iPr}Phebox ligand was observed by ^{1}H NMR spectroscopy. The Rh products observed in the reactions with cyclohexane-d_{12} and *n*-octane were identical by ^{1}H NMR spectroscopy. The identification of these products using NMR spectroscopy was difficult because of the complex spectra obtained.

Scheme 3.1

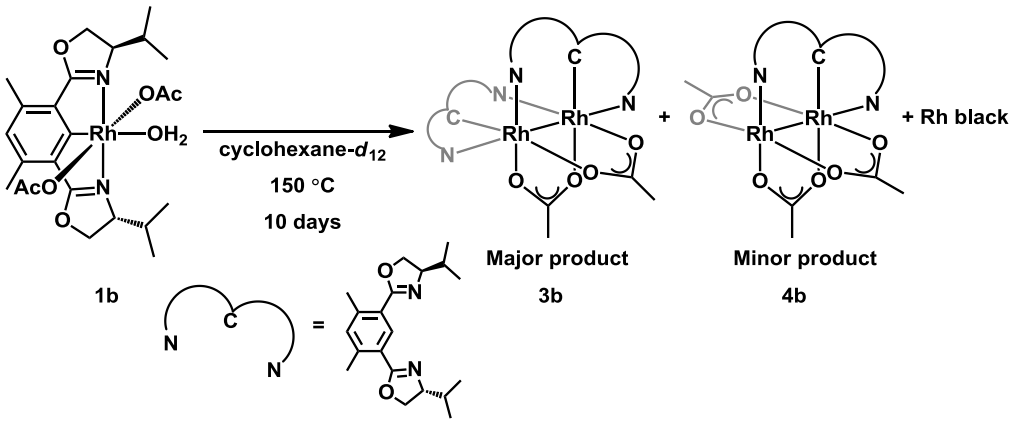

The Rh products were separated via column chromatography resulting in isolation of orange and green compounds. X-ray quality crystals of the orange and green products were grown from a pentane solution and a CH_2Cl_2 solution layered with pentane, respectively, at -15 °C. The structure of the orange product was determined to be the symmetrical complex, $[(^{iPr}\text{Phebox})\text{RhOAc}]_2$ (**3b**) (Figure 3.1). Each Rh^{II} center of **3b** is coordinated to two ^{iPr}Phebox ligands and bridged by two OAc ligands. The green product was determined to be the dimer, $(^{iPr}\text{Phebox})Rh_2(OAc)_3$ (**4b**) (Figure 3.2), using X-ray crystallographic analysis. One Rh^{II} center in **4b** is coordinated to the C_{aryl} and one N substituent of the ^{iPr}Phebox ligand. The other N substituent of the same pincer ligand is coordinated to the second Rh^{II} center. Three bridging OAc ligands are present in the molecule. It is worth noting that the Rh^{II} center bound to only to a N substituent of the pincer ligand has a square planar geometry, while the saturated Rh center exhibits an octahedral geometry. The Rh^{II}-Rh^{II} bonds lengths in **3b** and **4b** were 2.4650(9) and 2.4301(8) Å, respectively. These lengths fall within the range of 2.4-2.8 Å reported in the literature for neutral Rh^{II}-Rh^{II} dimers.[7] It is also possible that complex 4b exists as a RhI-RhIII

dimer. One Rh center contains an octahedral geometry, while the geometry of the second Rh center is square planar.

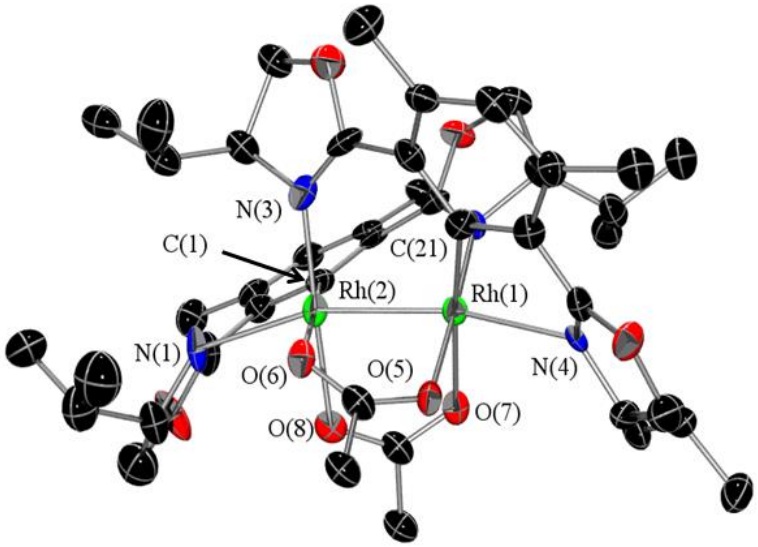

Figure 3.1. ORTEP diagram of [(^{iPr}Phebox)Rh(OAc)]$_2$ (**3b**) (thermal ellipsoids at 50% probability, H atoms omitted for clarity). Selected bond distances (Å) and angles (deg): Rh(1)-Rh(2) = 2.4650(9), Rh(1)-C(21) = 1.986(7), Rh(1)-N(2) = 2.010(6), Rh(1)-N(4) = 2.265(6), Rh(1)-O(5) = 2.065(5), Rh(1)-O(7) = 2.170(5), Rh(2)-C(1) =1.987(8), Rh(2)-N(1) = 2.256(6), Rh(2)-N(3) = 2.025(6), Rh(2)-O(6) = 2.159(5), Rh(2)-O(8) = 2.065(5), N(1)-Rh(2)-Rh(1) = 163.92(16), N(2)-Rh(1)-O(5) = 177.2(2), C(21)-Rh(1)-O(7) = 172.4(3), C(21)-Rh(1)-N(4) = 80.9(3), O(6)-Rh(2)-N(1) = 93.8(2), N(2)-Rh(1)-N(4) = 104.3(3), N(3)-Rh(2)-N(1) = 102.8(2), C(1)-Rh(2)-N(3) = 87.9(3), C(1)-Rh(2)-O(6) = 173.8(3), N(3)-Rh(2)-O(6) = 96.7(2).

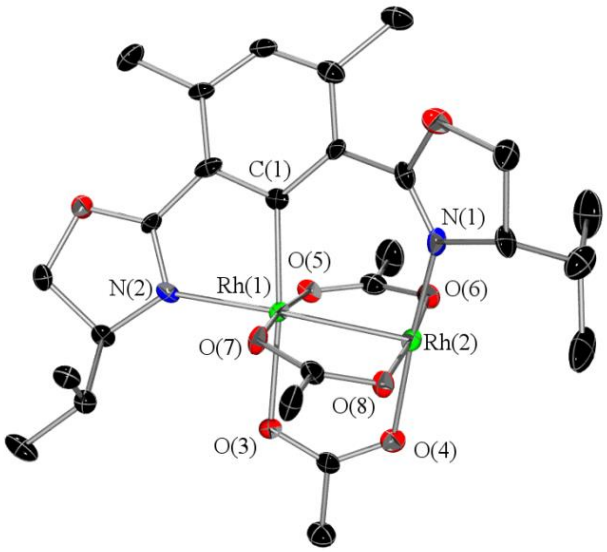

Figure 3.2. ORTEP diagram of [(^{iPr}Phebox)Rh(OAc)]$_2$ (**4b**) (thermal ellipsoids at 50% probability, H atoms omitted for clarity). Selected bond distances (Å) and angles (deg): Rh(1)-C(1) = 2.014(7), Rh(2)-N(1) = 1.9474(8), Rh(1)-N(2) = 2.073(5), Rh(1)-O(3) = 2.169(5), Rh(2)-O(4) = 2.039(6), Rh(1)-O(5) = 2.058(5), Rh(2)-O(6) = 2.034(6), Rh(1)-O(7) = 2.044(5), Rh(2)-O(8) = 2.059(5), Rh(1)-Rh(2) = 2.4301(8), O(3)-Rh(1)-Rh(2) = 84.87(13), C(1)-Rh(1)-Rh(2) = 101.5(2), N(2)-Rh(1)-O(3) = 92.7(2), C(1)-Rh(1)-O(3) = 171.6(2), C(1)-Rh(1)-O(7) = 96.7(2), N(1)-Rh(2)-O(4) = 176.0(3), O(4)-Rh(2)-O(8) = 91.6(2).

Despite the instability of the Rh complex at high temperatures, the Ir analogue was proposed to exhibit greater stability at the elevated temperatures required for C-H activation in this system. Intermolecular benzene C-H bond activation resulted when solutions of **2a** or (^{iPr}Phebox)Ir(OAc)$_2$(OH$_2$) (**2b**) were heated at 100 °C for 1.5 h. The corresponding Ir-phenyl products, (^{R}Phebox)Ir(OAc)(Ph) (**5a, b**), were formed in quantitative and 78 % yields respectively (eq. 3.1). Complexes **5a, b** were characterized using ^{1}H and ^{13}C NMR spectroscopy, EA, and X-ray crystallography (Figure 3.3). Nishiyama and coworkers also reported the X-ray structure of **5a** and our data is in agreement with their published structure. When benzene-d_6 was used as the substrate, the expected ^{1}H NMR signals for the product **5a-*d*$_5$**, were observed in solution; however, the signal corresponding to the methyl group of coordinated acetate (2.08 ppm) was quite broad. A broad signal at 1.56 ppm, attributed to acetic acid, was

also present. In contrast, when **5a** was isolated and then examined by ^{1}H NMR spectroscopy in benzene-d_6 (with no acetic acid present), the acetate signal at 2.07 ppm was very sharp. The addition of 1 equiv. of acetic acid to the benzene-d_6 solution of isolated **5a** at room temperature resulted in broadening of the acetate signal and the appearance of a second broad signal at 1.6 ppm for the added acetic acid. The ^{1}H NMR spectrum of **5a** was otherwise unchanged. At 40 °C the two broad acetate signals coalesce, resulting in a single resonance at 1.79 ppm. These observations indicate that the bound acetate ligand in complex **5a** exchanges with free acetic acid on the NMR timescale. The signals for the methyl groups of the oxazoline rings do not coalesce, indicating that the phenyl group remains at a fixed coordination site at the Ir^{III} center during the acetate/acetic acid exchange.

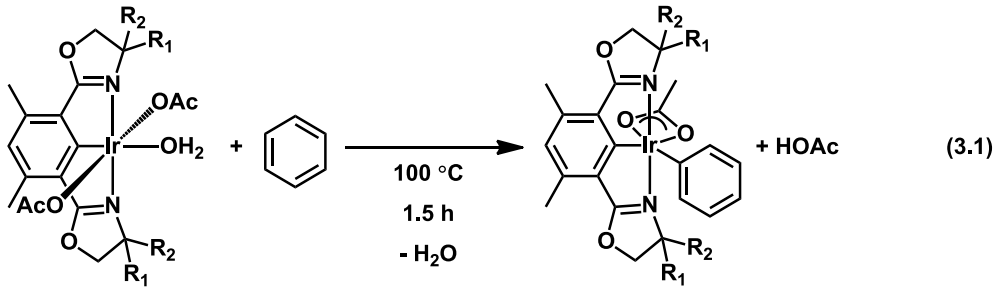

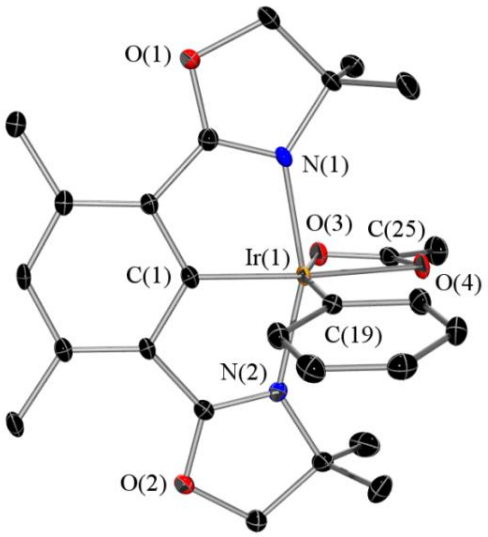

Figure 3.3. ORTEP diagram of (^{dm}Phebox)Ir(OAc)(Ph) (**5a**) (thermal ellipsoids at 50% probably, H atoms omitted for clarity). Selected bond distances (Å) and angles (deg): Ir(1)-C(1) = 1.923(2), Ir(1)-N(1) = 2.045(2), Ir(1)-N(2) = 2.046(2), Ir(1)-O(3) = 2.2410(18), Ir(1)-O(4) = 2.2348(17), Ir(1)-C(19) = 2.009(2), N(1)-Ir(1)-N(2) = 158.57(9), C(1)-Ir(1)-O(4) = 166.25(8). Bond lengths and angles obtained for complex **5a** agree with those reported by Nishiyama and coworkers.[5]

Nishiyama and co-workers reported that thermolysis of **2a** in neat heptane or octane solutions at 160 °C, over 70 h, in the presence of K_2CO_3 results in formation of (^{dm}Phebox)Ir(OAc)(*n*-alkyl) in 80 % and 78 % isolated yield, respectively.[5] We found that when **2a** was heated in neat *n*-octane at 150 °C (no added K_2CO_3), no reaction was observed even after heating for 6 days. When the temperature was increased to 180 °C, a small amount of a new Ir-hydride species was observed after 5 days. Finally, when the reaction mixture was heated at 200 °C for 72 h the new complex, (^{dm}Phebox)Ir(OAc)(H) (**6a**) was obtained in 96% yield (eq. 3.2). Removal of the volatiles from the reaction mixture afforded **6a** as a light orange solid, which was characterized by ^{1}H and ^{13}C NMR spectroscopy, single crystal X-ray diffraction and elemental analysis. In the ^{1}H NMR spectrum (benzene-d_6), the hydride resonance was clearly observed as a singlet at -33.8 ppm. Hydride signals for five-coordinate Ir^{III} hydrides are often found in this high upfield region,[8] while six-coordinate hydrides typically appear farther downfield.[8a,9] The

high upfield shift for the hydride in **6a** may indicate that the acetate is κ^1 in solution or that the structure is distorted significantly from an octahedral geometry. Two doublets (3.79 and 3.84 ppm, $^1J_{HH}$ = 8.3 Hz) are observed for the inequivalent methylene protons of the ^{dm}Phebox oxazoline rings and two singlets for the inequivalent methyl groups (1.29 and 1.33 ppm). The acetate resonance appears as a singlet at 2.06 ppm. Addition of one equivalent of acetic acid to isolated **6a** resulted in loss of the acetate signal and the appearance of one broad resonance in the ^{1}H NMR spectrum at 1.75 ppm corresponding to an averaged signal for the acetate ligand and acetic acid. These observations suggest an interaction of acetic acid with the acetate ligand similar to that observed with **5a**.

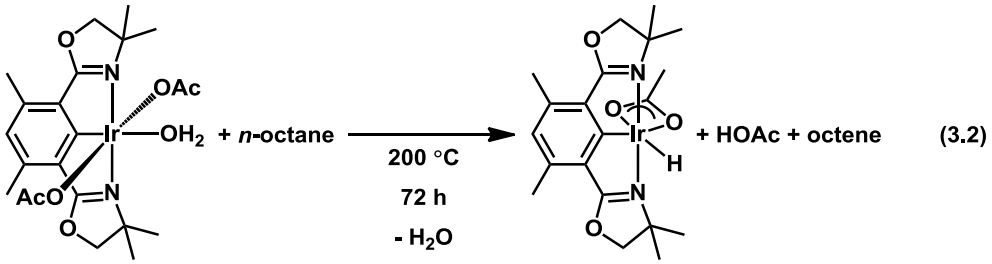

The X-ray data obtained for complex **6a** revealed a distorted octahedral structure in the solid state. The hydride ligand is located approximately trans to one oxygen of the κ^2-acetate ligand; the H(1)-Ir(1)-O(3) angle is 164.6(2)° rather than 180° (Figure 3.5). The C(1)-Ir(1)-O(4) angle is comparable at 167.92(9)° and the Ir-O bond distances are quite similar (2.251(2) and 2.243(2) Å), suggesting that the *trans*-effects of the hydride and aryl carbon of the ^{dm}Phebox ligand are comparable. The Ir-O bond distances are also comparable to the Ir-O distances observed in **2a**.[5] The Ir-H bond length of **6a** was determined to be 1.50(3) Å, which is within the

typical range for pincer Ir^{III}-H bond lengths (1.5-1.6 Å)[10] and is in close agreement with the Ir-H bond distance reported for (^{tBu}PCP)Ir(H)(κ^2-O,ONCH$_2$) (1.52(2) Å).[10c]

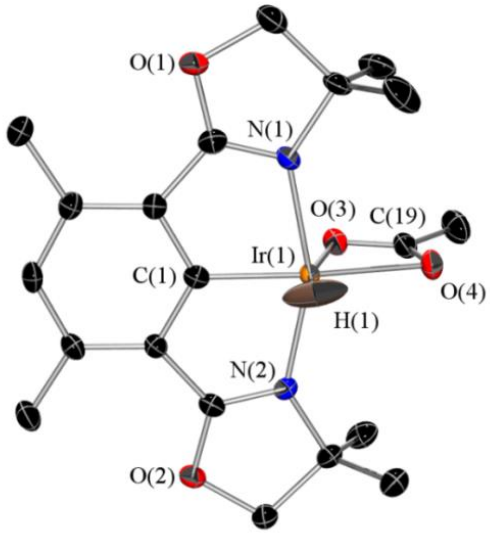

Figure 3.4. ORTEP diagram of (^{dm}Phebox)Ir(OAc)(H) (**6a**) (thermal ellipsoids at 50% probability, H atoms omitted for clarity). Selected bond distances (Å) and angles (deg): Ir(1)-C(1) = 1.923(2), Ir(1)-N(1) = 2.043(2), Ir(1)-N(2) = 2.055(2), Ir(1)-O(3) = 2.251(2), Ir(1)-O(4) = 2.243(2), Ir(1)-H(1) = 1.50(3), N(1)-Ir(1)-N(2) = 158.30(8), C(1)-Ir(1)-O(4) = 167.92(9), C(1)-Ir(1)-O(3) = 109.66(8), C(1)-Ir(1)-H(1) = 85.2(12).

Observation of the hydride species **6a** suggested that *β*-hydride elimination had occurred from an Ir-octyl complex. Indeed, we were able to observe the expected organic product of the reaction, octene, via GC analysis. After 72 h at 200 °C, a mixture of octenes, composed of *trans*-4-octene (20%), *trans*-3-octene (28%), *trans*-2-octene (32%), *cis*-3-octene (8%), and *cis*-2-octene (11%) was found (Scheme 3.2, Table 3.1). The product that would be obtained from terminal C-H bond activation, 1-octene, was not observed. The absence of this isomer was somewhat surprising given that Nishiyama and co-workers reported that only the primary *n*-alkyl product was observed in their reactions. In order to determine if 1-octene was a kinetic product

that was subsequently consumed under the conditions for dehydrogenation, the distribution of octene was monitored as a function of time (Table 3.1).

Scheme 3.2

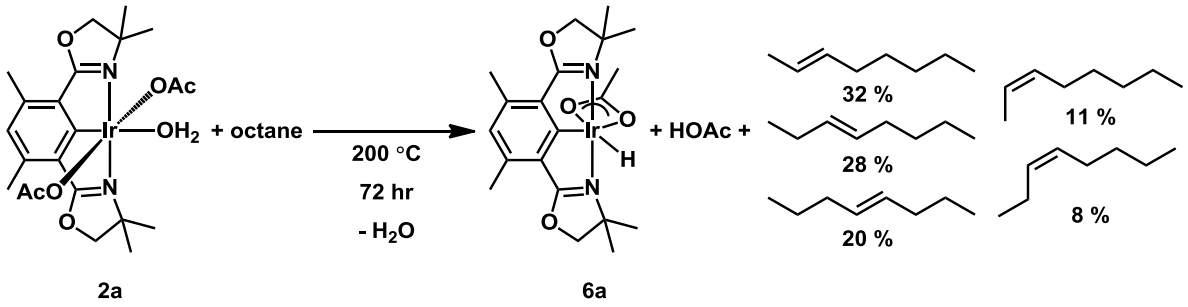

Table 3.1. Octene distribution as a function of time in the reaction of **2a** with octane[a].

Octene[b]	3 h (%)	6 h (%)	24 h (%)	48 h (%)	72 h (%)	120 h (%)
1-octene	20(2)	20(3)	6(1)	1(1)	0	0
trans-4-octene	0	0	5(1)	16(1)	20(1)	20(1)
trans-3-octene	0.6(1)	3(1)	13(2)	23(1)	28(1)	29(2)
trans-2-octene	6(1)	15(2)	25(1)	26(1)	32(1)	29(2)
cis-3-octene	0.5(1)	1(1)	4(1)	6(1)	8(1)	8(1)
cis-2-octene	2(1)	6(1)	10(1)	9(1)	11(1)	11(1)
Total octene	**29(3)**	**45(3)**	**63(4)**	**80(2)**	**98(1)**	**94(5)**

[a]All reactions run under a nitrogen atmosphere at 200 °C. [b]Yields determined by GC analysis using a mesitylene internal standard.

When the reaction of **2a** with octane was stopped after 3 h, a 20% yield of 1-octene (by far the major product considering ca. 30% conversion) was determined by GC analysis (Table 3.1). While at early reaction times (3-6 h), 1-octene was present as the major isomer, its concentration slowly decreased over time, until at 72 h 1-octene was no longer observed. The decrease in the concentration of 1-octene tracked with the increase in the concentrations of the four internal isomers (Table 3.1). The absence of the kinetic product of octane dehydrogenation at 72 h could be explained by isomerization of 1-octene by **6a**.[6j] Heating a 0.1 M solution of 1-

octene and 5.5 mol % **6a** in octane at 200 °C for 24 h resulted in isomerization of 1-octene to the same distribution of octene observed after 72 h of heating **2a** in *n*-octane, thus confirming that complex **6a** was an effective isomerization catalyst (Table 3.1). Together these experiments demonstrate that *n*-octane is dehydrogenated regioselectively to give 1-octene, followed by 1-octene isomerization by **6a**. Generation of 1-octene is presumed to occur via formation of the Ir *n*-alkyl derivative, (^{dm}Phebox)Ir(OAc)(*n*-octyl) (**7a**), in accord with Nishiyama's observations.[5] In support of this hypothesis when an octane solution of **7a** was heated at 200 °C for 24 hours, ^{1}H NMR spectroscopic analysis revealed conversion to the hydride complex **6a**.

An issue with the well known (^{R}PCP)Ir (R = alkyl) dehydrogenation systems which activate C-H bonds by oxidative addition to Ir^I is that the reactions are inhibited by nitrogen, water, and/or the alkene product.[6f,11] Nitrogen and alkenes coordinate to the open site at the Ir^I center blocking the site needed for alkane C-H activation. In the case of water, oxidative addition to the low valent Ir^I center is observed.[11] Roddick utilized fluorinated alkyl substituents on the PCP ligand to produce an Ir alkane dehydrogenation system that was not affected by nitrogen and water, and was more resistant to alkene inhibition than the non-fluorinated analog.[6j] Since **2a** activates C-H bonds by a different mechanism involving an Ir^{III} center, we were interested in assessing the effect of nitrogen, water, and alkenes on the octane dehydrogenation reaction. When solutions of octane and **2a** were degassed thoroughly prior to heating, the yield of octene was determined to be 30% (Table 3.2). In comparison, heating **2a** in octane under nitrogen resulted in a 29% yield of octene after 3 h. The nearly identical yields of these reactions indicate that nitrogen does not inhibit octane dehydrogenation by **2a**. The addition of 1-hexene (73 mM, 10 equiv. relative to **2a**) to the reaction mixture prior to heating resulted in a 33 % octene yield. Thus, olefin also does not inhibit the dehydrogenation reaction and the long

reaction time required to reach complete conversion is not due to product inhibition. When alkane dehydrogenation was performed with **2a** using a water-saturated octane solution (120 equiv. H_2O compared to **2a**), an increase in the yield of octene to 44% after 3 h was observed. Determination of the role of water in this system is currently under investigation. Overall, it is notable that C-H activation and functionalization by the Ir^{III} center of **2a** is not inhibited by the common small molecules, nitrogen, water, and alkene that have been found to adversely affect C-H activation at Ir^{I} centers.

Table 3.2. Octene yield obtained using **2a** and octane in the presence of various additives[a].

Additive	Octene % Yield
N_2	29(3)
none	30(3)
1-hexene (10 equiv.)	33(1)
H_2O (120 equiv.)	44(2)

[a]All reactions run in octane at 200 °C for 3 h. [b]Yields determined by GC analysis using mesitylene internal standard.

It is significant that during our study of alkane activation by complex **2a**, we did not observe the previously reported Ir-octyl species **7a**. Nishiyama and coworkers reported that they isolated **7a** from the reaction of **2a** with octane in the presence of one equivalent of K_2CO_3 and suggested that the addition of base stabilized 7**a** by reacting with the acetic acid generated from C-H cleavage.[12] Indeed we observed that if **7a** is treated with an equivalent of acetic acid, octane and **2a** are generated at 160 °C. In contrast, the Ir-Ph complex **5a** is generated in the presence of an equivalent of acetic acid. This difference is consistent with a thermodynamic advantage of aryl activation over alkane activation.[13] H/D exchange between benzene and various deuterated solvents (e. g. CD_3OD, TFA-*d*, and D_2O) was also not observed when **2a** was heated in these mixtures for prolonged periods at 100 °C; complex **5a** was formed in these reactions and the benzene showed no deuterium incorporation by GC/MS.[14]

If the role of the K_2CO_3 is to remove acetic acid product in the octane experiments to provide the driving force for the formation of **7a**, then reversible C-H activation would be expected in the absence of base. Indeed, when a solution of **7a** (1 mol %) in octane (1.4 mmol) with acetic acid-d_4 (1.8 mmol) was heated at 160 °C for 48 h, a small amount of deuterium incorporation into the terminal position of octane was observed (1.5(1)%; 1.5 TON (eq. 3.3)).

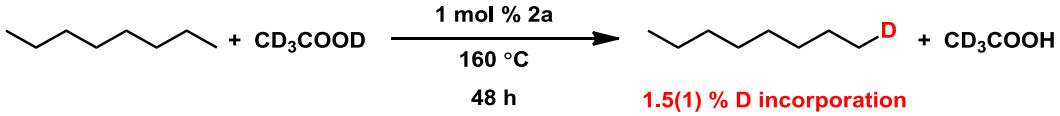

(3.3)

The amount of H/D exchanged observed is consistent with the slow octane activation reported by Nishyama where **2a** was heated for 70h at 160 °C in the presence of K_2CO_3 in order to produce good yields of **7a**.[5] Interestingly, we found that with weaker bases, $KHCO_3$ and K_2SO_4, incomplete conversion resulted with lower yields of the Ir-octyl product **7a** within the same 48 h reaction time at 160 °C. The results of a reaction containing 18-crown-6 (1,4,7,10,13,16-hexaoxacyclooctadecane) and K_2CO_3 were similar to that without the crown ether indicating that the cation does not play a significant role. When a soluble base, such as NEt_3, was utilized in the reaction complete consumption of **2a** was observed and the Ir-hydride complex **6a** was obtained in 67% yield by ^{1}H NMR analysis. Complex **7a** was not observed during the reaction or as a product. This result was exciting as it demonstrated that the reaction could be tuned by modifying the base utilized to remove acetic acid.

The role of the base in Nishyama's system is to trap the acetic acid released upon C-H activation to drive the equilibrium toward the alkyl product as shown in Scheme 3.3. An equilibrium favoring **2a** without base present was confirmed by the addition of acetic acid to a

sample of **7a** in octane which regenerated **2a** at 160 °C. The observation of H/D scrambling with acetic acid-d_4 at 160 °C supports that activation of an octane C-H bond by **2a** occurs reversibly at this temperature. In the absence of base, higher temperature can drive the C-H activation by promoting β-hydride elimination and formation of octene and **6a** (Scheme 3.3). Notably, it was demonstrated in an independent experiment that heating 7**a** in octane at 200 °C results in formation of **6a** and octene.

Scheme 3.3

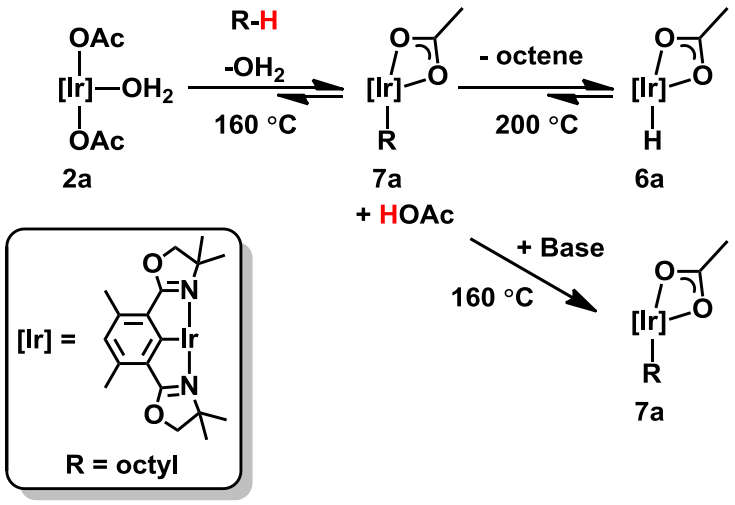

Conclusions

In summary, the Ir^{III} complex ^{dm}PheboxIr(OAc)$_2$(OH$_2$) (**2a**) was shown to dehydrogenate *n*-octane to yield octenes and the Ir^{III}-H complex **6a** in quantitative yield. In contrast, *n*-octane dehydrogenation by (^{iPr}Phebox)Rh(OAc)$_2$(OH$_2$) (**1b**) resulted in the formation of two different Rh^{II} dimers and a significant amount of Rh black and ^{iPr}Phebox. Alkane dehydrogenation by **2a** occurs at a higher temperature (200 °C) than the previously reported formation of the alkyl complex **7a**, which is observed in the presence of the base K_2CO_3 at 160 °C. The added base

acts to remove the acetic acid allowing observation of the alkyl complex **7a**. Higher temperatures promote β-hydride elimination from **7a** and generation of the Ir^{III} hydride **6a**. While catalytic alkane dehydrogenation was not observed, it is notable that this Ir^{III} C-H activation was not inhibited by nitrogen, water, or alkene, all significant issues for the ^{R}(PCP)Ir systems that activate C-H bonds by oxidative addition to Ir^{I}. Current efforts are focused on promoting catalytic alkane dehydrogenation with the (^{dm}Phebox)Ir system.

Experimental

General Considerations. Unless specified otherwise, all reactions were carried out under a dry nitrogen atmosphere using standard glovebox, Schlenk, or vacuum-line techniques. *n*-Octane, ≥ 98%, was used as received from Alfa Aesar. All other reagents were used as received. Solvents were purified before use: benzene and pentane were purified by passage through columns of activated alumina and molecular sieves. Deuterated solvents were purchased from Cambridge Isotope Laboratories. Benzene-d_6, cyclohexane-d_{12} were dried over sodium/benzophenone and dichloromethane-d_2, chloroform-d_1 were dried over CaH_2. NMR spectra were obtained on Bruker AV300 or AV500 MHZ spectrometers with chemical shifts (δ) reported in ppm downfield of tetramethylsilane. Octane dehydrogenation reactions were quantified using Agilent 7890A gas chromatograph with a 30 m x 0.32 mm Agilent GASPRO capillary column. ^{dm}Phebox, ^{iPr}Phebox, (^{iPr}Phebox)Rh$(OAc)_2(OH_2)$ (**1b**), and ^{R}PheboxIr$(OAc)_2(OH_2)$ (**2a** (R = CH_3), **2b** (R = ^{i}Pr, H) were prepared according to published procedures.[4] Elemental analyses were performed by Atlantic Microlab Inc. of Norcross, GA.

Synthesis, Characterization, and Reactivity

Rh dimers (3b, 4b). A sealable NMR tube was charged with **1b** (17.5 mg, 0.031 mmol), 75 μL THF-d_8, and 350 μL of alkane (cyclohexane-d_{12} or *n*-octane). After the tube was flame sealed,

the reaction mixture was heated at 150 °C for 10 days. Formation of Rh black was observed during the course of the reaction. After cooling to room temperature, the products were separated via silica gel column chromatography using 7:3 ethyl acetate/petroleum ether eluent. **[(^{iPr}Phebox)RhOAc]$_2$ (3b).** ^{1}H NMR ($CDCl_3$, 500 MHz): δ 6.46 (s, 2H, ^{iPr}Phebox-aryl), 4.56 (t, 2H, oxazoline), 4.34 (t, 4H, oxazoline), 4.26 (t, 3H, oxazoline), 3.76 (t, 3H, oxazoline), 2.59 (s, 6H, ^{iPr}Phebox-CH_3), 2.43 (s, 6H, ^{iPr}Phebox-CH_3), 1.83 (m, 4H, *iPr*), 1.62 (s, 3H, OAc), 1.52 (s, 3H, OAc), 1.02 (d, 12H, $^1J_{HH'}$ = 6.7 Hz), 0.94 (d, 12H, $^1J_{HH'}$ = 6.7 Hz), 0.77 (d, 12H, $^1J_{HH'}$ = 6.9Hz), 0.57 (d, 12H, $^1J_{HH'}$ = 7.1 Hz). **(^{iPr}Phebox)Rh$_2$(OAc)$_3$ (4b).** ^{1}H NMR ($CDCl_3$, 500 MHz): δ 6.64 (s, 1H, ^{iPr}Phebox-aryl), 4.80 (m, 1H, oxazoline), 4.96 (m, 2H, oxazoline), 4.36 (t, 1H, oxazoline), 4.26 (t, 1H, oxazoline), 4.06 (m, 2H, oxazoline), 2.63 (m, 1H, oxazoline-*iPr*), 2.57 (s, 3H, oxazoline-*iPr*), 2.57 (s, 3H, ^{iPr}Phebox-CH_3), 2.36 (s, 3H, ^{iPr}Phebox-CH_3), 2.22 (s, 3H, OAc), 1.67 (s, 3H, OAc), 1.45 (s, 3H, OAc), 1.76 (d, 3H, $^1J_{HH'}$ = 6.7 Hz, *iPr*), 1.72 (d, 3H, $^1J_{HH'}$ = 6.8 Hz, *iPr*), 1.08 (d, 3H, $^1J_{HH'}$ = 7.0 Hz, *iPr*), 0.97 (d, 3H, $^1J_{HH'}$ = 6.8 Hz, *iPr*).

(^{dm}Phebox)Ir(OAc)(C$_6$H$_5$) (5a). A 50 mL Teflon-stoppered reaction vessel was charged with a stir bar, **2a** (150 mg, 0.0239 mmol), and benzene (12.5 ml, 140 mmol). Oxygen was removed from the solution through three freeze-pump-thaw cycles and then heated at 100 °C. After 1.5 h the reaction mixture was cooled to room temperature and the volatiles were removed. The resulting bright orange solid was dried overnight *in vacuo*. Complex **5a** was isolated as a bright orange solid. Yield: 149 mg, 99%. ^{1}H NMR ($CDCl_3$, 500 MHz): δ 6.63 (s, 1H, ^{dm}Phebox-aryl), 6.63 (t, 2H, 3-Ph), 6.55 (t, 1H, 4-Ph), 6.42 (d, 2H, 2-Ph), 4.44 (d, 2H, $^1J_{HH'}$ = 8.3 Hz, OCH_2), 4.36 (d, 2H, $^1J_{HH'}$ = 8.3 Hz, OCH_2), 2.62 (s, 6H, Phebox-CH_3), 2.01 (s, 3H, OAc), 1.41 (s, 6H, CH_3), 1.04 (s, 6H, CH_3). ^{13}C NMR ($CDCl_3$, 125 MHz): δ 185.31 (OAc), 179.16 (Ph), 177.08 (C=N), 140.39, 134.76 (2-Ph), 125.48 (^{dm}Phebox-*C*H), 125.23 (3-Ph), 123.93, 121.95, 120.87 (4-

Ph), 82.22 (O*C*H_2C(CH_3)$_2$), 66.29 (OCH_2*C*(CH_3)$_2$), 26.95 (CH_3), 26.85 (CH_3), 25.42 (OAc), 18.81 (Phebox-CH_3). Anal. Calcd for $C_{26}H_{31}N_2O_4Ir$: C, 49.74; H, 4.98; N, 4.46. Found: C, 48.92; H, 4.89; N, 4.36.

^{iPr}PheboxIr(OAc)(C_6H_5) (5b). Following the general procedure above **5b** was prepared from **2b** (106 mg, 0.162 mmol) and isolated as a bright orange solid. Yield: 85 mg, 78%. ^{1}H NMR ($CDCl_3$, 500 MHz): δ 6.66 (t, 2H, 3-Ph), 6.63 (s, 1H, ^{dm}Phebox-aryl-H), 6.58 (t, 1H, 4-Ph), 6.41 (d, 2H, 2-Ph), 4.72 (t, 1H, OCH$_2$C*H*), 4.57 (m, 2H, OC*H*$_2$CH), 4.51 (t, 1H, OCH$_2$C*H*), 3.95 (m, 2H, OC*H*$_2$CH), 2.65 (s, 3H, Phebox-CH_3), 2.58 (s, 6H, Phebox-CH_3), 2.49 (m, 1H, C*H*(CH_3)$_2$), 2.04 (s, 3H, OAc), 2.00 (m, 1H, C*H*(CH_3)$_2$), 0.94 (d, 3H, J_{HH}= 7.1 Hz, CH(C*H*$_3$)$_2$), 0.83 (d, 3H, J_{HH}= 6.8 Hz, CH(C*H*$_3$)$_2$), 0.77 (d, 3H, J_{HH}= 7.1 Hz, CH(C*H*$_3$)$_2$), 0.11 (d, 3H, J_{HH} = 6.7 Hz, CH(C*H*$_3$)$_2$). ^{13}C NMR ($CDCl_3$, 125 MHz): δ 185.00 (OAc), 179.55 (Ph), 178.46 (C=N), 178.18 (C=N), 140.75, 140.43, 134.35 (2-Ph), 125.64 (3-Ph), 125.35, 125.21, 123.90, 122.33 (Phebox-CH), 121.23 (4-Ph), 71.18 (OCH$_2$*C*H), 70.28 (OCH$_2$*C*H), 67.30 (O*C*H$_2$CH), 29.30 (*C*H(CH_3)$_2$), 29.17 (*C*H(CH_3)$_2$), 24.88 (OAc), 19.66 (CH(*C*H$_3$)$_2$), 19.60 (CH(*C*H$_3$)$_2$), 18.89 (Phebox-CH_3), 18.82 (Phebox-CH_3), 14.77 (CH(*C*H$_3$)$_2$), 14.28 (CH(*C*H$_3$)$_2$). Anal. Calcd for $C_{28}H_{35}N_2O_4Ir$: C, 51.28; H, 5.39; N, 4.27. Found: C, 51.48; H, 5.68; N, 4.32.

^{dm}PheboxIr(OAc)(C_6D_5) (5a-*d_5*). A resealable Teflon-capped NMR tube was charged with **2a** (5.3 mg, 0.0084 mmol) and 0.43 mL benzene-d_6 were vacuum transferred to give a light green solution. Dioxane (0.8 μL, 0.0084 mmol) was added via microsyringe and the solution was degassed using three freeze/pump/thaw cycles. The mixture was heated at 100 °C for 2 h, resulting in a bright orange solution. Yield: 96%, determined by integration of Phebox-aryl-H signal against dioxane internal standard. ^{1}H NMR (C_6D_6, 500 MHz, 25 °C): δ 6.58 (s, 1H, Phebox-aryl-H), 3.68 (d, 2H, $J_{HH'}$ = 8.3 Hz, OCH_2), 3.57 (d, 2H, $J_{HH'}$ = 8.3 Hz, OCH_2), 2.68 (s,

6H, Phebox-CH_3), 2.08 (br s, 3H, OAc), 1.56 (br s, 3H, HOAc), 1.24 (s, 6H, CH_3), 0.95 (s, 6H, CH_3). ^{1}H NMR (C_6D_6, 500 MHz, 40 °C): δ 6.58 (s, 1H, Phebox-aryl-H), 3.68 (d, 2H, $J_{HH'}$ = 8.3 Hz, OCH_2), 3.57 (d, 2H, $J_{HH'}$ = 8.3 Hz, OCH_2), 2.68 (s, 6H, Phebox-CH_3), 1.79 (br s, 6H, OAc/HOAc), 1.24 (s, 6H, CH_3), 0.96 (s, 6H, CH_3).

Addition of acetic acid to 5a. A resealable Teflon-capped NMR tube was charged with **5a** (2.0 mg, 0.0032 mmol) and benzene-d_6 (0.40 mL). All of the ^{1}H NMR signals described above in the characterization of **5a** were observed. Acetic acid (0.2 μL, 0.0035 mmol) was added via microsyringe and the mixture was degassed using three freeze/pump/thaw cycles. In the ^{1}H NMR spectrum after addition of acetic acid all of the ^{dm}Phebox and phenyl ligand signals were observed. Notably, the acetate signal at 2.07 ppm was absent at room temperature. ^{1}H NMR (C_6D_6, 500 MHz, 25 °C): δ 6.95 (d, 2H, 2-Ph), 6.89 (t, 2H, 3-Ph), 6.76 (t, 1H, 4-Ph), 6.58 (s, 1H, Phebox-aryl-H), 3.67 (d, 2H, OCH_2), 3.57 (d, 2H, OCH_2), 2.68 (s, 6H, Phebox-CH_3), 1.23 (s, 6H, CH_3), 0.96 (s, 6H, CH_3).

General procedure for the reaction of 2a with *n*-octane. Five 25 mL resealable Teflon-stoppered reaction vessel were charged with **2a** and 1.5 mL of octane. Each vessel was sealed under a nitrogen atmosphere. Each vessel was heated at 200 °C for 20 minutes and then removed from heat and shaken to ensure complete solubility of **2a**. Each vessel was put back into the 200 °C bath and heated a specified amount of time (3, 6, 24, 48, or 72 h). After allowing the reaction to cool to room temperature, the volatiles were transferred to a 5 mL volumetric flask. The reaction vessel was washed twice with pentane and combined in the flask. Mesitylene (6 μL) was added as an internal standard and the mixture was diluted to a total volume of 5 mL using pentane. The volatile products were quantified by GC analysis.

^{dm}PheboxIr(OAc)(H) (6a). In a resealable Teflon-stoppered reaction vessel, complex **2a** (7.3 mg, 0.012 mmol) was heated in octane (2 mL) for 72 h. A bright orange powder was obtained after removing the volatiles in vacuo. Crystals were obtained at room temperature by layering a benzene solution of **6a** with pentane. Yield: 7.0 mg, 96%. ^{1}H NMR (C_6D_6, 500 MHz): δ 6.49 (s, 1H, Phebox-aryl-H), 3.84 (d, 2H, $J_{HH'}$ = 8.3 Hz, OCH_2), 3.79 (d, 1H, $J_{HH'}$ = 8.3 Hz, OCH_2), 2.64 (s, 6H, Phebox-CH_3), 2.06 (s, 3H, OAc), 1.33 (s, 6H, CH_3), 1.29 (s, 6H, CH_3), -33.78 (s, 1H, Ir-H). ^{13}C NMR (C_6D_6, 125 MHz): δ 185.78 (OAc), 178.59 (Ph), 177.20 (C=N), 139.38, 126.93 (Phebox-CH), 123.04, 81.65 ($OCH_2C(CH_3)_2$), 65.71 ($OCH_2C(CH_3)_2$), 27.27 (CH_3), 26.57 (CH_3), 26.32 (OAc), 18.89 (Phebox-CH_3). Anal. Calcd for $C_{20}H_{27}N_2O_4Ir$: C, 43.55; H, 4.93; N, 5.08. Found: C, 42.94; H, 4.79; N, 4.45.

Isomerization of 1-octene using 6a. A sealable NMR tube was loaded with **6a** (2.0 mg, 0.0036 mmol) and 600 μL of a 0.11 M solution of 1-octene in octane was added. The solution was degassed using 3 freeze-pump-thaw cycles and the tube was flame sealed. The reaction was heated at 200 °C for 24 h and then cooled to room temperature. The tube was opened and then the mixture was transferred to a 5 mL volumetric flask. The tube was washed two times with pentane and the washes were combined in the flask. Mesitylene (6 μL) was added as an internal standard and the solution was diluted to a total volume of 5 mL with more pentane. The volatiles were analyzed by GC; 15 TON; 90% conversion.

***n*-Octane dehydrogenation in the presence of 1-hexene.** A 25 mL resealable Teflon-stoppered reaction vessel was charged with **2a** (7.0 mg, 0.011 mmol) and 1.5 mL of octane. 1-Hexene (14 μL, 0.11 mmol) was added via microsyringe and the reaction was closed under a nitrogen atmosphere. The reaction was performed using the general procedure for octane dehydrogenation and the octene yield was determined by GC; 33(1)%.

***n*-Octane dehydrogenation in the presence of H_2O.** A 25 mL resealable Teflon-stoppered reaction vessel was charged with **2a** (7.3 mg, 0.012 mmol) and 1.5 mL of octane. HPLC grade H_2O (25 μL, 1.4 mmol, 120 equiv.) was added via microsyringe and the reaction was closed under a nitrogen atmosphere. The reaction was performed using the general procedure for octane dehydrogenation and octene yield was determined by GC; 44(2)%

H/D exchange between *n*-octane and acetic-d_4 using 2a. A sealable NMR tube was charged with **2a** (4.0 mg, 0.0064 mmol), octane (210 μL, 1.4 mmol), and acetic acid-d_4 (100 μL, 1.8 mmol). The solution was degassed using 3 freeze-pump-thaw cycles and the tube was flame sealed. After heating at 160 °C for 48 h the reaction was cooled to room temperature and opened. A 2 M dichloromethane-d_2 in benzene solution (50 μL, 0.10 mmol) was added and the reaction was analyzed by ^{2}H NMR spectroscopy; 1.5(1) % deuterium incorporation (determined by integration of the deuterated octane signal against CD_2Cl_2) into the terminal C-H bonds of octane.

General procedure for the reaction of 2a and *n*-octane in the presence of base. Following literature procedure,[5] a 25 mL resealable Teflon-stoppered a reaction vessel was charged with **2a**, base (1 equiv.) and octane (2 mL). The reaction was sealed under nitrogen and heated at 160 °C for 48 h. After cooling to room temperature, the volatiles were removed in vacuo. The orange residue was dissolved in benzene and transferred to a resealable NMR tube. After removal of the volatiles, benzene-d_6 was transferred to give a dark orange solution. An internal standard solution was added to the NMR tube and yields were determined by ^{1}H NMR spectroscopy.

Reaction of 2a with *n*-octane in the presence of K_2SO_4. Following the general procedure, **2a** (13 mg, 0.021 mmol), K_2SO_4 (3.6 mg, 0.021 mmol) were heated in octane. At the end of the

reaction 20 μL of a dioxane internal standard solution (0.23 M in benzene-d_6) was added. Integration of dioxane signal vs ^{dm}Phebox-aryl-H or Ir-H signal was used to obtain yields: 34% **7a**, ~1% **6a**, 41% **2a**.

Reaction of 2a with *n*-octane in the presence of $KHCO_3$. Following the general procedure, **2a** (13 mg, 0.021 mmol) $KHCO_3$ (2.1 mg, 0.021 mmol) were heated in octane. At the end of the reaction 20 μL of a dioxane internal standard solution was (0.23 M in benzene-d_6). Integration of dioxane signal vs ^{dm}Phebox-aryl-H or Ir-H signal was used to obtain yields: 50% **7a**, 11% **6a**, 11% **2a**.

Reaction of 2a with *n*-octane in the presence of 18-crown-6. Following the general procedure, **2a** (13 mg, 0.021 mmol), K_2CO_3 (2.9 mg, 0.21 mmol), 18-crown-6 (11 mg, 0.042 mmol) were heated in octane. At the end of the reaction 20 μL of a hexamethyldisiloxane internal standard solution was (0.094 M in benzene-d_6). Integration of dioxane signal vs ^{dm}Phebox-aryl-H or Ir-H signal was used to obtain yields: 37% **7a**, 31% **6a**; total yield of Ir products 68%.

Details of Solid State Structure Determination of 3b.

An orange prism, measuring 0.13 x 0.11 x 0.03 mm^3 was mounted on a glass capillary with oil. Data was collected at -173 °C on a Bruker APEX II single crystal X-ray diffractometer, Mo-radiation. Crystal-to-detector distance was 40 mm and exposure time was 60 seconds per frame for all sets. The scan width was 0.5°. Data collection was 99.3% complete to 25° in 9. A total of 55372 (merged) reflections were collected covering the indices, h = -16 to 16, k = -18 to 18, l = -29 to 29. 9362 reflections were symmetry independent and the R_{int} = 0.1431 indicated that the data was of less than average quality (0.07). Indexing and unit cell refinement indicated a primitive orthorhombic lattice. The space group was found to be P 2_1 2_1 2_1 (No.19). The data

was integrated and scaled using SAINT, SADABS within the APEX2 software package by Bruker.[15]

Solution by direct methods (SHELXS, SIR97[16]) produced a complete heavy atom phasing model consistent with the proposed structure. The structure was completed by difference Fourier synthesis with SHELXL97.[17,18] Scattering factors are from Waasmair and Kirfel.[19] Hydrogen atoms were placed in geometrically idealised positions and constrained to ride on their parent atoms with C---H distances in the range 0.95-1.00 Angstrom. Isotropic thermal parameters U_{eq} were fixed such that they were $1.2U_{eq}$ of their parent atom Ueq for CH's and $1.5U_{eq}$ of their parent atom U_{eq} in case of methyl groups. All non-hydrogen atoms were refined anisotropically by full-matrix least-squares. The structure contains large channels filled with disordered pentane.

Table 3.3. Crystal data and structure refinement for **3b**.

Empirical formula	$C_{49} H_{72} N_4 O_8 Rh_2$	
Formula weight	1050.93	
Temperature	100(2) K	
Wavelength	0.71073 Å	
Crystal system	Orthorhombic	
Space group	P 2_1 2_1 2_1	
Unit cell dimensions	a = 13.497(2) Å	α = 90°.
	b = 15.394(2) Å	β = 90°.
	c = 24.739(4) Å	γ = 90°.
Volume	5140.1(13) $Å^3$	
Z	4	
Density (calculated)	1.358 Mg/m^3	
Absorption coefficient	0.695 mm^{-1}	
F(000)	2192	
Crystal size	0.13 x 0.11 x 0.03 mm^3	
Theta range for data collection	1.72 to 25.35°.	
Index ranges	-16<=h<=16, -18<=k<=18, -29<=l<=29	
Reflections collected	55372	
Independent reflections	9362 [R(int) = 0.1431]	
Completeness to theta = 25.00°	99.3 %	
Max. and min. transmission	0.9795 and 0.9151	
Refinement method	Full-matrix least-squares on F^2	
Data / restraints / parameters	9362 / 14 / 570	
Goodness-of-fit on F^2	0.997	
Final R indices [I>2sigma(I)]	R1 = 0.0570, wR2 = 0.1049	
R indices (all data)	R1 = 0.1059, wR2 = 0.1225	
Absolute structure parameter	-0.01(4)	
Largest diff. peak and hole	0.656 and -0.546 $e.Å^{-3}$	

Details of Solid State Structure Determination of 4b.

A small dichroic purple/green prism, measuring 0.10 x 0.05 x 0.03 mm^3 was mounted on a glass capillary with oil. Data was collected at -173 °C on a Bruker APEX II single crystal X-ray diffractometer, Mo-radiation. Crystal-to-detector distance was 40 mm and exposure time was 60 seconds per frame for all sets. The scan width was 0.5^o. Data collection was 99.9% complete to 25^o in ϑ. A total of 13553 (merged) reflections were collected covering the indices,

h = -12 to 12, k = -12 to 12, l = -20 to 20. 6760 reflections were symmetry independent and the R_{int} = 0.0681 indicated that the data was of average quality (0.07). Indexing and unit cell refinement indicated a primitive monoclinic lattice. The space group was found to be P 2_1 (No.4). The data was integrated and scaled using SAINT, SADABS within the APEX2 software package by Bruker.[15]

Solution by direct methods (SHELXS, SIR97[16]) produced a complete heavy atom phasing model consistent with the proposed structure. The structure was completed by difference Fourier synthesis with SHELXL97.[17,18] Scattering factors are from Waasmair and Kirfel.[19] Hydrogen atoms were placed in geometrically idealized positions and constrained to ride on their parent atoms with C---H distances in the range 0.95-1.00 Angstrom. Isotropic thermal parameters U_{eq} were fixed such that they were $1.2U_{eq}$ of their parent atom Ueq for CH's and $1.5U_{eq}$ of their parent atom U_{eq} in case of methyl groups. All non-hydrogen atoms were refined anisotropically by full-matrix least-squares.

Table 3.4. Crystal data and structure refinement for **4b**.

Empirical formula	$C_{26} H_{36} N_2 O_8 Rh_2$	
Formula weight	710.39	
Temperature	100(2) K	
Wavelength	0.71069 Å	
Crystal system	Monoclinic	
Space group	P 2_1	
Unit cell dimensions	a = 9.7840(15) Å	α = 90°.
	b = 9.523(3) Å	β = 106.304(9)°.
	c = 15.7500(15) Å	γ = 90°.
Volume	1408.5(5) $Å^3$	
Z	2	
Density (calculated)	1.675 Mg/m^3	
Absorption coefficient	1.221 mm^{-1}	
F(000)	720	
Crystal size	0.10 x 0.05 x 0.03 mm^3	
Theta range for data collection	2.17 to 28.35°.	
Index ranges	-12<=h<=12, -12<=k<=12, -20<=l<=20	
Reflections collected	13553	
Independent reflections	6760 [R(int) = 0.0681]	
Completeness to theta = 25.00°	99.9 %	
Max. and min. transmission	0.9643 and 0.8876	
Refinement method	Full-matrix least-squares on F^2	
Data / restraints / parameters	6760 / 1 / 352	
Goodness-of-fit on F^2	0.970	
Final R indices [I>2sigma(I)]	R1 = 0.0494, wR2 = 0.0790	
R indices (all data)	R1 = 0.1106, wR2 = 0.0960	
Absolute structure parameter	0.03(5)	
Largest diff. peak and hole	0.906 and -1.304 $e.Å^{-3}$	

Details of Solid State Structure Determination of 5a.

An orange prism, measuring 0.17 x 0.14 x 0.08 mm^3 was mounted on a glass capillary with oil. Data was collected at -173 °C on a Bruker APEX II single crystal X-ray diffractometer, Mo-radiation. Crystal-to-detector distance was 40 mm and exposure time was 10 seconds per frame for all sets. The scan width was 0.5^o. Data collection was 100% complete to 25^o in ϑ. A total of 35783 (merged) reflections were collected covering the indices, h = -14 to 14, k = -10 to 10, l = -25 to 25. 5710 reflections were symmetry independent and the R_{int} = 0.0317 indicated

that the data was good (average quality 0.07). Indexing and unit cell refinement indicated a triclinic lattice. The space group was found to be P $\bar{1}$ (No.2). The data was integrated and scaled using SAINT, SADABS within the APEX2 software package by Bruker.[15]

Solution by direct methods (SHELXS, SIR97[16]) produced a complete heavy atom phasing model consistent with the proposed structure. The structure was completed by difference Fourier synthesis with SHELXL97.[17,18] Scattering factors are from Waasmair and Kirfel.[19] Hydrogen atoms were placed in geometrically idealized positions and constrained to ride on their parent atoms with C---H distances in the range 0.95-1.00 Angstrom. Isotropic thermal parameters U_{eq} were fixed such that they were $1.2U_{eq}$ of their parent atom Ueq for CH's and $1.5U_{eq}$ of their parent atom U_{eq} in case of methyl groups. All non-hydrogen atoms were refined anisotropically by full-matrix least-squares.

Table 3.5. Crystal data and structure refinement for **5a**.

Empirical formula	$C_{26} H_{31} Ir N_2 O_4$	
Formula weight	627.73	
Temperature	100(2) K	
Wavelength	0.71073 Å	
Crystal system	Triclinic	
Space group	P -1	
Unit cell dimensions	a = 8.9434(4) Å	α = 88.990(2)°.
	b = 9.2062(4) Å	β = 74.571(2)°.
	c = 14.8342(7) Å	γ = 78.459(2)°.
Volume	1152.73(9) $Å^3$	
Z	2	
Density (calculated)	1.809 Mg/m^3	
Absorption coefficient	5.827 mm^{-1}	
F(000)	620	
Crystal size	0.17 x 0.14 x 0.08 mm^3	
Theta range for data collection	2.26 to 28.35°.	
Index ranges	-11<=h<=11, -12<=k<=11, -19<=l<=19	
Reflections collected	35783	
Independent reflections	5710 [R(int) = 0.0317]	
Completeness to theta = 25.00°	100.0 %	
Max. and min. transmission	0.6528 and 0.4374	
Refinement method	Full-matrix least-squares on F^2	
Data / restraints / parameters	5710 / 0 / 305	
Goodness-of-fit on F^2	1.077	
Final R indices [I>2sigma(I)]	R1 = 0.0193, wR2 = 0.0448	
R indices (all data)	R1 = 0.0224, wR2 = 0.0458	
Largest diff. peak and hole	1.240 and -1.413 $e.Å^{-3}$	

Details of Solid State Structure Determination of 6a.

An orange prism, measuring 0.17 x 0.07 x 0.02 mm^3 was mounted on a glass capillary with oil. Data was collected at -173 °C on a Bruker APEX II single crystal X-ray diffractometer, Mo-radiation. Crystal-to-detector distance was 40 mm and exposure time was 10 seconds per frame for all sets. The scan width was 0.5^o. Data collection was 100% complete to 25^o in ϑ. A total of 83959 (merged) reflections were collected covering the indices, h = -19 to 19, k = -13 to 13, l = -20 to 20. 5620 reflections were symmetry independent and the R_{int} = 0.0472 indicated

that the data was excellent (average quality 0.07). Indexing and unit cell refinement indicated a primitive monoclinic lattice. The space group was found to be P 2_1/c (No.14). The data was integrated and scaled using SAINT, SADABS within the APEX2 software package by Bruker.[15]

Solution by direct methods (SHELXS, SIR97[16]) produced a complete heavy atom phasing model consistent with the proposed structure. The structure was completed by difference Fourier synthesis with SHELXL97.[17,18] Scattering factors are from Waasmair and Kirfel.[19] Hydrogen atoms (except for H1 on iridium) were placed in geometrically idealized positions and constrained to ride on their parent atoms with C---H distances in the range 0.95-1.00 Angstrom. Isotropic thermal parameters U_{eq} were fixed such that they were $1.2U_{eq}$ of their parent atom Ueq for CH's and $1.5U_{eq}$ of their parent atom U_{eq} in case of methyl groups. All non-hydrogen atoms were refined anisotropically by full-matrix least-squares. Because of extremely high data quality, the hydride H1 at a distance of 1.50(3)Å to the iridium metal center was refined anisotropically by full-matrix least-squares with soft restrains on the thermal parameters. One benzene solvent was found per two complex molecules

Table 3.5. Crystal data and structure refinement for **6a**.

Empirical formula	$C_{23}\ H_{30}\ Ir\ N_2\ O_4$	
Formula weight	590.69	
Temperature	100(2) K	
Wavelength	0.71073 Å	
Crystal system	Monoclinic	
Space group	$P\ 2_1/c$	
Unit cell dimensions	a = 14.5034(9) Å	α = 90°
	b = 10.1858(6) Å	β = 103.835(3)°
	c = 15.4427(10) Å	γ = 90°
Volume	2215.1(2) $Å^3$	
Z	4	
Density (calculated)	1.771 Mg/m^3	
Absorption coefficient	6.059 mm^{-1}	
F(000)	1164	
Crystal size	0.17 x 0.07 x 0.02 mm^3	
Theta range for data collection	2.42 to 28.55°	
Index ranges	$-19 \leq h \leq 19$,	
	$-13 \leq k \leq 13$,	
	$-20 \leq l \leq 20$	
Reflections collected	83959	
Independent reflections	5620 [R(int) = 0.0472]	
Completeness to θ = 25.00°	100.0 %	
Max. and min. transmission	0.8884 and 0.4257	
Refinement method	Full-matrix least-squares on F^2	
Data / restraints / parameters	5620 / 6 / 287	
Goodness-of-fit on F^2	1.048	
Final R indices [$I > 2\sigma(I)$]	$R_1 = 0.0188$, $wR_2 = 0.0363$	
R indices (all data)	$R_1 = 0.0288$, $wR_2 = 0.0394$	
Largest diff. peak and hole	0.794 and -0.598 $e.Å^{-3}$	

Notes to Chapter 3

1. (a) Arndsten, B. A.; Bergman, R. G.; Mobley, T. A.; Peterson, T. H. *Acc*. *Chem*. *Res*. **1995**, *28*, 154. (b) Shilov, A. E.; Shul'pin, G. B. *Chem*. *Rev*. **1997**, *97*, 2879. (c) Crabtree, R. H. *J*. *Chem*. *Soc*., *Dalton Trans*. **2001**, 2437. (d) Labinger, J. A.; Bercaw, J. E. *Nature* **2002**, *417*, 507. (e) Activation and Functionalization of C-H Bonds; Goldberg, K. I., Goldman, A. S., Eds.; ACS Symposium Series 885; American Chemical Society: Washington, DC, 2004.

2. (a) Zhong, H. A.; Labinger, J. A.; Bercaw, J. E. *J*. *Am*. *Chem*. *Soc*. **2002**, *124*, 1378. (b) Periana, R. A.; Bhalla, G.; Tenn, W. J., III; Young, K. J. H.; Liu, X. Y.; Mironov, O.; Jones, C. J.; Ziatdinov, V. R. *J*. *Mol Catal*. *A* **2004**, *220*, 7. (c) Conley, B. L.; Tenn, W. J., III; Young, K. J. H.; Ganesh, S. K.; Meier, S. K.; Ziatdinov, V. R.; Mironov, O.; Oxgaard, J.; Gonzales, J.; Goddard, W. A., III; Periana, R. A. *J*. *Mol*. *Catal*. *A* **2006**, *251*, 8. (d) Owen, J. S.; Labinger, J. A.; Bercaw, J. E. *J*. *Am*. *Chem*. *Soc*. **2006**, *128*, 2005.

3. Ito, J.; Nishiyama, H. *Eur*. *J*. *Inorg*. *Chem*. **2007**, 1114.

4. Ito, J.; Shiomi, T.; Nishiyama, H. *Adv*. *Synth*. *Catal*. **2006**, *348*, 1235.

5. Ito, J.; Kaneda, T.; Nishiyama, H. *Organometallics* **2012**, *31*, 4442.

6. (a) Crabtree, R. H.; Mihelcic, J. M.; Quirk, J. M. *J*. *Am*. *Chem*. *Soc*. **1979**, *101*, 7738. (b) Crabtree, R. H.; Mellea, M. F.; Mihelcic, J. M.; Quirk, J. M. *J*. *Am*. *Chem*. *Soc*. **1982**, *104*, 107. (c) Burk, M. J.; Crabtree, R. H.; McGrath, D. V. *J*. *Am*. *Chem*. *Soc*., *Chem*. *Commun*. **1985**, 1829. (d) Burk, M. J.; Crabtree, R. H. *J*. *Am*. *Chem*. *Soc*. **1987**, *109*, 8025. (e) Gupta, M.; Hagen, C.; Flesher, R. J.; Kaska, W. C.; Jensen, C. M. *Chem*. *Commun*. **1996**, 2083. (f) Liu, F.; Pak, E. B.; Singh, B.; Jensen, C. M.; Goldman, A. S. *J*. *Am*. *Chem*. *Soc*. **1999**, *121*, 4086. (g) Fekl, U.; Kaminsky, W.; Goldberg, K. I. *J*. *Am*. *Chem*. *Soc*. **2003**, *125*, 15286. (h) Kostelansky, C. N.; MacDonald, M. G.; White, P. S.; Templeton, J. L. *Organometallics* **2006**, *25*, 2993. (i) Khaskin,

E.; Zavalij, P. Y.; Vedernikov, A. N. *J. Am. Chem. Soc.* **2006**, *128*, 13054. (j) Adams, J. J.; Arulsamy, N.; Roddick, D. M. *Organometallics* **2012**, *31*, 1439.

7. (a) Clegg, W.; Garner, C. D.; Akhter, L.; Al-Samman, M. H. *Inorg. Chem.* **1983**, *22*, 2466. (b) Cotton, F. A.; Dunbar, K. R. *J. Am. Chem. Soc.* **1987**, *109*, 3142. (c) Barcelo, F.; Cotton, F. A.; Lahuerta, P.; Sanau, M.; Schwotzer, W.; Ubeda, M. A. *Organometallics* **1987**, *6*, 1105. (d) Kawamura, T.; Maeda, M.; Miyamoto, M.; Usami, H.; Imaeda, K.; Ebihara, M. *J. Am. Chem. Soc.* **1998,** *120*, 8136. (e) Choi, S.; Lin, Z. *J. Organomet. Chem.* **2000**, *608*, 42. (f) Ebihara, M.; Yang, Z.; Kawamura, T. *Acta Cryst.* **2006**, *E62*, 3031.

8. (a) Moulton, C. J.; Shaw, B. L. *Dalton Trans* **1976**, 1020. (b) Kanzelberger, M.; Singh, B.; Czerw, M.; Krogh-Jespersen, K.; Goldman, A. S. *J. Am. Chem. Soc.* **2000**, *122*, 11017. (c) Ben-Ari, E.; Gandelman, M.; Rozenberg, H.; Shimon, L. J.; Milstein, D. *J. Am. Chem. Soc.* **2003**, *125*, 4714. (d) Zhu, Y.; Chen, C.; Finnell, S. R.; Foxman, B. M.; Ozerov, O. *J. Am. Chem. Soc.* **2006**, *25*, 3190.; (e) Fan, L.; Parkin, S.; Ozerov, O. *J. Am. Chem. Soc.* **2006**, *128*, 12400. (f) Bernskoetter, W. H.; Hanson, S. K.; Buzak, S. K.; Davis, Z.; White, P. S.; Swartz, R.; Goldberg, K. I.; Brookhart, M. *J. Am. Chem. Soc.* **2009**, *131*, 8603.

9. (a) Kanzelberger, M.; Zhang, X.; Emge, T. J. Goldman, A. S.; Zhao, J.; Incarvito, C.; Hartwig, J. F. *J. Am. Chem. Soc.* **2003**, *125,* 13644. (b) Frech, C. M.; Shimon, L. J. W.; Milstein, D. *Organometallics* **2009**, *28*, 1900. (c) Segawa, Y.; Yamashita, M.; Nozaki, K. *J. Am. Chem. Soc.* **2009**, *131*, 9201.

10. (a) Zhang, X.; Kanzelberger, M.; Emge, T. J.; Goldman, A. S. *J. Am. Chem. Soc.* **2004**, *126*, 13192. (b) Zhang, X.; Emge, T. J.; Ghosh, R.; Goldman, A. S. *J. Am. Chem. Soc.* **2005**, *127*, 8250. (c) Zhang, X.; Emge, T. J.; Ghosh, R.; Krogh-Jespersen, K.; Goldman, A.S.

Organometallics **2006**, *25*, 1303. (d) Segawa, Y.; Yamashita, M.; Nozaki, K. *J*. *Am*. *Chem*. *Soc*. **2009**, *131*, 9201. (e) Huang, Z.; Zhou, J.; Hartwig, J. F. *J*. *Am*. *Chem*. *Soc*. **2010**, *132*, 11458.

11. Morales-Morales, D.; Lee, D. W.; Wang, Z.; Jensen, C. M. *Organometallics* **2001**, *20*, 1144.

12. When we synthesized **4a** using the published procedure, a mixture of **4a** and **3a** was always obtained (3:1 ratio determined by ^{1}H NMR spectroscopy in C_6D_6 against hexamethyldisiloxane internal standard).

13. *Organotransition Metal Chemistry*; Hartwig, J.; University Science Books: Sausalito, CA, 2011; pp 275-276.

14. The aromatic signals of the Ir-phenyl protons integrated to the expected values against the ^{dm}Phebox ligand by ^{1}H NMR spectroscopy.

15. Bruker (**2007**) APEX2 (Version 2.1-4), SAINT (version 7.34A), SADABS (version 2007/4), BrukerAXS Inc, Madison, Wisconsin, USA.

16. (a) Altomare, A.; Burla, C.; Camalli, M.; Cascarano, L.; Giacovazzo, C.; Guagliardi, A.; Moliterni, A. G. G.; Polidori, G.; Spagna, R. *J*. *Appl*. *Cryst*. **1999**, *32***,** 115-119. (b) Altomare, A.; Cascarano, G.; Giacovazzo, C.; Guagliardi, A. *J*. *Appl*. *Cryst*. **1993**, *26*, 343.

17. Sheldrick GM. **(1997)** SHELXL-97, Program for the Refinement of Crystal Structures. University of Göttingen, Germany.

18. Mackay, S.; Edwards, C.; Henderson, A.; Gilmore, C.; Stewart, N.; Shankland, K.; Donald, A. *MaXus: a computer program for the solution and refinement of crystal structures from diffraction data*. University of Glasgow, Scotland, **1997**.

19. Waasmaier, D.; Kirfel, A. *Acta Crystallogr*. A. **1995**, *51*, 416.

Chapter 4: Generation of (^{dm}Phebox)Ir(OAc)$_2$(OH)$_2$ Using Oxygen as a Hydrogen Acceptor

Introduction

Direct methods for the dehydrogenation of alkanes utilizing inexpensive and environmentally friendly oxidants would result in greener and more efficient industrial processes. These methods would presumably involve the activation of an alkane C-H bond to generate a metal alkyl complex, followed by β-hydride elimination to produce the alkene. The success of late transition metals in selective C-H bond activation coupled with their high proclivity for β-hydride elimination has led to many investigations of the use of low valent Ir, Pt, and Rh complexes as catalysts for alkane dehydrogenation reactions.[1,2] Notably, the thermodynamics of alkane dehydrogenation require the use of hydrogen acceptors or some physical means of removing hydrogen as it is generated. Some successful systems have used sacrificial olefins as hydrogen acceptors, but this obviously lessens the atom efficiency of the reaction by creating significant waste and increasing costs. Dehydrogenation systems without sacrificial acceptors have been also been developed, but these require high operating temperatures and the reactions are carried out in an open system to enable hydrogen release.[1f,3] It is challenging to find catalysts that are durable under these severe conditions.

Alkane dehydrogenation mediated by the Ir^{III} complex, (^{dm}Phebox)Ir(OAc)$_2$(OH$_2$) (**1a**) (^{dm}Phebox = 2,6-bis(4,4-dimethyloxazolinyl)-3,5-dimethylphenyl) was not inhibited by the olefin product, water or nitrogen, and cleanly generated the Ir^{III} hydride complex (^{dm}Phebox)Ir(OAc)H (**2a**).[4] The reaction of molecular oxygen with a variety of late metal hydride bonds has recently been reported[5] and the Ir^{III} hydride product **2a** presents the possibility of a reaction with oxygen and acetic acid to regenerate **1a** (eq 4.1). A reaction as shown in eq. 4.1 could allow oxygen to

be used as the oxidant in alkane dehydrogenation. Notably, attempts to use oxygen as the oxidant in (PCP)Ir catalyzed alkane dehydrogenation systems have been unsuccessful. (PCP)Ir^{III} complexes have been observed to decompose in the presence of oxygen. For example, oxygen induced reductive elimination of HX was demonstrated upon exposure of the five-coordinate ($^{t\text{Bu}}$PCP)Ir(H)(X) (X = Ph, CCPh, or H) species to oxygen at room temperature.[6] The Ir oxygen complexes ($^{t\text{Bu}}$PCP)Ir(O_2)n (n= 1, 2) were observed to form in this reaction followed by further intractable decomposition. However, with reports of oxygen insertion into late transition metal hydrides to generate metal hydroperoxide species, which typically decay to the corresponding metal hydroxide complexes,[7] the potential regeneration of **1a** from Ir-hydride complex **2a** with oxygen was investigated.

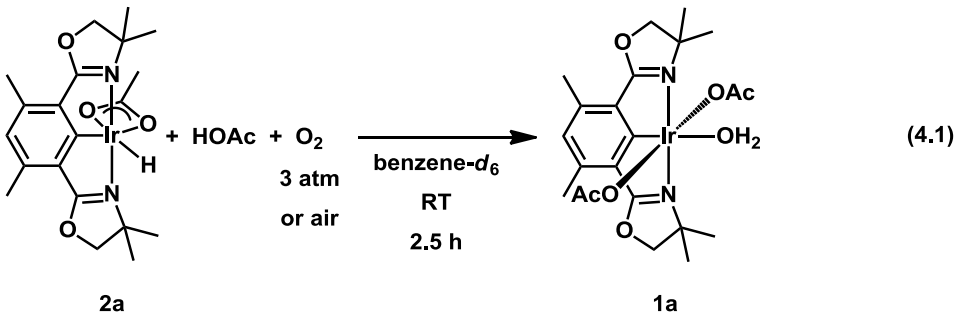

(4.1)

Results and Discussion

Generation of 1a Using Oxygen

The Ir-hydride acetate complex **2a** and 1 equiv. of acetic acid were generated during *n*-octane dehydrogenation by **1a** at 200 °C demonstrating the stability of **2a** to acetic acid at high temperatures. Complex **2a** was observed to be stable for prolonged periods (*e.g.* months) under an inert nitrogen atmosphere. At room temperature no reaction between **2a** and acetic acid (up to 10 equiv.) was also observed. H/D exchange between the hydride ligand and acetic acid-d_4 (3

equiv.) was observed at room temperature resulting in 50% deuterium incorporation after 2 h. In this reaction complete exchange of the protio OAc ligand for OAc-d_3 was also observed. We have previously described the exchange of acetic acid with the OAc ligand of (^{dm}Phebox)Ir(OAc)(Ph) in benzene solution at room temperature.[4] Exchange between HOAc (1 equiv.) and the OAc ligand of **2a** occurs at room temperature. A single broad resonance at 1.87 ppm, in the ^{1}H NMR spectrum, corresponding to both the added acetic acid and OAc is observed.

Exposure of a bright orange benzene-d_6 solution of **2a** and 1 equiv. acetic acid to ambient air resulted in a reaction at room temperature. After 2 h complex **1a** was formed in high yield (98%; determined by ^{1}H NMR spectroscopy using dioxane internal standard) and was observed to be the only Ir product of the reaction. The identity of **1a** was further confirmed by spiking the reaction with an authentic sample of the complex.[8] Over the course of the reaction, the hydride signal at -33.78 ppm disappeared. During the reaction, an intermediate Ir species (**3a**) was observed in the ^{1}H NMR spectrum (Figure 4.1). The signals diagnostic of **3a** are most clearly observed in the aromatic and oxazolinyl regions of the spectrum. After 10 minutes at room temperature **2a**, the intermediate species **3a**, and product **1a** were observed. The signal corresponding to the ^{dm}Phebox-aryl proton in both **2a** and **3a** was observed at 6.38 ppm. The signal for the same aromatic proton in **1a** was present at 6.48 ppm and integrated in a 9:1 ratio (**2a**,**3a**:**1a**). Two singlets indicative of the methyl substituents of the oxazoline rings for **3a** were observed at 1.24 and 1.48 ppm and are consistent with an asymmetrical geometry for the intermediate. In the oxazolinyl region of the ^{1}H NMR spectrum, two doublets were observed at 3.95 and 4.20 ppm corresponding to **3a**. During the course of the reaction these doublets shifted

downfield to 4.09 and 4.21 ppm (Figure 4.1, 1 h 45 min). An upfield shift in the signal indicative of ^{dm}Phebox-aryl proton of the intermediate was also observed.

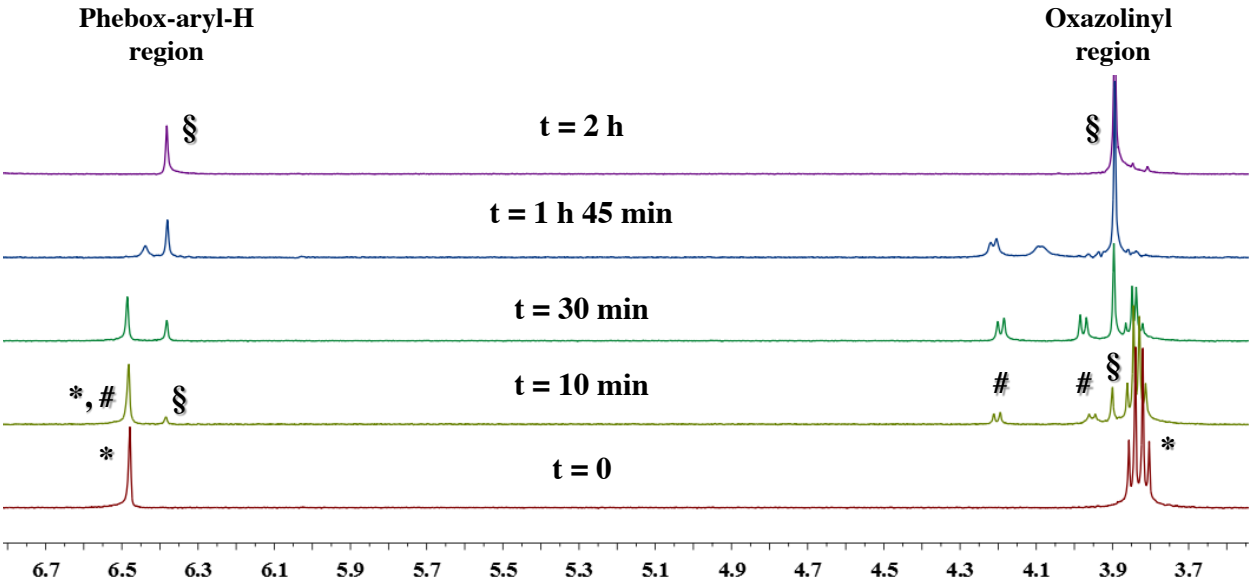

Figure 4.1. ^{1}H NMR spectral data in the aromatic and oxazolinyl regions over the course of the reaction of **2a** with acetic acid and air at room temperature in benzene-d_6; * = **2a**, # = intermediate **3a**, and § = **1a**.

Exposure of a bright orange benzene solution of **2a** and 1 equiv. of acetic acid to 3 atm of oxygen also resulted in formation of **1a** after 2 h (eq. 4.1). Formation of **1a** in high yields, 83%, was confirmed using ^{1}H NMR spectroscopy and dioxane internal standard. Additionally the formation of a brown solid was observed during the reaction. When the reaction was performed with added water, the yield of **1a** increased to 96% yield and no brown precipitate was observed. Monitoring the reaction by ^{1}H HNMR spectroscopy revealed the presence of intermediate **3a** during the reaction.

The reaction between **2a** and oxygen has been expanded to other carboxylate ligands, such as benzoate and pivalate. Complexes (^{dm}Phebox)Ir(X)H (X = OBz (**2b**), OPiv (**2c**)) could be obtained via carboxylate exchange at **2a**. The addition of 1 equiv. of benzoic acid solution to

2a in benzene-d_6 resulted in displacement of the OAc ligand for OBz after 10 min to generate **2b** in 99% NMR yield (eq. 4.2). After removal of acetic acid *in vacuo* complex **2b** remained. In the ^{1}H NMR spectrum of **2b** the hydride resonance was observed at -33.68 ppm. Three signals indicative of the benzoate protons were observed at 7.18 (1H), 7.22 (2H), and 8.55 (2H) consistent with carboxylate exchange at the Ir center. The pivalate derivative (^{dm}Phebox)Ir(OPiv)H **2c**, can also be generated *in situ* from the reaction of **2a** and 1 equiv. of pivalic acid solution after 10 min at room temperature in quantitative yield (eq. 4.2). The OPiv *tert*-butyl substituent was observed at 1.46 ppm and integrated to 9 protons relative to the two oxazoline methyl groups (each 6 protons) of the ^{dm}Phebox ligand. The hydride signal in the ^{1}H NMR spectrum of **2c** was observed at -33.83 ppm consistent with the spectral data obtained for **2a** and **2b**.

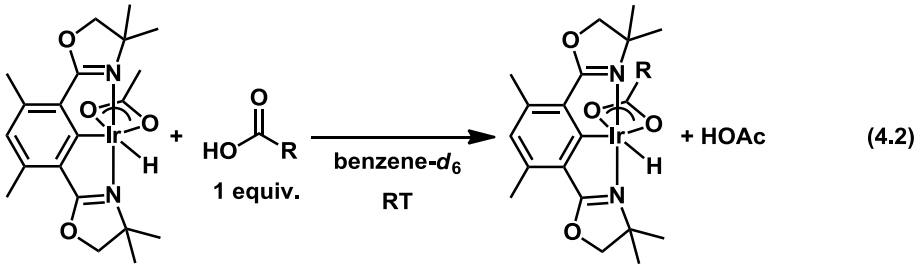

The addition of 1 equiv. of benzoic acid to a benzene-d_6 solution of **2b** resulted in broadening of the OBz signals. These signals also shifted upfield upon the addition of benzoic acid consistent with exchange between coordinated OBz and benzoic acid. For example, the OBz signal diagnostic of the *ortho* protons shifted from 8.55 to 8.28 ppm. Exposure of a benzene-d_6 solution of **2b** and 1 equiv. benzoic acid to air resulted in an immediate reaction.

After 10 min at room temperature an intermediate species (**3b**) and product **1b** were observed in the ^{1}H NMR spectrum. In the oxazolinyl region of the spectrum the two doublets at 3.99 and 3.81 ppm supported an asymmetrical geometry for **3b**. A singlet at 6.52 ppm belonged to the ^{dm}Phebox-aryl proton of the intermediate species **3b**. Additionally, a doublet at 8.39 ppm integrated to four protons and was consistent with the *ortho* aromatic protons of OBz, suggestive of the presence of 2 OBz ligands in **3b**. The presence of singlets in the oxazolinyl (3.75 ppm) and aromatic (6.55 ppm) regions of the spectrum at 10 min were suggestive of the presence of **1b**. A doublet in the OBz region at 8.11 ppm was also indicative of **1b**. Two singlets at 1.19 and 1.42 ppm corresponded to the two different methyl substituents of the oxazoline rings in **3b** along with a singlet at 1.34 consistent with formation of **1b**. The starting material was also present at this time as the major species in solution and the hydride signal at -33.81 ppm was observed. Complete disappearance of **2b** and intermediate **3b** was observed after 2 h, to generate complex **1b** in 80% yield (determined against dioxane internal standard). The species from the reaction of **2b** with air was spiked with an authentic sample of **1b** to confirm the identity of the product. Complex **1b** was independently synthesized from (^{dm}Phebox)$IrCl_2(OH_2)$ and 2 equiv. of AgOBz in CH_2Cl_2 at 60 °C for 24 h in 75% isolated yield. In the ^{1}H NMR spectrum of **1b** two triplets at 7.22 and 7.32 ppm and a doublet at 7.66 ppm correlated to the two OBz ligands. A singlet at 4.55 ppm corresponded to the four protons of the oxazoline rings and is indicative of a symmetrical complex.

Upon the addition of 1 equiv. of pivalic acid to a benzene-d_6 solution of **2c**, exchange between the OPiv ligand and pivalic acid was observed indicated by the presence of a broad signal at 1.25 ppm for the *tert*-butyl groups. Exchange between the OPiv ligand and pivalic acid is consistent with the exchange discussed above for the OAc and OBz derivatives. When the

solution was exposed to air the formation of **2c** was observed by ^{1}H NMR spectroscopy. After 10 min at room temperature (Figure 4.2), the presence of an intermediate species (**3c**) similar to **3a** was indicated by the appearance of two new doublets, integrating in a 1:1 ratio in the oxazolinyl region at 3.94 and 4.18 ppm. A singlet at 6.43 ppm was also assigned to intermediate **3c** as the ^{dm}Phebox-aryl proton. Additionally, two singlets at 1.49 and 1.20 ppm were assigned as the oxazoline methyl groups and each integrated to six protons. After 3 h complex **1c** was formed in 97% NMR yield and was the only species present in solution. The identity of **1c** was confirmed by independent synthesis of the product using (^{dm}Phebox)IrCl$_2$(OH$_2$) and 2 equiv. of AgOPiv in CH_2Cl_2 at 60 °C for 24 h. In the ^{1}H NMR spectrum of **1c** a singlet at 0.84 ppm integrating to 18 protons was observed at indicative of the OPiv ligands. Another singlet at 4.57 ppm (4H) was consistent with the oxazoline protons and confirmed the symmetrical geometry of **1c**.

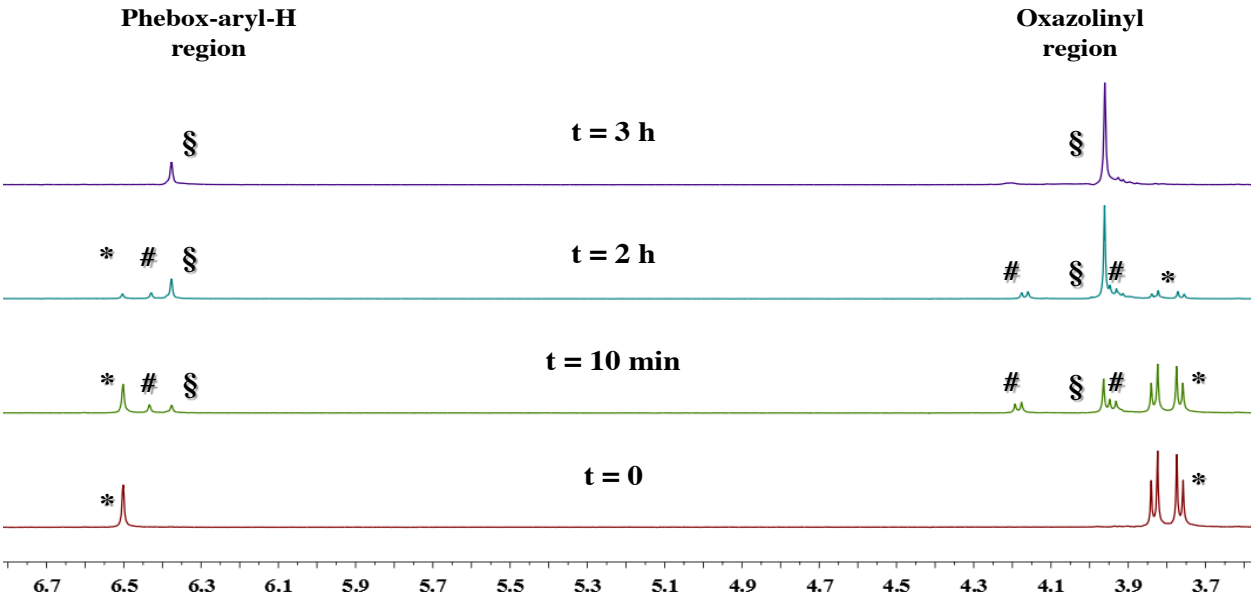

Figure 4.2. ^{1}H NMR spectral data in the aromatic and oxazolinyl regions over the course of the reaction of **2c** with pivalic acid and air at room temperature in benzene-d_6; * = **2c**, # = intermediate **3c**, and § = **1c**.

The effect of acid on the conversion of Ir-hydride **2a** to complex **1a** was examined. When a strong acid such as HBF_4 etherate or HOTf (1 equiv.) was added to a benzene solution of **2a**, an immediate color change occurred upon mixing (orange to yellow). In the ^1H NMR spectrum, the signal consistent with the hydride ligand at -33.78 ppm had disappeared concomitantly with the appearance of broad signals corresponding to a new ^{dm}Phebox complex. A broad signal at 1.63 ppm was indicative of an acetate ligand and not free acetic acid. Hydrogen was not observed in the ^1H NMR spectrum. Cooling the reaction mixture to 233 K in toluene-d_8 did not result in a more resolved NMR spectrum. When 2 equiv. of HBF_4 etherate was added, similar broad signals and chemical shifts were observed by ^1H NMR spectroscopy.

X-ray quality crystals were obtained from the reaction of **2a** and 2 equiv. of HBF_4. The structure of the compound was determined to be [(^{dm}Phebox)Ir(HOAc)(OH_2)][BF_4] (**4a**) (eq. 4.3, Figure 4.2). This structure is questionable as it suggested that the oxidation state at the metal center was Ir^{II}. The ^1H NMR spectral data are consistent with a diamagnetic species as the chemical shifts are observed within the range expected for a diamagnetic compound. Arguably, if the aqua ligand were a hydroxide then the oxidation state at the metal center would be Ir^{III} and would be consistent with the ^1H NMR chemical shifts for **4a**. A second possibility is that the bound acetic acid is actually OAc which would also result in an Ir^{III} diamagnetic species. The X-ray crystallographic data provided evidence for an extensive hydrogen bonding network between the BF_4 counterion and the acetic acid and aqua ligands. The Ir pincer bond lengths of complex **4a** in Figure 4.2 are similar to those observed for complex **2a**. In **4a** the C(1)-Ir(1) bond length, 1.923(9) Å, is identical to the bond length reported for complex **2a**. Additionally the Ir-N bond distances between the two complexes are quite similar (2.072(2) Å and 2.046(7) Å in **4a** vs. 2.055(2) Å and 2.043(2) Å in **2a**). The evidence from the X-ray crystallographic and ^1H NMR

data suggested that the addition of 1 equiv. of HBF_4 likely protonated the Ir-hydride bond of **2a** to generate hydrogen. A signal for hydrogen was not observed in the ^1H NMR spectra acquired during the reaction. When a second equiv. of HBF_4 was added, protonation at the OAc ligand occurred to generate acetic acid. When a benzene-d_6 solution of **4a** was exposed to oxygen a black solid immediately precipitated from the reaction solution. This solid was soluble in THF-d_8 and examination by ^1H NMR spectroscopy showed the formation of multiple intractable products, thus supporting decomposition of complex **4a**. The species formed in the reaction of **2a** with strong acids did not react as productively with oxygen as solutions of **2a** and acetic acid.

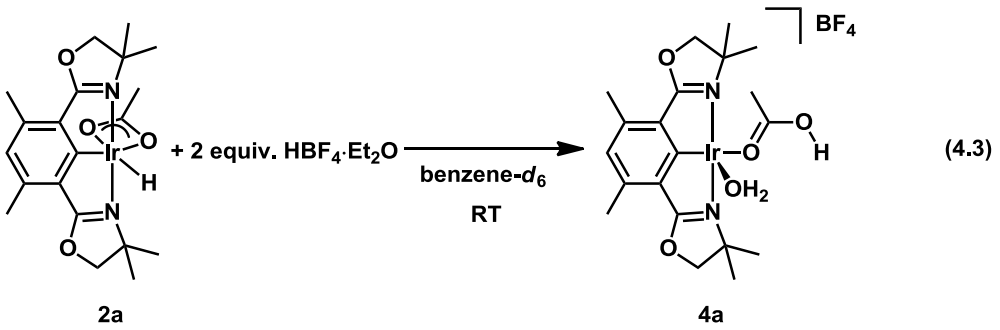

2a 4a (4.3)

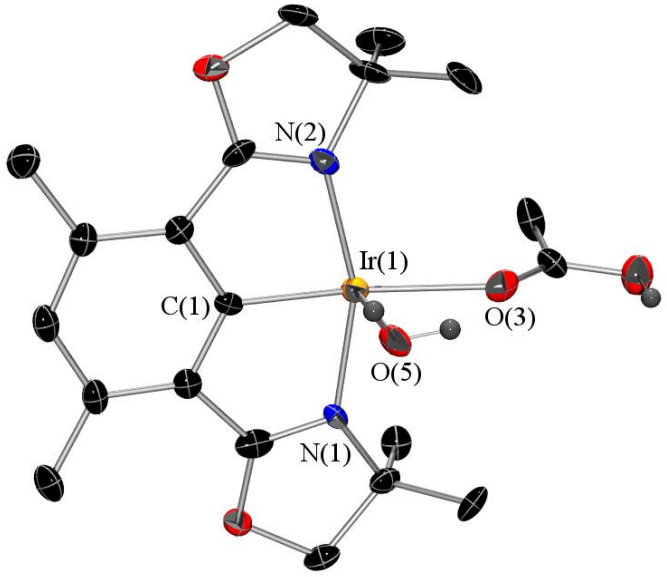

Figure 4.3. ORTEP diagram of [(^{dm}Phebox)Ir(HOAc)(OH_2)][BF_4] (**4a**) (thermal ellipsoids at 50% probability, H atoms and BF_4 counterion omitted for clarity). Selected bond distances (Å) and angles (deg): Ir(1)-C(1) = 1.923(9), Ir(1)-N(1) = 2.046(7), Ir(1)-N(2) = 2.072(7), Ir(1)-O(3) = 2.217(7), Ir(1)-O(5) = 2.256(6), N(1)-Ir(1)-N(2) = 158.6(3), C(1)-Ir(1)-O(3) = 171.8(3), C(1)-Ir(1)-O(5) = 93.5(3), C(1)-Ir(1)-N(1) = 78.9(3). C(1)-Ir(1)-N(2) = 79.7(3).

The intermediate species observed in the reaction of **2a** with acetic acid and oxygen was thought to most likely result from an initial reaction of **2a** with oxygen. To probe this hypothesis, the reaction of **2a** and oxygen in the absence of acid was explored. Surprisingly, exposure of a benzene-d_6 solution of **2a** to 3 atm of O_2 at room temperature did not result in an immediate reaction by ^{1}H NMR spectroscopy. Over the course of 3.5 h at room temperature the solution slowly darkened from a bright orange color to dark green. At this time complete consumption of **2a** was observed and a new complex (**5a**) was present in the ^{1}H NMR spectrum. The ^{1}H NMR data was representative of the formation of an asymmetrical species. Two doublets were present in the oxazolinyl region at 3.84 and 3.91 ppm each representative of two protons. Singlets at 1.25 (6H), 1.46 (6H), and 2.66 (6H) ppm were consistent with the two different methyl substituents on the oxazoline rings and the methyl group in the ^{dm}Phebox backbone. A signal indicative of coordinated OAc was observed at 1.89 ppm and integrated to three protons.

Integration of the ^{dm}Phebox-aryl proton at 6.42 ppm against an internal standard (dioxane) showed that this species was formed in 50% yield. No other products were observed in the spectrum and no precipitate was present in the NMR tube, which is highly suggestive of the formation of a paramagnetic species in this reaction.

The reaction of **2a** and oxygen was also explored in the presence of base. When 1 equiv. of NBu_4OAc was present in the reaction mixture slow formation of **1a** was observed by ^{1}H NMR spectroscopy (24 h). After 48 h complex **1a** was present in modest yield (62% vs hexamethyldisiloxane internal standard) along with three minor (^{dm}Phebox)Ir containing products (21% vs internal standard). The reaction in the presence of H_2O (1 μL) resulted in the formation of **1a** in 63% NMR yield, suggestive that the low yields obtained in these reactions did not result from a limiting amount of H_2O. The slow formation of **1a** in the absence of acetic acid may be attributed to difficulty associated with opening the κ^2-acetate ligand. If the initial step in formation of **1a** is dissociation the acetate ligand to generate an open site, then the added acetic acid may assist in decoordination of OAc. Over time in the presence of NBu_4OAc complex **1a** was formed, but at a slower rate in comparison to when acetic acid was used.

Complex **5a** is tentatively proposed to be an Ir-OOH species that results from the direct reaction of **2a** and oxygen. In order to determine if **5a** was an intermediate in the reaction of **2a** and acetic acid with oxygen, acetic acid was added to a benzene-d_6 solution of **5a** (Scheme 4.1). If this complex were present during formation of **1a** then an immediate reaction with acetic acid should occur to generate **1a**. Upon the addition of 1 equiv. of acetic acid no reaction was observed by ^{1}H NMR spectroscopy and the reaction mixture did not change color. The addition of a second equiv. of acetic acid also did not result in an immediate reaction. When the solution was left at room temperature for 72 h complex **1a** was generated in 83% yield based on **5a** (47%

based on **2a**). In the absence of HOAc, **1a** was generated in 14% yield based on **2a** after 72 h. The slow reaction of **5a** with acetic acid strongly suggests that this species is not the same as intermediate **3a**. Additionally the ^{1}H NMR spectra of intermediates **3a** and **5a** are not the same, which further supports this hypothesis.

Scheme 4.1

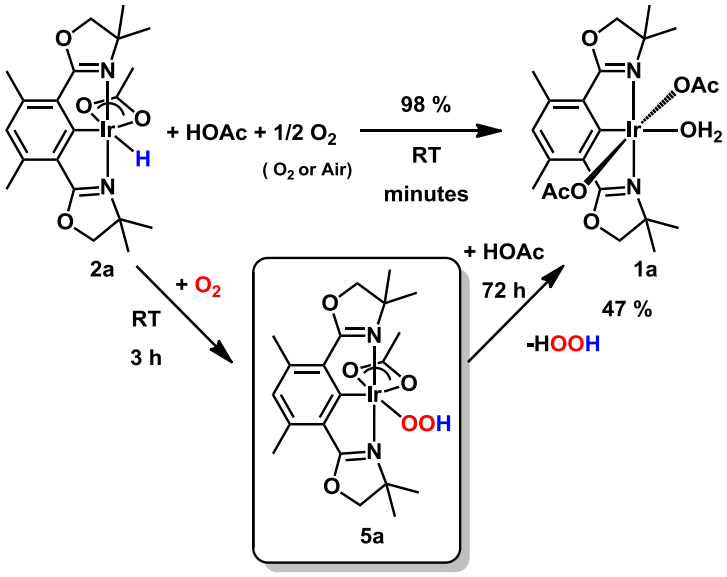

Based upon the ^{1}H NMR data described above the identity of **5a** has been tentatively proposed to be (^{dm}Phebox)Ir(OAc)OOH (**5a**). The OOH ligand may be formed from the insertion of oxygen in the Ir-hydride bond. In order to probe the presence of an OOH ligand, an assay for the detection of hydrogen peroxide was performed.[9] Isolated **5a** was subjected to an excess of H_2SO_4 and then added to an aqueous solution of $KMnO_4$. The formation of hydrogen peroxide in 73(6)% was detected using a $KMnO_4$ titration assay. Intermediate **3a** may also contain an OOH ligand. However, the formation of hydrogen peroxide was not observed in the reaction of **2a** and acetic acid with oxygen. The absence of this product may be the result of

disproportionation of hydrogen peroxide by the Ir product **1a**; the addition of 50 equiv. of a 30% hydrogen peroxide solution to a benzene solution of **1a** resulted in immediate bubbling. After 20 h gas evolution had ceased and complex **1a** was still present in solution without any decomposition to metal black. This result indicates that **1a** is a catalyst for hydrogen peroxide disproportionation to oxygen and water.

Multiple attempts were made to obtain IR data for intermediate **5a**. Complex **5a** was generated in benzene using $^{16}O_2$ and $^{18}O_2$ in separate experiments. In the solid state **5a** was stable, but for prolonged periods the solid was stored at -15 °C. In the IR spectrum of the unlabeled complex a band was observed at 954 cm^{-1} suggestive of an O-O stretching frequency. The expected isotopic shift to approximately 899 cm^{-1} (based upon a harmonic oscillator model) for **5a** generated using $^{18}O_2$ was not observed. Many attempts using both KBr pellets and nujol mulls did not result in suitable IR spectroscopic data.

Attempts to obtain X-ray quality crystals using various conditions did not result in high quality crystals. Complex **5a** could be cleanly generated in benzene and toluene. When concentrated toluene solutions of **5a** were stored at -80 °C, globular solids were obtained that were not sufficient for diffraction studies. Layering a toluene solution of **5a** with pentane also generated globular solids at -80 °C. Recrystallizations of isolated **5a** using acetonitrile (neat or solutions layered with three times the amount of pentane) or CH_2Cl_2 (neat or solutions layered with three times the amount of pentane or Et_2O) did not result in viable X-ray quality crystals at -80 or -15 °C. Instead high quality crystals of the final product complex **1a** were obtained.

Along with the formation of **1a**, a second species was observed when benzene-d_6 solutions of **5a** (without added acetic acid) were left at room temperature for 72 h. This species was asymmetrical as indicated by the two doublets in the oxazolinyl region at 3.57 and 3.67 ppm

that each integrated to two protons. A singlet at 2.07 ppm was consistent with this species having an OAc ligand and integrated to three protons against the oxazoline signals. The yields of this complex and **1a** at 72 h were 13% and 14%, respectively, based on **2a**. A potential product of this reaction is (^{dm}Phebox)Ir(OAc)OH (**6a**), which would result from oxygen atom loss from **5a**. Decomposition of M-OOH species to the corresponding M-OH has been observed in the literature.[5a,b] Attempts to obtain the direct precursor to **6a**, (^{dm}Phebox)Ir(Cl)OH(OH_2) by independent synthesis using (^{dm}Phebox)IrCl_2(OH_2) (**7a**) and Ag_2O in CH_2Cl_2 resulted in recovery of **7a**.

Synthesis of metal hydroxide and alkoxide compounds from TFA adducts has been demonstrated using Pt and Ir complexes.[10,11] Therefore steps were taken to independently synthesize **6a** from (^{dm}Phebox)Ir(TFA)Cl were undertaken. Complex (^{dm}Phebox)Ir(TFA)(OH_2)Cl (**8a**) can be easily prepared from **7a** and 1 equiv. of AgTFA in CH_2Cl_2 at room temperature and has been characterized using ^{1}H and ^{19}F NMR spectroscopy and X-ray crystallography. In the ^{1}H NMR spectrum of **8a**, a singlet at 4.63 ppm was observed for the oxazoline protons. Typically, two unique doublets are observed for the oxazolinyl protons of an asymmetrical (^{dm}Phebox)Ir species. It is unclear what causes the two different oxazoline protons to appear as a singlet in the ^{1}H NMR spectrum. A signal at -74.80 ppm was present in the ^{19}F NMR spectrum indicative of the TFA ligand. The X-ray crystallographic data obtained for **8a** confirmed the asymmetry present in the molecule and suggested the presence of a water ligand (Figure 4.4). In the ^{1}H NMR spectrum a broad signal suggestive of coordinated water was observed at 6.42 ppm. The Ir-OH_2 bond length was 2.2302(17) Å and is consistent with the reported bond Ir-OH_2 length of **1a** (2.206(3)Å).[12] The Ir-O(3) bond length, 2.0801(17) Å, is

slightly longer than the Ir-OAc bond lengths, 2.037(3) and 2.058(3) Å, of **1a** and consistent with TFA being a weaker ligand than OAc.

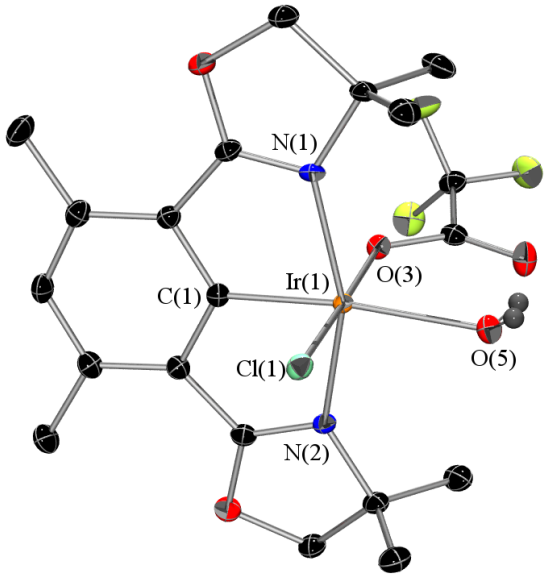

Figure 4.4. ORTEP diagram of (^{dm}Phebox)Ir(TFA)(OH_2)Cl (**8a**) (thermal ellipsoids at 50% probably, H atoms omitted for clarity). Selected bond distances (Å) and angles (deg): Ir(1)-C(1) = 1.936(2), Ir(1)-N(1) = 2.0669(19), Ir(1)-N(2) = 2.0639(19), Ir(1)-O(3) = 2.0801(17), Ir(1)-O(5) = 2.2302(17), Ir(1)-C1(1) = 2.3206(6), N(1)-Ir(1)-N(2) = 158.51(8), C(1)-Ir(1)-O(3) = 91.21(8), C(1)-Ir(1)-O(5) = 173.88(8), N(1)-Ir(1)-O(5) = 106.18(7), C(1)-Ir(1)-Cl(1) = 89.26(7), O(3)-Ir(1)-Cl(1) = 177.33(5).

When a toluene-d_8 solution of **8a** and 10 equiv. of KOH were heated at 60 °C for 24 h the formation of a new product was observed by ^{1}H NMR spectroscopy. In the oxazoline region two doublets were present at 3.60 and 3.67 ppm each integrating to two protons. A singlet at 4.36 ppm integrating to one proton was suggestive of a hydroxide ligand and a singlet at 6.52 ppm corresponded to the ^{dm}Phebox-aryl proton (1H). In the ^{19}F NMR spectrum a signal for TFA was observed at -74.66 ppm. Attempts to scale this reaction up resulted in decomposition of the starting material and the formation of an intractable brown solid. Alternative methods to synthesize **6a** were not been taken.

Loss of the hydride ligand in the reaction of **2a** and oxygen would be consistent with oxygen insertion into the Ir^{III}-hydride bond. The insertion of oxygen into an Ir^{III} –H bond to form an Ir^{III}-OOH intermediate was proposed in the hydrogenation of oxygen by $Cp^*IrH(TsDPEN)$ (TsDPEN = rac-$H_2NCHPhCHPhN(SO_2C_6H_4CH_3)^-$) (Scheme 4.2).[13] DFT calculations point to a hydrogen abstraction type mechanism similar to that proposed for O_2 insertion into a Pd^{II}-H bond.[14] Ison and coworkers have also proposed an Ir^{III}-OOH intermediate in the catalytic oxidation of alcohols using $[Cp^*IrCl]_2$.[15] More recently, Nocera and coworkers observed oxygen insertion into an Ir-H bond and isolated a binuclear Ir hydroperoxide complex (Scheme 4.2).[16] A reasonable suggestion for the identity of intermediate **3a** from the reaction of **2a** and acetic acid is (^{dm}Phebox)Ir(OAc)(HOAc)OOH as shown in Scheme 4.3. Coordination of acetic acid to the Ir center may result in the difference in chemical shifts observed for the ^{dm}Phebox ligands in **3a** and **5a**.

Scheme 4.2

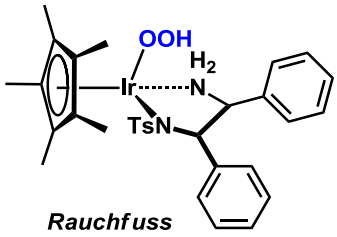

Rauchfuss

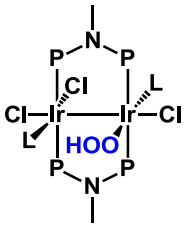

Nocera

L = $NCCH_3$

-OCH_2CF_3 groups on P omitted for clarity

Scheme 4.3

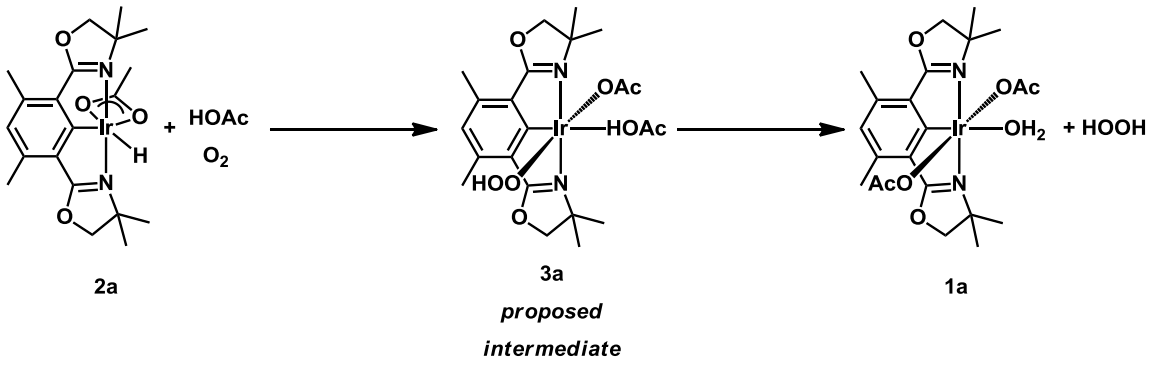

Generation of 1a Using Ethylene

In order to determine if alternative hydrogen acceptors to oxygen could be utilized, we explored the reactivity of **2a** and HOAc with ethylene. Olefins have long been employed as hydrogen acceptors in catalytic alkane dehydrogenation systems. The mechanism of hydrogen transfer typically involves olefin insertion into a metal hydride bond followed by reductive elimination of alkane. When a benzene solution of **2a** with 1 equiv. of acetic acid was exposed to 3 atm of ethylene, a reaction occurred immediately as evidenced by a color change in solution from bright orange to yellow. Analysis of the mixture by ^{1}H NMR spectroscopy immediately after mixing showed two new doublets at 3.94 and 4.20 ppm corresponding to a second species present in solution. This species reacted to form the final product, **1a**, during the course of the reaction (eq. 4.4). After 2 h at room temperature, 15% of the intermediate was present and 14% of **1a** had formed. Allowing the reaction to remain at room temperature for 21 h resulted in a 56-66% yield of **1a**. When the reaction was performed in the presence of excess acetic acid (3 equiv.) a 52% yield of **1a** was obtained. In contrast, exposure of a benzene solution of only complex **2a** to 3 atm of ethylene did not result in an observable reaction as determined by ^{1}H NMR spectroscopy. Heating the reaction mixture overnight at 100 °C also did not result in any

reaction. The importance of acetic acid in this scenario is two-fold. Not only is it required to generate **1a** in reasonable yields, but it is also needed to promote ethylene insertion in the Ir-hydride bond. To date the reaction of **2a** and acetic acid with ethylene has been irreproducible, which is suggestive of a radical mechanism for ethylene insertion. Additionally, the formation of ethane in this reaction has not been observed by ^{1}H NMR spectroscopy. Further experiments are required to provide additional insight into this reaction.

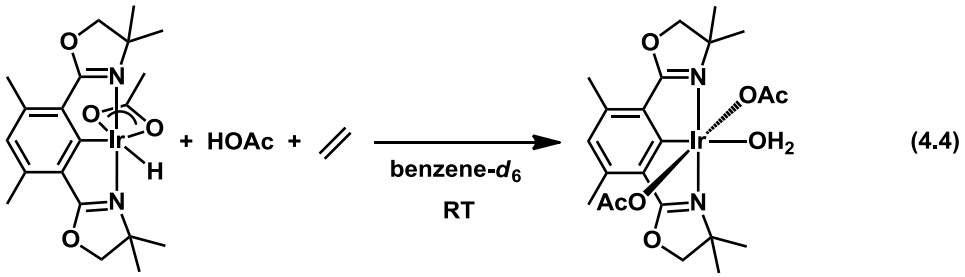

2a **1a** (4.4)

The proposed catalytic cycle for alkane dehydrogenation using complex **1a** and oxygen is shown in Scheme 4.4. In the first step of the cycle C-H activation of alkane occurs to generate an Ir-alkyl species. Formation of alkene occurs in the second step by β-hydride elimination from the Ir-alkyl complex to generate **2a**, which has been described in Chapter 3. To complete the cycle, oxygen can be used as the hydrogen acceptor resulting in regeneration of **C**. In the reaction with oxygen an Ir-hydroperoxide species is a likely intermediate. This intermediate then may react further to generate **1a** and hydrogen peroxide. Hydrogen peroxide may be produced in the reaction however, it would not be observed as **1a** has been demonstrated to catalyze hydrogen peroxide disproportionation.

Scheme 4.4

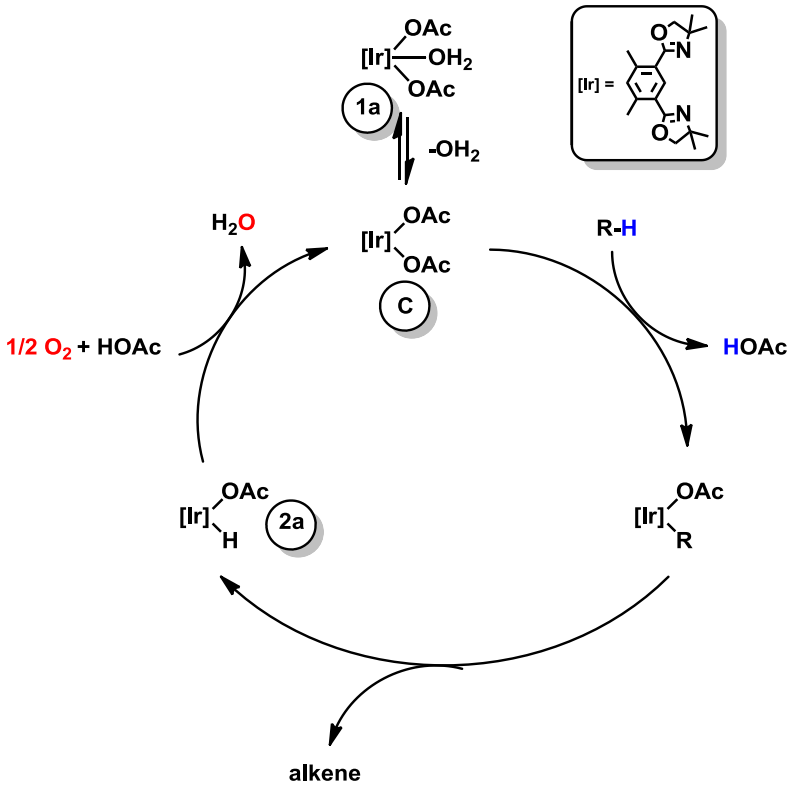

Attempted Catalytic Dehydrogenation Reactions

The system shown in Scheme 4.4 was probed for catalytic alkane dehydrogenation using oxygen from air and ethylene respectively, as hydrogen acceptors. Complex **1a** was tested as a catalyst in neat *n*-octane at 200 °C in the presence of air using a Parr reaction vessel. After 3 or 6 h the reaction mixture was analyzed by GC/MS. Octene and octanone were observed with approximately 4-6 TONs under these conditions. However, reactions conducted in the Parr vessel in the absence of Ir resulted in similar TONs for octene and octanone. This result suggested that *n*-octane functionalization was catalyzed by something in the reaction vessel and not by an Ir species. Dehydrogenation of *n*-octane using **1a** and air was explored in glass Teflon-stoppered reaction vessels. After 3 h at 200 °C the volatiles of the reaction were analyzed by

GC/MS and 1 TON for the functionalized products was observed. When the data was background corrected (background reactions also performed in glass vessels), the TONs for the formation of octene and octanone were similar suggestive of no Ir catalysis. At the end of the reaction the solutions were colorless and Ir black was observed indicative of decomposition of **1a**. As a result of the background activity observed when the Parr vessels were used, reactions using catalytic conditions were performed in glass vessels.

The formation of Ir black prompted exploration of the stability of **1a** in the presence of air. At 160 °C in the presence of air, decomposition of **1a** to Ir black was observed in both *n*-octane and hexafluorobenzene after 72 h. In contrast to the alkane dehydrogenation reactions, benzene C-H activation by **1a** could be conducted under air at 100 °C to generate (^{dm}Phebox)Ir(OAc)Ph in quantitative yield. These results suggested that **1a** is not stable to oxygen at temperatures above 100 °C. Since alkane C-H activation by **1a** is not compatible with oxygen at high temperatures, a stepwise approach was taken towards catalysis (Scheme 4.5). For example, solutions of **1a** and *n*-octane in Teflon-stoppered glass vessels were heated at 200 °C for 24 and 72 h. After cooling to room temperature, the reaction vessels were opened to air and stirred for 2 h. The mixtures were then degassed using three freeze-pump-thaw cycles and heated at 200 °C for 24 or 72 h. After several cycles at 24 or 72 h intervals the volatiles were diluted to 5 mL and analyzed by GC. Ideally, the reaction performed using 72 h time intervals (2 cycles) should generate 2 TONs for octene. In reality, only 1.4 TONs (not corrected for background) were observed. In the ^{1}H NMR spectrum of the Ir material at the end of the reaction, ^{dm}Phebox ligand, complex **1a**, and intermediate **3a** were observed. Prior to obtaining the NMR data, the reaction vessel was opened under air. Therefore Ir-hydride present at the end of the reaction should react with oxygen to generate **3a**. Broad signals in the ^{1}H NMR spectrum

were also observed indicative of formation of multiple intractable products. Decomposition of **1a** to Ir black was also observed, consistent with the formation of free pincer ligand. Under these conditions step-wise dehydrogenation catalysis was not feasible.

Scheme 4.5

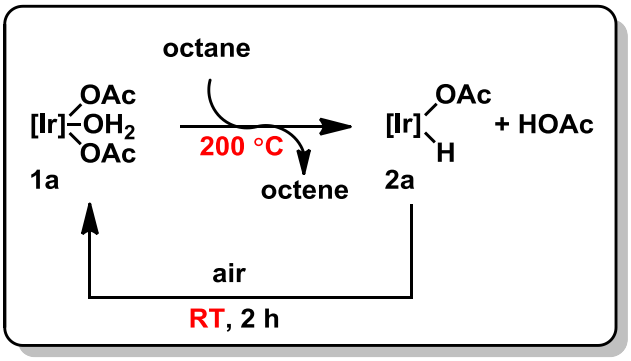

Catalytic *n*-octane dehydrogenation was also probed using ethylene as the hydrogenation acceptor. A Parr reaction vessel was charged with **1a**, *n*-octane, and 8 atm of ethylene. After 72 h at 200 °C the reaction was analyzed by GC and ^{1}H NMR spectroscopy. Octene was not observed as a product of the reaction. In the ^{1}H NMR spectrum of the Ir material a new asymmetrical compound was present (Figure 4.5). Two doublets were observed at 3.78 and 3.84 ppm in the oxazolinyl region consistent with an asymmetrical product. Three new doublet of doublets (dd) were observed at 3.72, 4.95, and 7.27 ppm consistent with a vinyl ligand. This Ir product was assigned as (^{dm}Phebox)Ir(OAc)(C_2H_3) (**9a**) (eq. 4.5). The doublet of doublets at 7.27 ppm corresponds to the vinylic proton H_a and the two doublets upfield are the geminal protons (H_b and H_c). These assignments were made based upon the observed coupling constants of the alkene protons. Complex **9a** likely resulted from C-H activation of ethylene by **1a** to generate acetic acid and the Ir-vinyl product. This is unsurprising as complex **1a** is effective at

cleaving sp^2 C-H bonds at temperatures lower than 200 °C. Attempts to independently synthesize **9a** in *n*-octane at 140 °C from **1a** and 3 atm of ethylene did not result in a reaction. Complex **1a** was recovered from this reaction. The starting material **1a** is not very soluble in *n*-octane at 140 °C and so alternative solvents (without C-H bonds that can compete with ethylene for C-H activation) are necessary to explore ethylene activation.

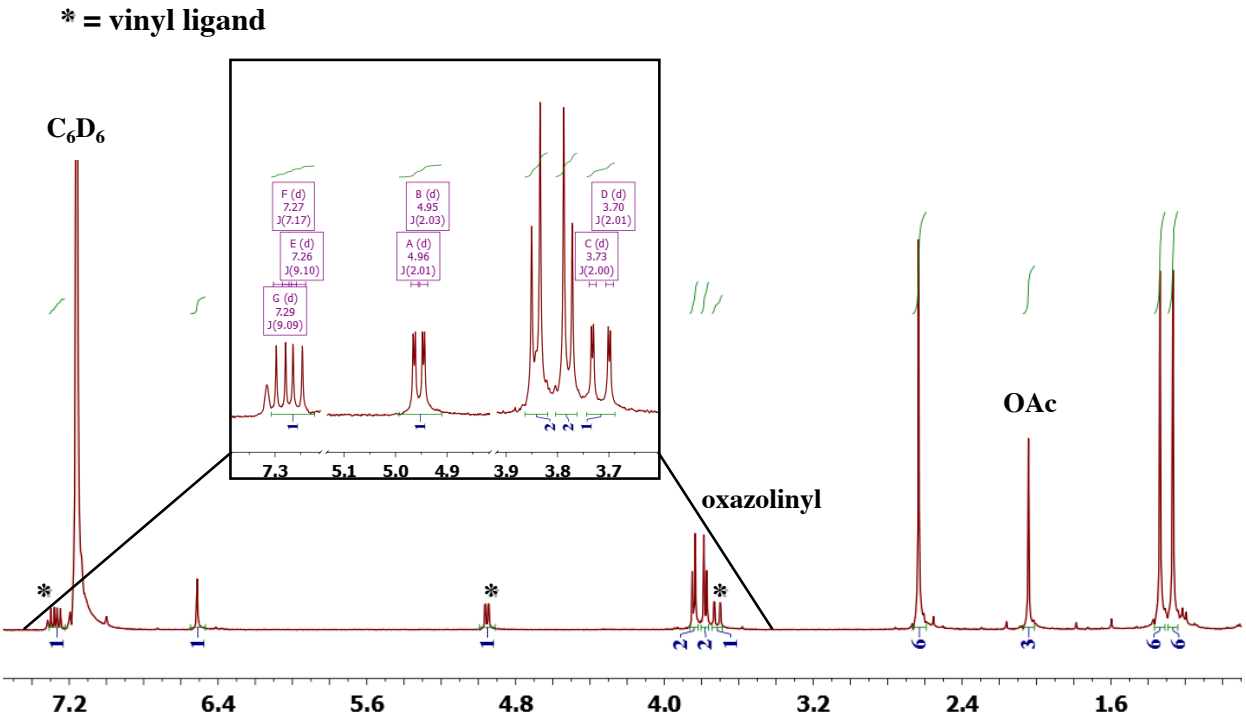

Figure 4.5. ^{1}H NMR spectrum of (^{dm}Phebox)Ir(OAc)(C_2H_3) (**9a**) in benzene-d_6 obtained from the reaction of **1a** and ethylene at 200 °C in *n*-octane. The ^{1}H NMR signals consistent with the vinyl ligand are denoted by *.

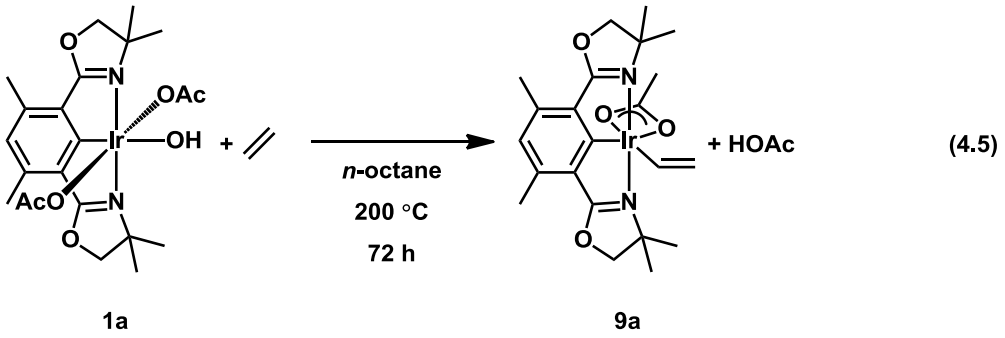

Attempts to Synthesize Ir-methyl Complex to Examine Potential Oxygen Insertion

Oxygen insertion into metal alkyl bonds has been observed in several different late transition metal systems. This reaction is of interest as this is a potential route to the transformation of methane to methanol. Methane activation by **1a** may yield complex (^{dm}Phebox)Ir(OAc)CH_3 (**10a**), which could react productively with oxygen to produce methanol. Complex **10a** has not been previously reported and so several methods were utilized to try to prepare this species. Methane activation by **1a** was explored in several different solvents. When **1a** and 20 atm of methane were heated in hexafluorobenzene at 200 °C for 6 days no reaction was observed and **1a** was recovered from the reaction. Complex **10a** may be formed under these conditions, but react with HOAc to reform **1a**. The CH_4 activation reaction was repeated in the presence of K_2CO_3 to remove any HOAc formed and trap **10a** if it was formed. The Ir starting material was recovered from the reaction and methane activation was not observed. When solvents, such as water and HOAc were used decomposition of **1a** to Ir black was observed at elevated temperatures (180-250 °C).

Alternative routes to the synthesis of **10a** were taken that did not involve methane activation. The reaction of (^{dm}Phebox)Ir$Cl_2(OH_2)$ (**7a**) with methylating reagents CH_3Li, $ZnMe_2$ and CH_3MgBr were explored. When 1 equiv. of CH_3Li was added to a THF-d_8 solution of **7a** at

room temperature the formation of a new product was observed. In the ^{1}H NMR spectrum broad signals were present indicative of the new species along with signals corresponding to **7a**. When the reaction was conducted with 4 equiv. of CH_3Li at room temperature or -35 °C in THF the formation of multiple species was observed by ^{1}H NMR spectroscopy. Signals consistent with a methyl ligand (-1 to 2 ppm) were not found in the spectrum. When 3 equiv. of CH_3MgBr was added to a THF solution of **7a** at -35 °C a reaction was observed by ^{1}H NMR spectroscopy. Broad signals assigned to the ^{dm}Phebox ligand were observed, but no signal was observed for a methyl ligand. The reaction of **7a** with $ZnMe_2$ was explored in THF-d_8 at 100 °C. No reaction was observed in this case even after heating at 100 °C for 4 days in the presence of 4 equiv. of $ZnMe_2$. Under these conditions the desired product **10a** was not observed and so other starting materials were explored.

A different precursor to **10a**, (^{dm}Phebox)Ir(OAc)Cl (**11a**) was prepared. An advantage of using **11a** as the starting material is that water is not present in the molecule. Complex **11a** can be cleanly generated from **7a** and 1 equiv. of AgOAc in CH_2Cl_2 at room temperature and has been characterized by ^{1}H and ^{13}C NMR spectroscopy and X-ray crystallography. In the ^{1}H NMR spectrum of **11a** two doublets were observed at 3.82 and 3.94 ppm in the oxazoline region, each integrating to two protons, consistent with an asymmetrical complex. A singlet indicative of the OAc ligand was present at 1.78 ppm and integrated to three protons. The X-ray crystallographic data obtained (Figure 4.6) was also consistent with an asymmetrical complex. The Ir-O bond lengths observed for the κ^2-acetate ligand are consistent with the bond lengths reported for complex **2a**.

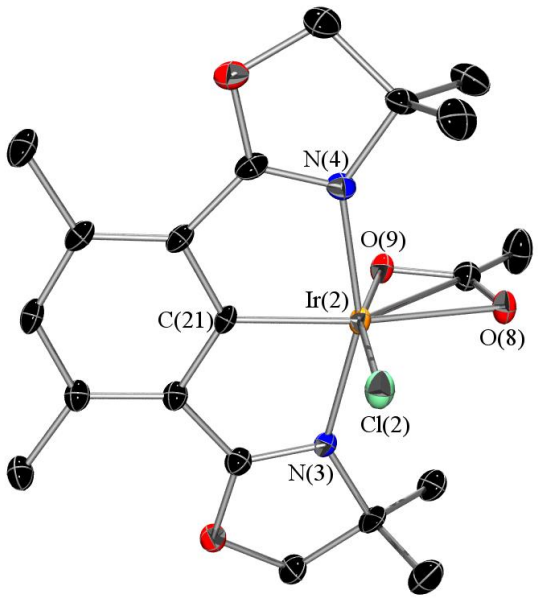

Figure 4.6. ORTEP diagram of (^{dm}Phebox)Ir(OAc)Cl (**11a**) (thermal ellipsoids at 50% probably, H atoms omitted for clarity). Selected bond distances (Å) and angles (deg): Ir(2)-C(21) = 1.927(3), Ir(2)-N(3) = 2.064(2), Ir(2)-N(4) = 2.052(2), Ir(2)-O(8) = 2.255(2), Ir(2)-O(9) = 2.097(2), Ir(2)-C1(2) = 2.3268(8), N(3)-Ir(2)-N(4) = 158.22(9), C(21)-Ir(1)-O(8) = 165.56(10), C(21)-Ir(2)-O(9) = 105.26(10), N(3)-Ir(2)-O(9) = 90.25(9), C(21)-Ir(2)-Cl(2) = 90.50(8), O(9)-Ir(2)-Cl(2) = 164.24(6).

The addition of 1 equiv. of CH_3Li to complex **11a** in benzene-d_6 resulted in the formation of new broad signals by ^{1}H NMR spectroscopy after 1 h. At this time 50% of the starting material remained and so a second equiv. of CH_3Li was added resulting in complete conversion to the broad species. The broad signals in the ^{1}H NMR spectrum were attributed to the ^{dm}Phebox ligand and a broad signal at 1.57 ppm integrating to three protons was consistent with a methyl ligand. The product expected from this reaction, complex **10a** was not expected to be a fluxional species. The Ir-hydride complex **2a** does not exhibit fluxional behavior on the NMR timescale. When 3 eqiuv. of CH_3MgBr was added to a THF solution of **11a** at -35 °C a similar broad species was observed by ^{1}H NMR spectroscopy. In contrast to the reactions described above, when 1 equiv. of $ZnMe_2$ was added to a benzene-d_6 solution of 8 no reaction was observed at room temperature. Upon heating at 60 °C for 2 h the formation of two new products along with

the presence of **11a** was observed by ^{1}H NMR spectroscopy. Heating the reaction overnight at 60 °C did not result in any change in the reaction. A second equiv. of $ZnMe_2$ was added to the reaction and the mixture was heated at 60 °C for 5 h. No change was observed in the ^{1}H NMR spectrum. Further heating at 100 °C for 24 did not result in any further reaction. Interestingly, when 0.5 equiv. of $ZnMe_2$ was used the same product distribution was observed. The reaction of **11a** with various methylating reagents has not led to any isolable products.

Conclusions

We have demonstrated that (^{dm}Phebox)Ir(OAc)$_2$(OH$_2$) (**1a**) can be generated efficiently from (^{dm}Phebox)Ir(OAc)(H) (**2a**) and acetic acid when oxygen is used as the hydrogen acceptor. The identity of the intermediate (**3a**) in this reaction has been difficult to determine using NMR spectroscopy and we have not been able to grow suitable crystals for analysis by X-ray crystallography. A reasonable proposal for this species is (^{dm}Phebox)Ir(OAc)(HOAc)OOH. The intermediate generated from **2a** and oxygen (**5a)** is notably different than the intermediate **3a**, which was observed during when acetic acid was present in the reaction. During this reaction only 50% of **5a** was generated from **2a**. The rest of **2a** likely generated a paramagnetic species, which does not form **1a** after 72 h at room temperature. Intermediates **3a** and **5a** are not the same as indicated by the ^{1}H NMR spectral data. The different yields of **1a** (based on **2a**) obtained from the decay of these species in the presence of acetic acid also supports that these intermediates are different. Generation of the dicarboxylate complex **1a-c** from the Ir-hydride species **2a-c** and oxygen appears to be general for different carboxylate ligands. Ethylene can also be used as a hydrogen acceptor, but the mechanism of this reaction may not be as straightforward as olefin insertion into (PCP)Ir hydride bonds and may involve a radical mechanism as the reaction has not been reproducible. Surprisingly, ethane was not observed in

this reaction. Complex **1a** is not stable to oxygen at temperatures above 100 °C and ^{1}H NMR spectroscopy and GC/MS have not provided insight into the potential products of this reaction. Alternative pincer ligands to ^{dm}Phebox may be necessary to achieve higher stability in the presence of oxygen at the elevated temperature required for C-H activation. Arene C-H activation by **1a** was compatible with oxygen at 100 °C and so if alkane dehydrogenation can be promoted at lower temperatures catalysis may be achieved using oxygen as a hydrogen acceptor. The results described in this chapter disclose the first example of using oxygen as a hydrogen acceptor for alkane dehydrogenation, albeit in a stoichiometric manner, and provide further insight into the elements required to perform this transformation.

Experimental

General Considerations. Unless specified otherwise, all reactions were carried out under a dry nitrogen atmosphere using standard glovebox, Schlenk, or vacuum-line techniques. AgOAc, AgOBz, AgTFA, and HBF_4 etherate were purchased from Aldrich and used as received. Oxygen (research grade) and ethylene were obtained from Praxair. Solvents were purified before use: toluene, benzene, and pentane were purified by passage through columns of activated alumina and molecular sieves. Deuterated solvents were purchased from Cambridge Isotope Laboratories. Benzene-d_6 was dried over sodium/benzophenone, and dichloromethane-d_2, chloroform-d_1 were dried over CaH_2. NMR spectra were obtained on Bruker AV300 or AV500 MHZ spectrometers with chemical shifts (δ) reported in ppm downfield of tetramethylsilane. ^{dm}Phebox,[8] (^{dm}Phebox)Ir(OAc)$_2$(OH$_2$) (**1a**),[8] (^{dm}Phebox)Ir(OAc)(H) (**2a**)[4], (^{dm}Phebox)IrCl$_2$(OH$_2$) (**7a**)[8] and AgOPiv[17] were prepared according to published procedures. Elemental analyses were performed by Atlantic Microlab Inc. of Norcross, GA.

Synthesis and Characterization of Complexes

(^{dm}Phebox)Ir(OBz)H (2b). A Teflon-stoppered NMR tube was charged with **2a** (2.5 mg, 0.0045 mmol), 450 μL of benzene, and 23 μL of a 0.20 M HOBz in benzene-d_6 solution (0.0045 mmol). After 10 min at room temperature the volatiles were removed in vacuo and benzene-d_6 (450 μL) was added. Dioxane was added to the reaction mixture as the internal standard (10 μL of 0.023 M dioxane in benzene-d_6 solution). Yield: 99%. ^{1}H NMR (C_6D_6, 500 MHz): δ 8.55 (d, 2H, *ortho*-OBz), 7.22 (t, 2H, *meta*-OBz), 7.18 (para-OBz), 6.52 (s, 1H, ^{dm}Phebox-aryl), 3.80 (d, 2H, $^1J_{HH'}$ = 8.1 Hz, OCH_2), 3.72 (d, 2H, $^1J_{HH'}$ = 8.1 Hz, OCH_2), 2.65 (s, 6H, Phebox-CH_3), 1.29 (s, 6H, CH_3), 1.22 (s, 6H, CH_3), -33.68 (s, 1H, hydride).

(^{dm}Phebox)Ir(OPiv)H (2c). A Teflon-stoppered NMR tube was charged with **2a** (2.6 mg, 0.0047 mmol), 450 μL of benzene, and 24 μL of a 0.20 M HOPiv in benzene-d_6 solution (0.0047 mmol). After 10 min at room temperature the volatiles were removed *in vacuo* and the solid was dissolved in benzene (450 μL) and then the volatiles were removed *in vacuo* again. The orange solid was dissolved in benzene-d_6 (450 μL). Dioxane was added to the reaction mixture as the internal standard (10 μL of 0.023 M dioxane in benzene-d_6 solution). Yield: 99%. ^{1}H NMR (C_6D_6, 500 MHz): δ 6.50 (s, 1H, ^{dm}Phebox-aryl), 3.83 (d, 2H, $^1J_{HH'}$ = 8.2 Hz, OCH_2), 3.76 (d, 2H, $^1J_{HH'}$ = 8.2 Hz, OCH_2), 2.65 (s, 6H, Phebox-CH_3), 1.46 (s, 9H, OPiv), 1.31 (s, 6H, CH_3), 1.25 (s, 6H, CH_3), -33.83 (s, 1H, hydride).

(^{dm}Phebox)Ir(OBz)$_2$(OH$_2$) (1b). A 10 mL Teflon-stoppered reaction vessel was charged with **7a** (52 mg, 0.090 mmol), AgOBz (41 mg, 0.18 mmol), and 3 mL of CH_2Cl_2. The reaction mixture was heated at 60 °C for 24 h and then the volatiles were removed *in vacuo*. Complex **1b** was dissolved in benzene (5 mL) and the mixture was filtered through Celite on a glass fritted filter. The volatiles were lyophilized overnight to give **1b** as a bright yellow solid. Yield: 49 mg,

73%. ^{1}H NMR ($CDCl_3$, 500 MHz): δ 7.67 (d, 2H, *ortho*-OBz), 7.32 (t, 1H, *para*-OBz), 7.22 (t, 2H, *meta*-OBz), 6.70 (s, 1H, ^{dm}Phebox-aryl), 4.55 (s, 4H, OCH_2), 2.72 (s, 6H, Phebox-CH_3), 1.46 (s, 12H, CH_3), -33.82 (s, 1H, hydride). ^{13}C NMR ($CDCl_3$, 125 MHz): δ 178.34 (OBz), 177.56 (C=N), 170.66, 140.48, 134.34, 130.83, 129.08, 127.60, 126.93, 126.21, 82.21 ($OCH_2C(CH_3)_2$), 65.46 ($OCH_2C(CH_3)_2$), 27.16 (CH_3), 18.85 (Phebox-CH_3). Anal. Calcd for $C_{32}H_{35}N_2O_7Ir$: C, 51.10; H, 4.70; N, 3.70. Found: C, 50.62; H, 4.72; N, 3.73.

(^{dm}Phebox)Ir(OPiv)$_2$(OH$_2$) (1c). A 10 mL Teflon-stoppered reaction vessel was charged with **7a** (71 mg, 0.12 mmol), AgOPiv (51 mg, 0.24 mmol), and 4 mL of CH_2Cl_2. The reaction mixture was heated at 60 °C for 24 h and then the volatiles were removed *in vacuo*. Complex **1c** was dissolved in benzene (5 mL) and the mixture was filtered through Celite on a glass fritted filter. The volatiles were lyophilized overnight to give **1b** as a bright yellow solid. Yield: 71 mg, 83%. ^{1}H NMR ($CDCl_3$, 500 MHz): δ 6.64 (s, 1H, ^{dm}Phebox-aryl), 4.59 (s, 4H, OCH_2), 2.68 (s, 6H, Phebox-CH_3), 1.44 (s, 12H, CH_3), 0.88 (s, 18H, OPiv). ^{13}C NMR ($CDCl_3$, 125 MHz): δ 190.66 (OPiv), 177.59 (C=N), 140.41, 126.99, 125.68, 82.53 ($OCH_2C(CH_3)_2$), 66.04 ($OCH_2C(CH_3)_2$), 39.21 (OPiv), 28.02 (OPiv), 27.14 (CH_3), 18.73 (Phebox-CH_3).

[(^{dm}Phebox)Ir(HOAc)(OH$_2$)][BF$_4$] (4a). A Teflon-stoppered NMR tube was charged with **2a** (3.5 mg, 0.0063 mmol) and benzene-d_6 (450 μL) and then HBF_4 etherate (1.7 μL, 0.013 mmol) was added to the orange solution. Upon mixing the solution immediately became bright yellow in color and a yellow solid began to precipitate. The X-ray structure for **4a** was obtained using some of the yellow crystals that crashed out of solution. ^{1}H NMR (C_6D_6, 500 MHz): δ 6.39 (s, 1H, ^{dm}Phebox-aryl), 4.05 (br s, 2H, OCH_2), 3.86 (d, 2H, $^{1}J_{HH'}$ = 8.3 Hz, OCH_2), 2.54 (s, 6H, Phebox-CH_3), 1.63 (br s, 3H, OAc), 1.27 (s, 6H, CH_3), 0.90 (s, 6H, CH_3).

(^{dm}Phebox)Ir(TFA)(OH_2)Cl (8a). A 50 mL round bottom was charged with **7a** (79 mg, 0.14 mmol), 4 mL CH_2Cl_2 and AgTFA (30 mg, 0.14 mmol). The mixture was stirred at room temperature overnight. The orange solution was filtered through Celite and glass wool to remove AgCl and the volatiles were removed in vacuo to give a bright orange/yellow solid. Yield: 89 mg, 97%. ^{1}H NMR (CD_2Cl_2, 300 MHz): δ 6.72 (s, 1H, ^{dm}Phebox-aryl), 6.42 (s, 2H, OH_2), 4.63 (s, 4H, OCH_2), 2.68 (s, 6H, Phebox-CH_3), 1.56 (s, 6H, CH_3), 1.39 (s, 6H, CH_3). ^{19}F NMR (C_6D_6, 300 MHz): δ -74.80 (TFA).

(^{dm}Phebox)Ir(OAc)Cl (11a). A 50 mL round bottom flask was charged with **7a** (56 mg, 0.097 mmol), 3 mL CH_2Cl_2, and AgOAc (16 mg, 0.097 mmol). The mixture was stirred at room temperature overnight to give a bright orange/yellow solution and white solid. The solution was filtered through Celite and glass wool and the volatiles were removed in vacuo to give an orange solid. The solid was dried overnight in vacuo. Yield: 53 mg, 93%. ^{1}H NMR (C_6D_6, 500 MHz): δ 6.38 (s, 1H, ^{dm}Phebox-aryl), 3.94 (d, 2H, $^1J_{HH'}$ = 8.3 Hz, OCH_2), 3.82 (d, 2H, $^1J_{HH'}$ = 8.3 Hz, OCH_2), 2.55 (s, 6H, Phebox-CH_3), 1.78 (s, 3H, OAc), 1.60 (s, 6H, CH_3), 1.19 (s, 6H, CH_3). ^{13}C NMR (C_6D_6, 125 MHz): δ 189.28 (OAc), 176.90 (C=N), 169.29, 140.50, 127.25, 125.63, 82.10 ($OCH_2C(CH_3)_2$), 65.81 ($OCH_2C(CH_3)_2$), 26.96 (CH_3), 26.71 (CH_3), 23.68 (OAc), 18.72 (Phebox-CH_3).

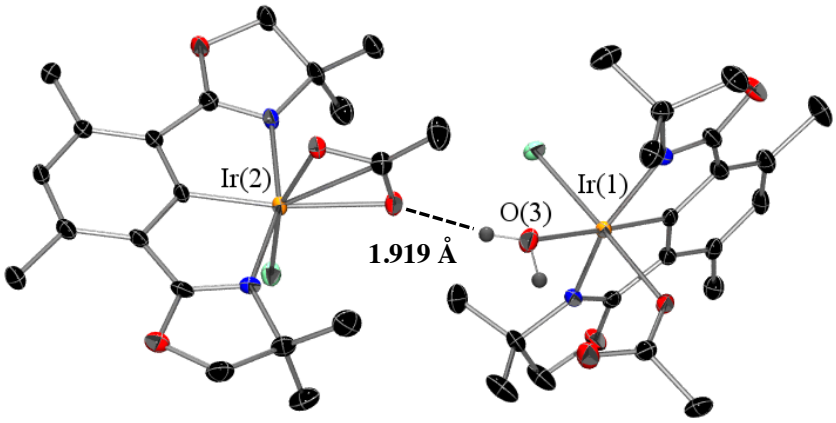

Figure 4.7. ORTEP diagram of (^{dm}Phebox)Ir(OAc)Cl (**11a**) (thermal ellipsoids at 50% probably, H atoms omitted for clarity). Two independent molecules were found in the asymmetric unit. The molecule containing Ir(2) is consistent with the ^{1}H NMR spectral data discussed above. The second molecule containing Ir(1) is most likely a result of the crystallization method. A hydrogen bond has been observed in the X-ray data between the protons bound to O(3) and the κ^2-acetate ligand.

Reactions with Oxygen

Reaction of 2a and HOAc with air. A Teflon-stoppered NMR tube was charged with **2a** (2.3 mg, 0.0042 mmol), 450 µL of benzene-d_6 and 25 µL of a 0.17 M HOAc in benzene-d_6 solution (0.0042 mmol). Dioxane was added to the reaction mixture as the internal standard (10 µL of 0.023 M dioxane in benzene-d_6 solution). The solution was degassed using three freeze-pump-thaw cycles and then opened to air. The bright orange colored solution immediately became yellow in color after mixing the solution. After 2 h at room temperature the yield of **1a** was determined to be 98%. Integration of dioxane signal vs the ^{dm}Phebox-aryl-H signal was used to obtain yield.

Reaction of 2a and HOAc with oxygen. A Teflon-stoppered NMR tube was charged with **2a** (2.6 mg, 0.0047 mmol), 450 µL of benzene-d_6 and 27 µL of a 0.17 M HOAc in benzene-d_6 solution (0.0047 mmol). Dioxane was added to the reaction mixture as the internal standard (10 µL of 0.023 M dioxane in benzene-d_6 solution). The solution was degassed using three freeze-

pump-thaw cycles and then charged with 3 atm of oxygen. The bright orange colored solution immediately became yellow in color after mixing the solution. After 2 h at room temperature the yield of **1a** was determined to be 83%. Integration of dioxane signal vs the ^{dm}Phebox-aryl-H signal was used to obtain yield.

Reaction of 2a and HOAc with oxygen with added H_2O. A Teflon-stoppered NMR tube was charged with **2a** (2.5 mg, 0.0047 mmol), 450 μL of benzene-d_6 and 27 μL of a 0.17 M HOAc in benzene-d_6 solution (0.0047 mmol). HPLC grade water was added to the reaction (1 μL). Dioxane was added to the reaction mixture as the internal standard (10 μL of 0.023 M dioxane in benzene-d_6 solution). The solution was degassed using three freeze-pump-thaw cycles and then charged with 3 atm of oxygen. The bright orange colored solution immediately became yellow in color after mixing the solution. After 2.5 h at room temperature the yield of **1a** was determined to be 96%. Integration of dioxane signal vs the ^{dm}Phebox-aryl-H signal was used to obtain yield.

Reaction of 2b and HOBz with air. Complex **2b** was prepared *in situ* in a Teflon-stoppered NMR tube from **2a** (2.5 mg, 0.0045 mmol) and 23 μL (0.0045 mmol) of a 0.20 M HOBz solution in benzene-d_6 as described above. The volatiles were removed *in vacuo*. The orange solid was dissolved in benzene-d_6 (450 μL) and a second equiv. of HOBz solution was added (23 μL, 0.0045 mmol). Dioxane (10 μL of 0.023 M dioxane in benzene-d_6 solution) was added to the tube as an internal standard and the solution was degassed using three freeze-pump-thaw cycles. The mixture was exposed to air and after 2.5 h at room temperature the yield of **1b** was determined to be 80%. Integration of dioxane signal vs ^{dm}Phebox-aryl-H signal was used to obtain yield.

Reaction of 2c and HOPiv with air. Complex **2c** was prepared *in situ* in a Teflon-stoppered NMR tube from **2a** (2.6 mg, 0.0047 mmol) and 24 μL (0.0047 mmol) of a 0.20 M HOPiv solution in benzene-d_6 as described above. The volatiles were removed *in vacuo*. The orange solid was dissolved in benzene-d_6 (450 μL) and a second equiv. of HOPiv solution was added (24 μL, 0.0047 mmol). Dioxane (10 μL of 0.023 M dioxane in benzene-d_6 solution) was added to the tube as an internal standard and the solution was degassed using three freeze-pump-thaw cycles. The mixture was exposed to air and after 3 h at room temperature the yield of **1c** was determined to be 97%. Integration of dioxane signal vs ^{dm}Phebox-aryl-H signal was used to obtain yield.

Intermediate 5a. A Teflon-stoppered NMR tube was charged with **2a** (3.6 mg, 0.0065 mmol) and benzene (450 μL). The solution was degassed using three freeze-pump-thaw cycles and the tube was charged with 3 atm of oxygen. After 3.5 h at room temperature, the solution was jungle green in color. Yield: 50% against dioxane internal standard. Complex **5a** was isolated as a green solid after lyophilization of benzene. ^{1}H NMR (CD_6D_6, 500 MHz): δ 6.42 (s, 1H, ^{dm}Phebox-aryl), 4.26 (br s, 1H, OOH), 3.91 (d, 2H, $^1J_{HH'}$ = 8.0 Hz, OCH_2), 3.84 (d, 2H, $^1J_{HH'}$ = 8.2 Hz, OCH_2), 2.66 (s, 6H, Phebox-CH_3), 1.89 (s, 3H OAc), 1.46 (s, 6H, CH_3), 1.25 (s, 6H, CH_3). ^{13}C NMR (C_6D_6, 200 MHz): δ 177.24, 139.82, 127.16, 124.29, 82.00 ($OCH_2C(CH_3)_2$), 65.42 ($OCH_2C(CH_3)_2$), 26.72 (CH_3), 26.56 (CH_3), 23.88 (OAc), 18.74 (Phebox-CH_3).

Detection of hydrogen peroxide. A solid sample of **5a** (2.5 mg) was dissolved in concentrated H_2SO_4 (400 μL, 7.5 mmol) at room temperature to afford a pale yellow solution. The resulting solution was then added in a single aliquot to an aqueous room temperature solution of $KMnO_4$ (4.4×10^{-4} M, 3 mL). Electronic absorption spectra of the $KMnO_4$ solution were recorded before and after addition of the acidified **5a** solution. The amount of H_2O_2 liberated from the acidified

solution was determined by the change in $KMnO_4$ concentration,[9] which resulted in the detection of H_2O_2 in 73(6)% yield (assuming the molecular weight of **5a** to be 584 g/mol) based upon three experimental trials.

Disproportionation of hydrogen peroxide by 1a. A Teflon-stoppered NMR tube was charged with **1a** (3.2 mg, 0.0051 mmol) and 450 μL of benzene-d_6. Then 50 equiv. of 30% aqueous HOOH solution (25 μL, 0.25 mmol) were added and immediate evolution of oxygen was observed. After 21 h at room temperature gas evolution was no longer observed. Complex **1a** was still present in the ^{1}H NMR spectrum.

Example of catalytic conditions for *n*-octane dehydrogenation in the presence of air. A 25 mL glass Teflon-stoppered reaction vessel was charged with **1a** (1.6 mg, 0.0026 mmol) and 2.5 mL of *n*-octane under air. The mixture was heated at 200 °C for 3 h and then the volatiles were transferred to a 5 mL volumetric flask. The glass vessel was rinsed with pentane and combined. Mesitylene (6 μL) was added as the internal standard and the solution was diluted up to 5 mL with pentane. The volatiles were analyzed by GC and GC/MS. An aliquot of the solution was transferred to a J. Young tube and the volatiles were removed *in vacuo*. The Ir residue was dissolved in benzene-d_6 and analyzed by ^{1}H NMR spectroscopy. The formation of Ir black was observed in the reaction along with the presence of multiple intractable products as observed in the ^{1}H NMR spectrum.

Example of stepwise catalytic conditions for *n*-octane dehydrogenation. A 25 mL glass Teflon-stoppered reaction vessel was charged with **1a** (5.0 mg, 0.0080 mmol) and 3 mL of *n*-octane. The mixture was degassed using three freeze-pump-thaw cycles and then heated at 200 °C. After 72 h the mixture was cooled to room temperature and then exposed to air and stirred for 2 h. The mixture was degassed using three freeze-pump-thaw cycles and then heated at 200

°C for 72 h. After cooling to room temperature the volatiles were transferred to a 5 mL volumetric flask. The glass vessel was rinsed with pentane and combined. An internal standard (mesitylene 6 μL) was added the solution was diluted up to 5 mL using pentane. The volatiles were analyzed by GCMS. An aliquot of the solution was transferred to a J. Young tube and the volatiles were removed *in vacuo*. The Ir residue was dissolved in benzene-d_6 and analyzed by ^{1}H NMR spectroscopy. Complex **1a** was observed in the spectrum along with the formation of ^{dm}Phebox. Generation of free pincer ligand is consistent with the formation of Ir black in the reaction.

Reactions with Ethylene

Reaction of 2a and ethylene. A Teflon-stoppered NMR tube was charged with **2a** (3.2 mg, 0.0058 mmol), 450 μL of benzene-d_6 and 3 equiv. of a 0.17 M HOAc in benzene-d_6 solution (100 μL, 0.017 mmol). Dioxane was added to the reaction mixture as the internal standard (10 μL of 0.023 M dioxane in benzene-d_6 solution). The solution was degassed using three freeze-pump-thaw cycles and then charged with 3 atm of ethylene. The bright orange colored solution slowly became yellow in color overnight. The yield of **1a** was determined to be 52%. Integration of dioxane signal vs ^{dm}Phebox-aryl-H signal was used to obtain yield.

(^{dm}Phebox)Ir(OAc)(C_2H_3) (9a). A Parr reaction vessel was charged with **1a** (10 mg, 0.016 mmol), 2 mL of *n*-octane, and sealed under a nitrogen atmosphere. The vessel was then charged with 8 atm of ethylene and heated to 200 °C. After 72 h the mixture was cooled to room temperature. Mesitylene (6 μL) was added to the solution and the volatiles were analyzed by GC. An aliquot of the solution was transferred to a J. Young tube and the volatiles were removed *in vacuo*. The Ir residue was dissolved in benzene-d_6 and analyzed by ^{1}H NMR spectroscopy. ^{1}H NMR (C_6D_6, 500 MHz): δ 7.27 (dd, 1H, $^3J_{HaHb}$ = 16.3 Hz, $^3J_{HaHc}$ = 9.1 Hz, H_a),

6.51 (s, 1H, ^{dm}Phebox-aryl), 4.95 (dd, 1H, $^{3}J_{HcHa}$ = 9.1 Hz, $^{2}J_{HcHb}$ = 2.0 Hz, H_c), 3.84 (d, 2H, $^{1}J_{HH'}$ = 8.3 Hz, OCH_2), 3.78 (d, 2H, $^{1}J_{HH'}$ = 8.3 Hz, OCH_2), 3.71 (dd, 1H, $^{3}J_{HbHa}$ = 16.3 Hz, $^{2}J_{HbHc}$ = 2.0 Hz, H_b), 2.63 (s, 6H, Phebox-CH_3), 2.04 (s, 3H, OAc), 1.34 (s, 6H, CH_3), 1.27 (s, 6H, CH_3).

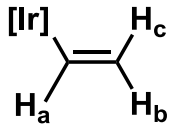

Details of Solid State Structure Determination of 4a.

A yellow prism, measuring 0.10 x 0.05 x 0.03 mm^3 was mounted on a loop with oil. Data was collected at -173 °C on a Bruker APEX II single crystal X-ray diffractometer, Mo-radiation. Crystal-to-detector distance was 40 mm and exposure time was 100 seconds per frame for all sets. The scan width was 0.5°. Data collection was 99.6% complete to 25° in ϑ. A total of 34746 reflections were collected covering the indices, h = -26 to 26, k = -10 to 10, l = -35 to 35. 4819 reflections were symmetry independent and the R_{int} = 0.1732 indicated that the data was of less than average quality (0.07). Indexing and unit cell refinement indicated a C-centered monoclinic lattice. The space group was found to be C 2/c (No.15). The data was integrated and scaled using SAINT, SADABS within the APEX2 software package by Bruker.[18]

Solution by direct methods (SHELXS, SIR97[19]) produced a complete heavy atom phasing model consistent with the proposed structure. The structure was completed by difference Fourier synthesis with SHELXL97.[20,21] Scattering factors are from Waasmair and Kirfel.[22] Hydrogen atoms were placed in geometrically idealized positions and constrained to ride on their parent atoms with C---H distances in the range 0.95-1.00 Angstrom. Isotropic thermal parameters U_{eq} were fixed such that they were 1.2U_{eq} of their parent atom Ueq for CH's and

1.5U_{eq} of their parent atom U_{eq} in case of methyl groups. All non-hydrogen atoms were refined anisotropically by full-matrix least-squares. Presence of water is confirmed by a network of hydrogen bonds between H_2O and BF_4. Similarly, a hydrogen of the acetic acid hydrogen bonds to fluorine. Only one half of a benzene molecule accompanies the complex and anion

Table 4.1. Crystal data and structure refinement for **4a**.

Empirical formula	$C_{23}\ H_{32}\ B\ F_4\ Ir\ N_2\ O_5$	
Formula weight	695.52	
Temperature	100(2) K	
Wavelength	0.71073 Å	
Crystal system	Monoclinic	
Space group	C 2/c	
Unit cell dimensions	a = 22.059(5) Å	α = 90°.
	b = 8.4388(18) Å	β = 106.994(15)°.
	c = 29.485(7) Å	γ = 90°.
Volume	5249(2) $Å^3$	
Z	8	
Density (calculated)	1.760 Mg/m^3	
Absorption coefficient	5.151 mm^{-1}	
F(000)	2736	
Crystal size	0.10 x 0.05 x 0.03 mm^3	
Theta range for data collection	1.93 to 25.39°.	
Index ranges	-26<=h<=26, -10<=k<=10, -35<=l<=35	
Reflections collected	34746	
Independent reflections	4819 [R(int) = 0.1732]	
Completeness to theta = 25.39°	99.6 %	
Max. and min. transmission	0.8608 and 0.6269	
Refinement method	Full-matrix least-squares on F^2	
Data / restraints / parameters	4819 / 57 / 339	
Goodness-of-fit on F^2	1.028	
Final R indices [I>2sigma(I)]	R1 = 0.0523, wR2 = 0.0824	
R indices (all data)	R1 = 0.1082, wR2 = 0.0966	
Largest diff. peak and hole	1.261 and -1.283 $e.Å^{-3}$	

Details of Solid State Structure Determination of 8a.

A yellow prism, measuring 0.25 x 0.10 x 0.05 mm^3 was mounted on a loop with oil. Data was collected at -173 °C on a Bruker APEX II single crystal X-ray diffractometer, Mo-radiation. Crystal-to-detector distance was 40 mm and exposure time was 10 seconds per frame for all sets. The scan width was 0.5^o. Data collection was 100% complete to 25^o in ϑ. A total of 80551 reflections were collected covering the indices, h = -40 to 40, k = -20 to 20, l = -14 to 14. 6081 reflections were symmetry independent and the R_{int} = 0.0490 indicated that the data

was of better than average quality (0.07). Indexing and unit cell refinement indicated a C-centered monoclinic lattice. The space group was found to be P C 2/c (No.15). The data was integrated and scaled using SAINT, SADABS within the APEX2 software package by Bruker.[18]

Solution by direct methods (SHELXS, SIR97[19]) produced a complete heavy atom phasing model consistent with the proposed structure. The structure was completed by difference Fourier synthesis with SHELXL97.[20,21] Scattering factors are from Waasmair and Kirfel.[22] Hydrogen atoms were placed in geometrically idealized positions and constrained to ride on their parent atoms with C---H distances in the range 0.95-1.00 Angstrom. Isotropic thermal parameters U_{eq} were fixed such that they were $1.2U_{eq}$ of their parent atom Ueq for CH's and $1.5U_{eq}$ of their parent atom U_{eq} in case of methyl groups. All non-hydrogen atoms were refined anisotropically by full-matrix least-squares.

Table 4.2. Crystal data and structure refinement for **8a**.

Empirical formula	$C_{41}\ H_{52}\ Cl_4\ F_6\ Ir_2\ N_4\ O_{10}$	
Formula weight	1401.07	
Temperature	100(2) K	
Wavelength	0.71073 Å	
Crystal system	Monoclinic	
Space group	C 2/c	
Unit cell dimensions	a = 30.145(5) Å	α = 90°.
	b = 15.075(2) Å	β = 106.508(11)°.
	c = 11.1245(16) Å	γ = 90°.
Volume	4846.9(13) $Å^3$	
Z	4	
Density (calculated)	1.920 Mg/m^3	
Absorption coefficient	5.787 mm^{-1}	
F(000)	2728	
Crystal size	0.25 x 0.10 x 0.05 mm^3	
Theta range for data collection	2.28 to 28.52°.	
Index ranges	-40<=h<=40, -20<=k<=20, -14<=l<=14	
Reflections collected	80551	
Independent reflections	6081 [R(int) = 0.0490]	
Completeness to theta = 25.00°	100.0 %	
Max. and min. transmission	0.7607 and 0.3256	
Refinement method	Full-matrix least-squares on F^2	
Data / restraints / parameters	6081 / 0 / 309	
Goodness-of-fit on F^2	1.084	
Final R indices [I>2sigma(I)]	R1 = 0.0183, wR2 = 0.0413	
R indices (all data)	R1 = 0.0232, wR2 = 0.0439	
Largest diff. peak and hole	1.084 and -1.476 e.$Å^{-3}$	

Details of Solid State Structure Determination of 11a.

A yellow block, measuring 0.15 x 0.10 x 0.05 mm^3 was mounted on a loop with oil. Data was collected at -173 °C on a Bruker APEX II single crystal X-ray diffractometer, Mo-radiation. Crystal-to-detector distance was 40 mm and exposure time was 10 seconds per frame for all sets. The scan width was 0.5^o. Data collection was 99.6% complete to 25^o in ϑ. A total of 59985 reflections were collected covering the indices, h = -11 to 11, k = -15 to 15, l = -32 to 32. 10626 reflections were symmetry independent and the R_{int} = 0.0312 indicated that the data was of

brilliant (average quality 0.07). Indexing and unit cell refinement indicated a primitive monoclinic lattice. The space group was found to be P $\bar{1}$ (No.2). The data was integrated and scaled using SAINT, SADABS within the APEX2 software package by Bruker.[18]

Solution by direct methods (SHELXS, SIR97[19]) produced a complete heavy atom phasing model consistent with the proposed structure. The structure was completed by difference Fourier synthesis with SHELXL97.[20,21] Scattering factors are from Waasmair and Kirfel.[22] Hydrogen atoms were placed in geometrically idealized positions and constrained to ride on their parent atoms with C---H distances in the range 0.95-1.00 Angstrom. Isotropic thermal parameters U_{eq} were fixed such that they were $1.2U_{eq}$ of their parent atom Ueq for CH's and $1.5U_{eq}$ of their parent atom U_{eq} in case of methyl groups. All non-hydrogen atoms were refined anisotropically by full-matrix least-squares.

Table 4.3. Crystal data and structure refinement for **11a**.

Empirical formula	$C_{40}\ H_{54}\ Cl_2\ Ir_2\ N_4\ O_9$	
Formula weight	1190.17	
Temperature	100(2) K	
Wavelength	0.71073 Å	
Crystal system	Triclinic	
Space group	P -1	
Unit cell dimensions	a = 8.4268(11) Å	α = 100.079(6)°.
	b = 11.3203(16) Å	β = 92.120(7)°.
	c = 24.008(3) Å	γ = 109.374(7)°.
Volume	2116.1(5) $Å^3$	
Z	2	
Density (calculated)	1.868 Mg/m^3	
Absorption coefficient	6.467 mm^{-1}	
F(000)	1164	
Crystal size	0.15 x 0.10 x 0.05 mm^3	
Theta range for data collection	1.73 to 28.54°.	
Index ranges	-11<=h<=11, -15<=k<=15, -32<=l<=32	
Reflections collected	59985	
Independent reflections	10626 [R(int) = 0.0312]	
Completeness to theta = 25.00°	99.6 %	
Max. and min. transmission	0.7381 and 0.4438	
Refinement method	Full-matrix least-squares on F^2	
Data / restraints / parameters	10626 / 0 / 534	
Goodness-of-fit on F^2	1.051	
Final R indices [I>2sigma(I)]	R1 = 0.0225, wR2 = 0.0421	
R indices (all data)	R1 = 0.0300, wR2 = 0.0438	
Largest diff. peak and hole	1.098 and -1.125 $e.Å^{-3}$	

Notes to Chapter 4

1. (a) Crabtree, R. H.; Mihelcic, J. M.; Quirk, J. M. *J*. *Am*. *Chem*. *Soc*. **1979**, *101*, 7738. (b) Crabtree, R. H.; Mellea, M. F.; Mihelcic, J. M.; Quirk, J. M. *J*. *Am*. *Chem*. *Soc*. **1982**, *104*, 107. (c) Burk, M. J.; Crabtree, R. H.; McGrath, D. V. *J*. *Am*. *Chem*. *Soc*., *Chem*. *Commun*. **1985**, 1829. (d) Burk, M. J.; Crabtree, R. H. *J*. *Am*. *Chem*. *Soc*. **1987**, *109*, 8025. (e) Gupta, M.; Hagen, C.; Flesher, R. J.; Kaska, W. C.; Jensen, C. M. *Chem*. *Commun*. **1996**, 2083. (f) Liu, F.; Pak, E. B.; Singh, B.; Jensen, C. M.; Goldman, A. S. *J*. *Am*. *Chem*. *Soc*. **1999**, *121*, 4086. (g) Fekl, U.; Kaminsky, W.; Goldberg, K. I. *J*. *Am*. *Chem*. *Soc*. **2003**, *125*, 15286. (h) Kostelansky, C. N.; MacDonald, M. G.; White, P. S.; Templeton, J. L. *Organometallics* **2006**, *25*, 2993. (i) Khaskin, E.; Zavalij, P. Y.; Vedernikov, A. N. *J*. *Am*. *Chem*. *Soc*. **2006**, *128*, 13054. (j) Adams, J. J.; Arulsamy, N.; Roddick, D. M. *Organometallics* **2012**, *31*, 1439.

2. Choi, J.; MacArthur, A. H. R.; Brookhart, M.; Goldman, A. S. *Chem*. *Rev*. **2011**, *111*, 1761.

3. (a) Liu, F.; Goldman, A. S. *Chem*. *Commun*. **1999**, 655. (b) Fujii, T.; Saito, Y. *J*. *Chem*. *Soc*.*; Chem*. *Commun*. **1990**, 757. (c) Fujii, T.; Saito, Y. *J*. *Chem*. *Soc*., *Dalton Trans*. **1993**, 517. (d) Aoki, T.; Crabtree, R. H. *Organometallics* **1993**, *12*, 294. (e) Xu, W.; Rosini, G. P.; Gupta, M.; Jensen, C. M.; Kaska, W. C.; Krogh-Jespersen, K.; Goldman, A. S. *Chem*. *Commun*. **1997**, 2273. (f) Krogh-Jespersen, K.; Czerw, M.; Summa, N.; Renkema, K. B.; Achord, P. D.; Goldman, A. S. *J*. *Am*. *Chem*. *Soc*. **2002**, *124*, 11404.

4. Allen, K. E.; Heinekey, D. M.; Goldman, A. S.; Goldberg, K. I. *Organometallics*, **2013**, *32*, 1579.

5. (a) Wick, D. D.; Goldberg, K. I. *J*. *Am*. *Chem*. *Soc*. **1999**, *121*, 11900. (b) Denney, M. C.; Smythe, N. A.; Cetto, K. L.; Kemp, R. A.; Goldberg, K. I. *J*. *Am*. *Chem*. *Soc*. **2006**, *128*, 2508. (c) Keith, J. M.; Muller, R. P.; Kemp, R. A.; Goldberg, K. I.; Goddard, W. A., III: Oxgaard, J.

Inorg. *Chem*. **2006**, *45*, 9631. (d) Konnick, M. M.; Gandhi, B. A.; Guzei, I. A.; Stahl, S. S. *Angew*. *Chem*. *Int*. *Ed*. **2006**, 45, 2904. (e) Heiden, Z. M.; Rauchfuss, T. B. *J*. *Am*. *Chem*. *Soc*. **2007**, *129*, 14303. (f) Look, J. L.; Wick, D. D.; Mayer, J. M.; Goldberg, K. I. *Inorg*. *Chem*. **2009**, *48*, 1356. (g) Grice, K. A.; Goldberg, K. I. *Organometallics* **2009**, *28*, 953. (h) Taylor, R. A.; Law, D. J.; Sunely, G. J.; White, A. J. P.; Britovsek, G. J. P. *Angew*. *Chem*. *Int*. *Ed*. **2009**, *48*, 5900. (i) Boisvert, L.; Denney, M. C.; Hanson, S. K.; Goldberg, K. I. *J*. *Am*. *Chem*. *Soc*. **2009**, *131*, 15802. (j) Szajha-Fuller, E.; Bakac, A. *Inorg*. *Chem*. **2010**, *49*, 781.

6. Williams, D. B.; Kaminsky, W.; Mayer, J. M.; Goldberg, K. I. *Chem*. *Commun*. **2008**, 4195.

7. Boisvert, L.; Goldberg, K. I. *Acc*. *Chem*. *Res*. **2012**, *45*, 899.

8. Ito, J.; Shiomi, T.; Nishiyama, H. *Adv*. *Synth*. *Catal*. **2006**, *348*, 1235.

9. For examples of hydrogen peroxide detection see: (a) Coggins, M. K.; Sun, X.; Kwak, Y.; Solomon, E. I.; Rybak-Akimova, E.; Kovacs, J. A. *J*. *Am*. *Chem*. *Soc*. **2013**, *135*, 5631. (b) Kim, S.; Saracini, C.; Siegler, M. A.; Drichko, N.; Karlin, K. D. *Inorg*. *Chem*. **2012**, *51*, 12603.

10. Smythe, N. A.; Grice, K. G.; Williams, B. S.; Goldberg, K. I. *Organometallics* **2009**, *28*, 277.

11. Meier, S. K.; Young, K. J. H.; Ess, D. H.; Tenn, W. J., III; Oxgaard, J.; Goddard, W. A., III; Periana, R. A. *Organometallics* **2009**, *28*, 5923.

12. Ito, J.; Kaneda, T.; Nishiyama, H. *Organometallics* **2012**, *31*, 4442.

13. Heiden, Z. M.; Rauchfuss, T. B. *J*. *Am*. *Chem*. *Soc*. **2007**, *129*, 14303.

14. Chowdhury, S.; Himo, F.; Russo, N.; Sicilia, E. *J*. *Am*. *Chem*. *Soc*. **2010**, *132*, 4178.

15. Jiang, B.; Feng, Y.; Ison, E. A. *J*. *Am*. *Chem*. *Soc*. **2009**, *130*, 14462.

16. Teets, T. S.; Nocera, D. G. *J*. *Am*. *Chem*. *Soc*. **2011**, *133*, 17796.

17. Endo, K.; Grubbs, R. H. *J*. *Am*. *Chem*. *Soc*. **2011**, *133*, 8525.

18. Bruker (**2007**) APEX2 (Version 2.1-4), SAINT (version 7.34A), SADABS (version 2007/4), BrukerAXS Inc, Madison, Wisconsin, USA.

19. (a) Altomare, A.; Burla, C.; Camalli, M.; Cascarano, L.; Giacovazzo, C.; Guagliardi, A.; Moliterni, A. G. G.; Polidori, G.; Spagna, R. *J*. *Appl*. *Cryst*. **1999**, *32***,** 115-119. (b) Altomare, A.; Cascarano, G.; Giacovazzo, C.; Guagliardi, A. *J*. *Appl*. *Cryst*. **1993**, *26*, 343.

20. Sheldrick GM. **(1997)** SHELXL-97, Program for the Refinement of Crystal Structures. University of Göttingen, Germany.

21. Mackay, S.; Edwards, C.; Henderson, A.; Gilmore, C.; Stewart, N.; Shankland, K.; Donald, A. *MaXus: a computer program for the solution and refinement of crystal structures from diffraction data*. University of Glasgow, Scotland, **1997**.

22. Waasmaier, D.; Kirfel, A. *Acta Crystallogr*. A. **1995**, *51*, 416.

Chapter 5: Exploration of (Phebox)Ir Phenyl Complex for Arene Functionalization

Introduction

Efficient processes for the direct oxidation of benzene to phenol have important implications for commodity chemicals. Currently, phenol is obtained from benzene by indirect routes involving several steps.[1] The Hock process is the largest contributor to world production of phenol, and generates the alcohol product from benzene and propylene. In this process cumene, produced from benzene and propylene, is oxidized to cumene hydroperoxide, which undergoes cleavage to generate phenol and acetone. As long as there is a market for acetone that tracks with the demand for phenol this process remains economically feasible. Phenol can also be obtained from the acetoxylation of benzene although this method has not been employed industrially.[1] In this indirect route phenyl acetate is initially formed, which undergoes hydrolysis to generate acetic acid and phenol. A direct route to the formation of phenol from benzene using a transition metal catalyst would result selectively in the desired functionalized product.

Pd catalysts have been shown to effectively mediate the formation of phenyl acetate from benzene, but these systems utilize expensive hypervalent iodide oxidants.[2] Alternatively, Rh and Ir mediated arene functionalization has been demonstrated using borane reagents by Hartwig and coworkers.[3] Another method of C-H functionalization involves the insertion of small molecules, such as CO, into metal alkyl bonds.[4] There are few examples of CO insertion into M-aryl bonds,[5] and more specifically even fewer reports of insertion into Ir-aryl bonds.[6] Jones and coworkers found that when neutral $Cp^*Ir(CN)Cl$ complexes (CN = phenylpyridine or phenylimine) were subjected to 1 atm of CO at room temperature, insertion of CO into the Ir-aryl bond occurred (Scheme 5.1).[7] Interestingly, when Davies and coworkers subjected the cationic complex $[Cp^*Ir(CN')(NCCH_3)][PF_6]$ (CN′ = 4,4-dimethyl-2-oxazolinylbenzene) to CO, insertion

into the Ir-aryl bond did not occur (Scheme 5.1).[8] Instead CO coordination to the Ir^{III} center and loss of $NCCH_3$ was observed. In order to better understand what factors contribute to promoting CO insertion into Ir-aryl bonds, a wider range of complexes must be explored. Previously we reported C-H activation of benzene by (Phebox)Ir$(OAc)_2(OH_2)$ which generated (Phebox)Ir(OAc)Ph in high yields (Chapter 3).[9] This compound is stable on the bench indefinitely and can be easily isolated. We were interested in exploring the reactivity of (^{iPr}Phebox)Ir(OAc)Ph (**1a**) with various oxidants and small molecules like CO in order to probe the potential of functionalization of the phenyl group.[10]

Scheme 5.1

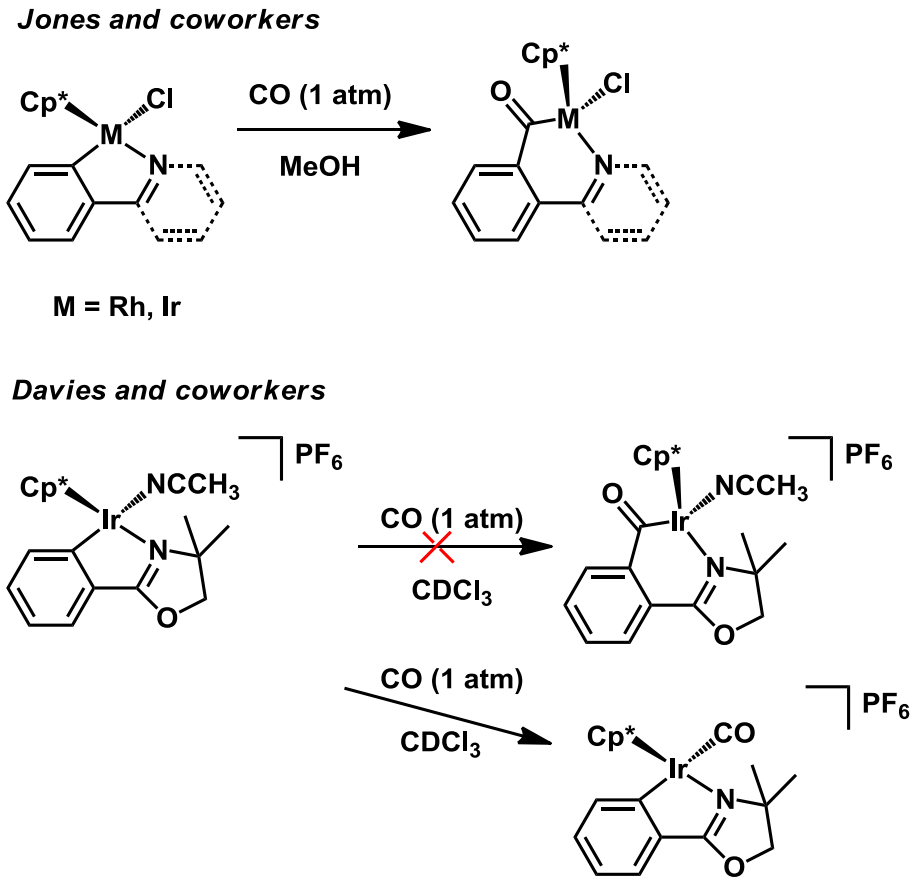

Results and Discussion

The reaction of complex **1a** with a variety of oxidants was explored in CD_2Cl_2. Upon the addition of 1 equiv. of $(C_6F_5)I(TFA)_2$ to a solution of **1a** at room temperature an immediate color change in the bright orange solution to black was observed. In the ^1H NMR spectrum recorded immediately after the addition of oxidant, the sharp signals corresponding to the ^{iPr}Phebox ligand had broadened. The multiplets indicative of the phenyl ligand had disappeared and benzene was present. After 24 h the solution became tan in color and new signals were observed in the ^1H NMR spectrum, but these signals did not correspond to dissociated ^{iPr}Phebox ligand. The volatiles were separated from the Ir material and subsequently analyzed by GC/MS. Notably, C_6F_5I was identified in the volatiles, but there was no evidence of the desired product $C_6F_5(X)$ (X = OAc or TFA).

In the ^1H NMR spectrum of the nonvolatile material, signals corresponding to two Ir products were observed. The major Ir species (**2a**) of this reaction is a symmetrical product, while the minor product (**3a**) appears to be asymmetrical. Complex **2a** can be separated from **3a** by a silica gel column using ethyl acetate. Two doublets, consistent with a symmetrical product, were observed at 0.68 and 0.98 ppm and a multiplet at 2.33 ppm were assigned to the isopropyl substituents. The multiplets corresponding to the oxazoline protons were observed at 4.22 and 4.81 ppm, (1H and 3H respectively) and a singlet at 6.80 ppm was assigned to the aromatic proton of the pincer backbone. In the ^{19}F NMR spectrum a singlet observed at -74.4 ppm was attributed to TFA. Complex **2a** has been tentatively assigned as (^{iPr}Phebox)Ir$(TFA)_2$ based on the absence of OAc signals in the ^1H NMR spectrum (Scheme 5.2). The identity of this product has not yet been confirmed by independent synthesis.

Scheme 5.2

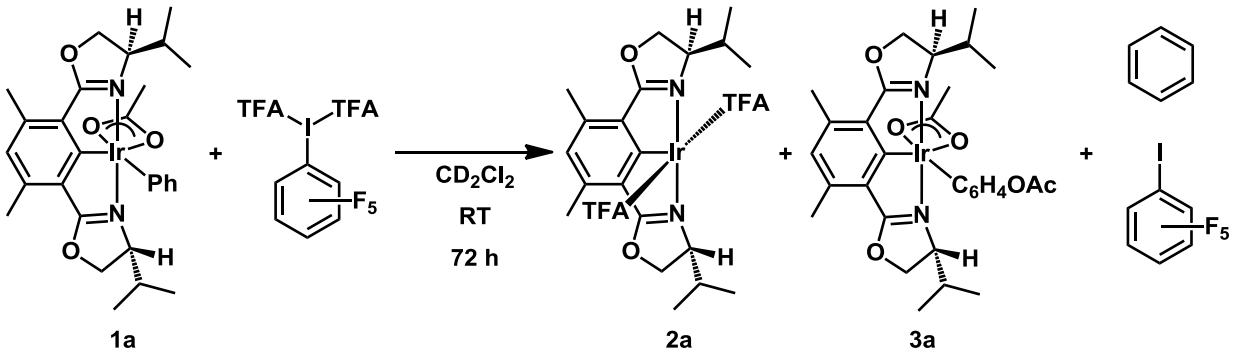

In the ^{1}H NMR spectrum of **3a** four multiplets were observed in the aromatic region each integrating to one proton. These signals are suggestive of an Ir-phenyl compound where one of the sites on the phenyl ligand has been substituted. A singlet at 6.76 ppm is indicative of the aromatic proton in the ^{iPr}Phebox backbone. Multiplets consistent with the oxazolinyl protons were observed at 3.93, 4.61, and 4.81 ppm. The *iso*propyl substituents of the oxazoline rings were observed as a doublet at 0.13 ppm and multiple overlapping doublets at 0.80 ppm. The doublet at 0.13 ppm was easily distinguishable, while the three remaining doublets for the *iso*propyl substituents were difficult to assign due to overlap with the symmetrical product and another minor product. Complex **3a** could not be recovered from the silica column and therefore clean ^{1}H NMR data was not obtained. The identity of **3a** has been tentatively assigned as (^{iPr}Phebox)Ir(OAc)(C_6H_4OAc) (Scheme 5.2). A signal at 1.86 ppm was suggestive of either an OAc ligand or OAc substituent of the phenyl ring. This species likely resulted from nucleophilic attack by carboxylate at the phenyl ligand. The proton source for the formation of benzene in this reaction is unclear at this time.

When 1 equiv. of $PhI(OAc)_2$ was added to a CD_2Cl_2 solution of **1a** at room temperature no immediate reaction occurred. The reaction was heated at 60 °C for 72 h, which did not result

in a reaction between the oxidant and **1a**. During this time phenyl iodide was observed in the ^{1}H NMR spectrum, but there was no change in the aromatic signals corresponding to **1a**. When the mixture was heated at 100 °C for 24 h the formation of benzene was observed concomitantly with a decrease in the intensity of the coordinated phenyl aromatic signals. Signals for free ^{iPr}Phebox ligand were not observed at any point during the reaction and there was no visible Ir black. Multiple signals were observed in the oxazolinyl and *iso*propyl regions of the spectrum after heating the reaction mixture at 100 °C suggesting the formation of multiple species. The volatiles of the reaction were separated from the Ir material and examined by GC/MS. The desired product phenyl acetate was not observed.

No immediate reaction was observed when 1 equiv. of PhIO was added to a CD_2Cl_2 solution of **1a** at room temperature. After the solution was heated at 60 °C for 2 h a new asymmetrical product was present in the ^{1}H NMR spectrum and was identified by the appearance of four doublets at 0.85, 0.92, 0.97, and 1.23 ppm in the *iso*propyl region (Figure 5.1). The ratio of starting material to the new product was 1:1 at this point in the reaction. Benzene was also observed in the ^{1}H NMR spectrum, likely resulting from loss of the phenyl ligand. Further heating of the mixture at 60 °C overnight resulted in the formation of multiple species and benzene. In the ^{1}H NMR spectrum, a small amount of Ir-phenyl starting material remained at this time and the aromatic signals corresponding to the phenyl ligand were still observable at 6.37 (d), 6.55 (t), and 6.61 (t) ppm. In the oxazoline region of the spectrum a large, complex signal was observed from 4.53 to 4.95 ppm, indicative of a number of ^{iPr}Phebox containing species. Consistent with this observation, in the isopropyl region multiple doublets were observed 1.46 to 1.22 ppm and 1.07 to 0.73 ppm. Formation of functionalized arene, such as phenyl acetate, was not observed by GC/MS.

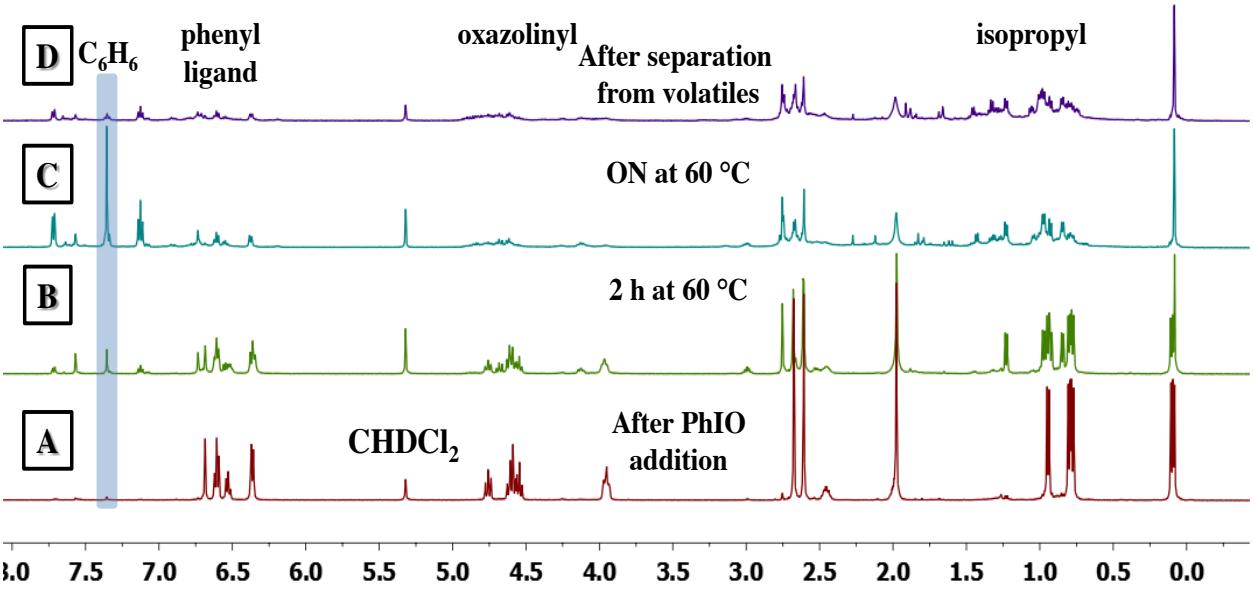

Figure 5.1. ^{1}H NMR spectral data acquired over the course of the reaction of **1a** with 1 equiv. PhIO in CD_2Cl_2. Figure A: immediately after the addition of PhIO to the solution **1a** was the only species observed. Figure B: the reaction mixture after heating for 2 h at 60 °C, a new asymmetrical product was present along with **1a**. Figure C: after heating the reaction at 60 °C overnight, multiple products were present. Figure D: after separation of the volatiles for GC/MS analysis, no change in the ^{1}H NMR spectrum of the Ir products.

The reaction of **1b** with CO was studied at room temperature. When CO was bubbled through a solution of **1b** in benzene or CH_3OH a new product was observed. The bright orange colored solution immediately became pale yellow upon CO exposure. In the ^{1}H NMR spectrum of the product three aryl signals were observed at 6.80 (t, 1H), 6.69 (t, 2H), and 6.45 (d, 2H) ppm indicative of a phenyl ring. These signals were significantly shifted in comparison to the phenyl signals observed for complex **1b**. The new product was characterized as (^{dm}Phebox)Ir(CO)(OAc)Ph (***trans*-4b**) using ^{13}C NMR and IR spectroscopy, and X-ray crystallography (eq. 5.1). In order to determine the ^{13}C NMR chemical shift for coordinated CO, (^{dm}Phebox)Ir(^{13}CO)(OAc)Ph was synthesized. In the ^{13}C NMR spectrum of the labeled complex the signal at 169.99 ppm was indicative of coordinated CO. The CO stretching frequency observed for ***trans*-4b** was 2033 cm^{-1}, suggestive of an electrophilic Ir^{III} center.

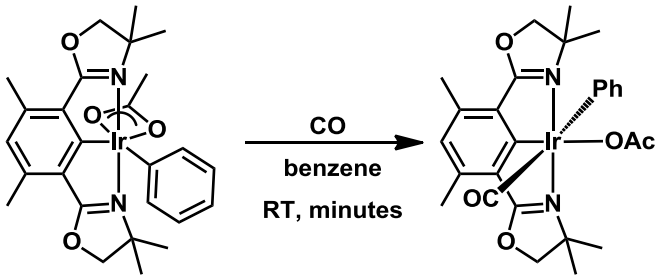

1b *trans*-4b (5.1)

The X-ray crystallographic data obtained for ***trans*-4b** revealed a distorted octahedral geometry about the Ir^{III} center (Figure 5.2). The N(1)-Ir(1)-N(2) bond angle is 156.8(3)° consistent with other (^{dm}Phebox)Ir complexes. The C(27)-Ir(1)-(C19) bond angle is 179.4(4)° confirming that CO is trans to the phenyl ligand. The Ir(1)-O(3) (2.168(6) Å) bond length is longer than the reported Ir^{III}-O acetate bond lengths (2.037(3) and 2.058(3) Å) in (^{dm}Phebox)Ir$(OAc)_2(OH_2)$.[11] The Ir(1)-C(27) bond length, 1.955(10) Å, is slightly longer than the reported Ir-CO bond length of (PCP)Ir(CO)(CH_3)Ph (1.916(7) Å) where CO is located *trans* to the CH_3 ligand.[12]

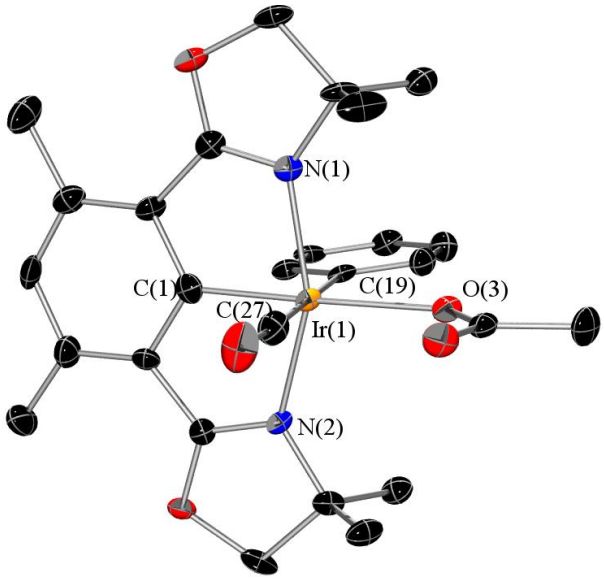

Figure 5.2. ORTEP diagram of ([dm]Phebox)Ir(CO)(OAc)Ph (***trans*-4b**) (thermal ellipsoids at 50% probably, H atoms omitted for clarity). Selected bond distances (Å) and angles (deg): Ir(1)-C(1) = 1.941(9), Ir(1)-C(19) = 2.113(8), Ir(1)-C(27) = 1.955(10), Ir(1)-N(1) = 2.072(7), Ir(1)-N(2) = 2.064(7), Ir(1)-O(3) = 2.168(6), N(2)-Ir(1)-N(1) = 156.8(3), C(27)-Ir(1)-(C19) = 179.4(4), C(1)-Ir(1)-C(27) = 90.4(4), N(1)-Ir(1)-O(3) = 102.3(2), C(19)-Ir(1)-O(3) = 87.6(3).

Complex ***trans*-4b** is air sensitive and unstable at room temperature. When a benzene-d_6 solution of ***trans*-4b** was left at room temperature overnight, a new product was observed in ^{1}H NMR spectrum. This new product could also be cleanly obtained by heating a benzene or CH_3OH solution of ***trans*-4b** overnight at 60 °C. Three signals at 7.26 (d, 2H), 6.91 (t, 2H), 6.82 (t, 1H) in the ^{1}H NMR spectrum were indicative of a new species bearing a phenyl ligand. A singlet at 2.11 ppm corresponded to the OAc ligand, which had shifted upfield in comparison to the chemical shift of the OAc ligand of ***trans*-4b** (2.68 ppm). The identity of this new product was determined to be ([dm]Phebox)Ir(OAc)(CO)Ph (***cis*-4b**) using ^{13}C NMR and IR spectroscopy, and X-ray crystallography (Scheme 5.3). The labeled complex ([dm]Phebox)Ir(OAc)(^{13}CO)Ph was synthesized in order to determine the ^{13}C NMR chemical shift for coordinated CO. In the ^{13}C NMR spectrum the signal indicative of the CO ligand had shifted downfield to 182.54 ppm from

169.09 ppm in ***trans*-4b**. The CO stretching frequency of ***cis*-4b** (2023 cm^{-1}) was red shifted relative to ***trans*-4b**.

Scheme 5.3

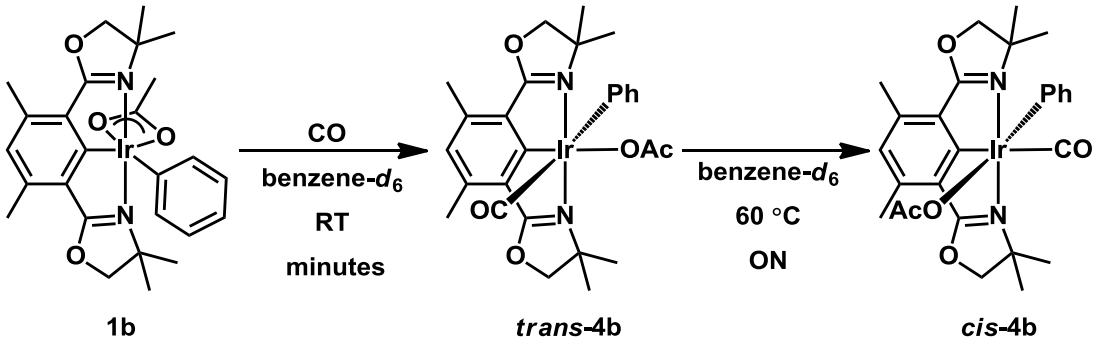

The X-ray crystallographic data demonstrated that ***cis*-4b** also has a distorted octahedral geometry similar to the *trans* isomer (Figure 5.3). The N(2)-Ir(1)-N(1) (155.46(11)°) bond angle is consistent with the angle observed for ***trans*-4b**. The C(27)-Ir(1)-C(1) bond angle is 178.54(12)°, indicating that CO occupies the position *trans* to the aryl ring of the ^{dm}Phebox ligand. The Ir-CO bond length is 1.963(3) Å, which is similar to the Ir-CO bond length observed in ***trans*-4b**. This bond is longer than the Ir-CO bond length of (PCP)Ir(CO)$(Ph)_2$ (1.906(3) Å) where the CO ligand is located *trans* to the PCP backbone.[12] The Ir-OAc, Ir(1)-O(3), bond length is 2.156(2) Å, which is again consistent with the Ir(1)-O(3) bond length of 2.168(6) Å for ***trans*-4b.**

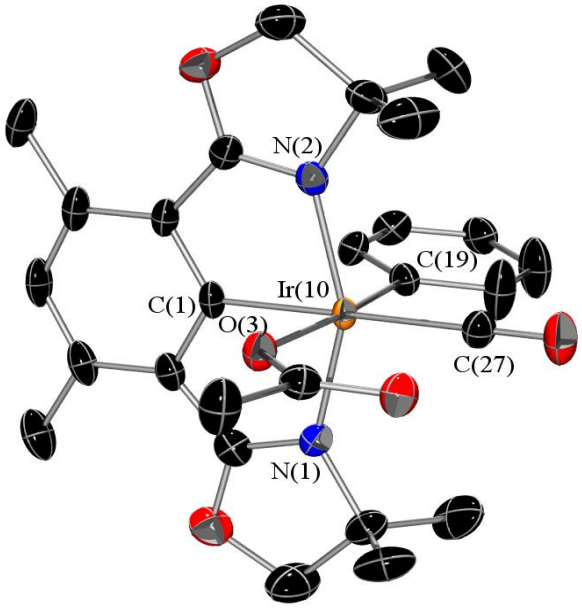

Figure 5.3. ORTEP diagram of (^{dm}Phebox)IrOAc)(CO)Ph (***cis*-4b**) (thermal ellipsoids at 50% probably, H atoms omitted for clarity). Selected bond distances (Å) and angles (deg): Ir(1)-C(27) = 1.963(3), Ir(1)-C(1) = 2.000(3), Ir(1)-N(1) = 2.056(3), Ir(1)-N(2) = 2.053(3), Ir(1)-C(19) = 2.068(3), Ir(1)-O(3) = 2.156(2), N(2)-Ir(1)-N(1) = 155.46(11), C(27)-Ir(1)-C(19) = 90.42(13), C(27)-Ir(1)-C(1) = 178.54(12), C(1)-Ir(1)-O(3) = 83.12(10), N(2)-Ir(1)-C(19) = 91.57(11).

The absence of CO insertion into the Ir-phenyl bond of **1b** is unsurprising as CO coordinates *trans* to the phenyl ligand. Formation of ***trans*-4b** as the initial product from the reaction with CO is suggestive of the κ^2-OAc ligand opening up to provide an open site *trans* to the phenyl ligand. In order for insertion to occur the CO ligand needs be oriented *cis* to the phenyl ligand as in ***cis*-4b**. Formation of ***cis*-4b** from ***trans*-4b** most likely occurs via dissociation of a ligand to generate a five coordinate complex, which can then undergo isomerization.

Attempts to observe CO insertion into the Ir-phenyl bond of ***cis*-4b** were explored at elevated temperatures. When a benzene-d_6 solution of ***cis*-4b** was heated at 200 °C for 72 h, with or without an atm of CO present, two products were formed and ***cis*-4b** remained in the reaction mixture. The ratio of ***cis*-4b** to the two products was 2:1:1. The three singlets observed at 6.4 to 6.5 ppm corresponded to three different ^{dm}Phebox aryl protons in the ^{1}H NMR spectrum and

were indicative of the three different species present. Interestingly, the aromatic signals corresponding to the phenyl ligand had disappeared without the formation of benzene, suggestive of deuterium incorporation into the ligand. When the reaction was conducted in protiated benzene the aromatic signals corresponding to the phenyl ligand were observed at the end of the reaction. The ^{1}H NMR signals corresponding to the ^{dm}Phebox ligand of ***cis*-4b** had not shifted and a new set of pincer signals were indicative of formation of ***trans*-4b**. Additionally, the signals consistent with the OAc ligands in ***trans*-** and ***cis*-4b** were unchanged. The third product of the reaction was determined to be (^{dm}Phebox)Ir(OAc)(Ph-d_5) (**1b-d_5**) by independent synthesis via C-D activation using either **1b** or (^{dm}Phebox)Ir(OAc)$_2$(OH)$_2$. This result also supported that the missing aryl signals for ***trans*-** and ***cis*-4b** were a result of arene exchange with benzene-d_6 (Scheme 5.4).

Scheme 5.4

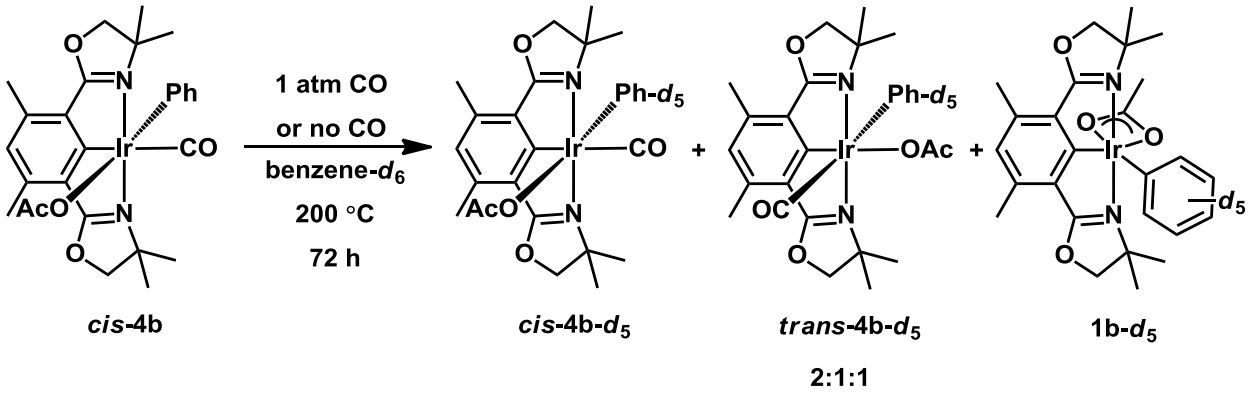

C-H activation by ***cis*-4b** most likely occurs via ligand loss, either OAc or CO, to generate a five coordinate complex. It is likely that CO loss would occur to generate a neutral Ir^{III} complex, especially in benzene, in contrast to OAc loss which would result in a cationic complex. C-H activation in the monoacetate system (^{dm}Phebox)Ir(OAc)(R) (R = Ph (**1b**), H

(**5b**)) resulted in retention of the OAc ligand which suggests that a mechanism other than CMD may be operating. A sigma bond metathesis mechanism is also possible in which OAc is not involved. In comparison to benzene activation using (^{dm}Phebox)Ir(OAc)$_2$(OH)$_2$, which occurred at 100 °C in 1.5 h, C-H cleavage in the monoacetate systems occurs at a higher temperature and over a longer period of time. When **1b** was heated at 150 °C in benzene-d_6 for 24 h, arene exchange to form **1b-*d*$_5$** occurred and the product was obtained in 98% yield (Scheme 5.5). Complex **1b** was also obtained in 76% yield by arene exchange between **5b** and benzene-d_6 at 200 °C over the course of 24 h (Scheme 5.5). Based on these results, it is reasonable to propose that when ***cis*-4b** in was heated in benzene-d_6 at 150 °C ligand loss occurred to generate an open site. Arene exchange via C-D activation then occurred to form **1b-*d*$_5$**. Complex **1b-*d*$_5$** can coordinate CO to form ***trans*-4b**, which can undergo isomerization to generate ***cis*-4b**.

Scheme 5.5

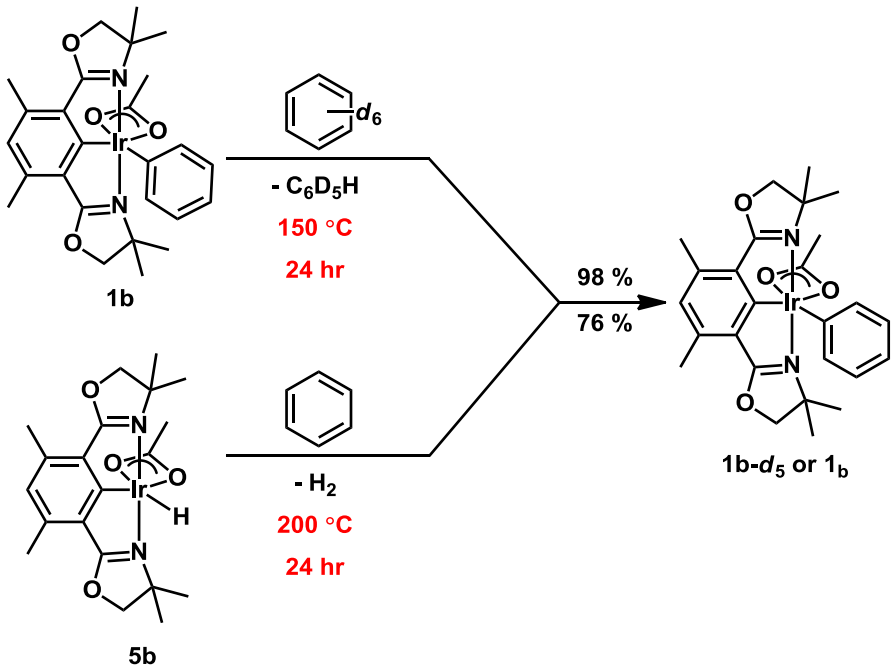

Conclusions

When hypervalent iodide oxidants were added to solutions of (^{iPr}Phebox)Ir(OAc)Ph (**1a**) benzene was formed in all the cases. The method by which benzene is generated in these reactions is unclear. Free ^{iPr}Phebox ligand and Ir black were not observed in these reactions, which suggested that benzene formation does not occur as a result of complete decomposition of the Ir material. The symmetrical product that resulted from the reaction of (^{iPr}Phebox)Ir(OAc)Ph (**1b**) with $C_6F_5I(TFA)_2$ is most likely (^{iPr}Phebox)Ir$(TFA)_2$ (**2a**), which may result from TFA exchange with the OAc ligand and benzene loss from **1a**. The asymmetrical product observed in this reaction is proposed to be (^{iPr}Phebox)Ir(OAc)(C_6H_4OAc) (**3a**). The ^{1}H NMR spectral data suggests that substitution at the phenyl ligand most likely resulted from nucleophilic attack at the *meta* position of the arene by OAc. Functionalization of the aryl ring by OAc is more likely than TFA as OAc is the better nucleophile. The reaction using $C_6F_5I(TFA)_2$ is the only method that appears to result in functionalization at the phenyl ring under these conditions.

Insertion of CO in the Ir-phenyl bond of (^{dm}Phebox)Ir(OAc)Ph (**2b**) was not observed under the conditions employed. Instead coordination of CO to **2b** initially resulted in the formation of ***trans*-4b**. This complex cleanly isomerized to the more stable isomer ***cis*-4b** at room temperature or at 60 °C overnight. When ***cis*-4b** was heated in benzene at 150 °C with or without CO present, arene exchange was observed by ^{1}H NMR spectroscopy. Insertion products were also not observed in this reaction. In order to induce CO insertion, complexes with weaker Ir-phenyl bonds may need to be developed. Additionally, the examination of neutral and cationic Ir complexes employing similar ligand sets is needed to better understand how metal ion Lewis acidity influences CO insertion into metal aryl bonds.

Experimental

General Considerations. Unless specified otherwise, all reactions were carried out under a dry nitrogen atmosphere using standard glovebox, Schlenk, or vacuum-line techniques. $(C_6F_5)I(TFA)_2$ and $PhI(OAc)_2$ were used as received from Aldrich. CO was obtained from Praxair. All other reagents were used as received from other suppliers. Benzene and pentane were purified by passage through columns of activated alumina and molecular sieves. Deuterated solvents were purchased from Cambridge Isotope Laboratories. Benzene-d_6 was dried over sodium/benzophenone and dichloromethane-d_2 and chloroform-d_1 were dried over CaH_2. NMR spectra were obtained on Bruker AV300 or AV500 MHZ spectrometers with chemical shifts (δ) reported in ppm downfield of tetramethylsilane. Products from the reactions of **1a** with oxidants were probed using Agilent 7890A gas chromatograph with a 30 m x 0.32 mm Agilent HP5-MS capillary column. (^{iPr}Phebox)Ir(OAc)Ph (**1a**) and (^{dm}Phebox)Ir(OAc)Ph (**1b**) were prepared using literature procedures.[9]

Reactions with Hypervalent Iodide Oxidants

Reaction of 1a with $C_6F_5I(TFA)_2$. A Teflon-stoppered NMR tube was charged with **1a** (5.4 mg, 0.0082 mmol), $C_6F_5I(TFA)_2$ (4.4 mg, 0.0085 mmol), and 450 μL CD_2Cl_2. The solution immediately became black in color and upon standing became tan colored after 24 h at room temperature. The volatiles were vacuum transferred to a separate Teflon-stoppered NMR tube and checked by ^{1}H NMR spectroscopy. This sample was diluted with CH_2Cl_2 and analyzed using GC/MS. The nonvolatile residue was dissolved in CD_2Cl_2 and analyzed by ^{1}H NMR spectroscopy. The Ir products were separated using a short silica gel column and ethyl acetate. A yellow fraction was obtained and analyzed by ^{1}H NMR spectroscopy. This fraction contained the symmetrical product, **3a**, discussed above. Product **4a** was not stable to air and decomposed

under the workup conditions. See Figure 5.4 for ^{1}H NMR data acquired during and after the reaction.

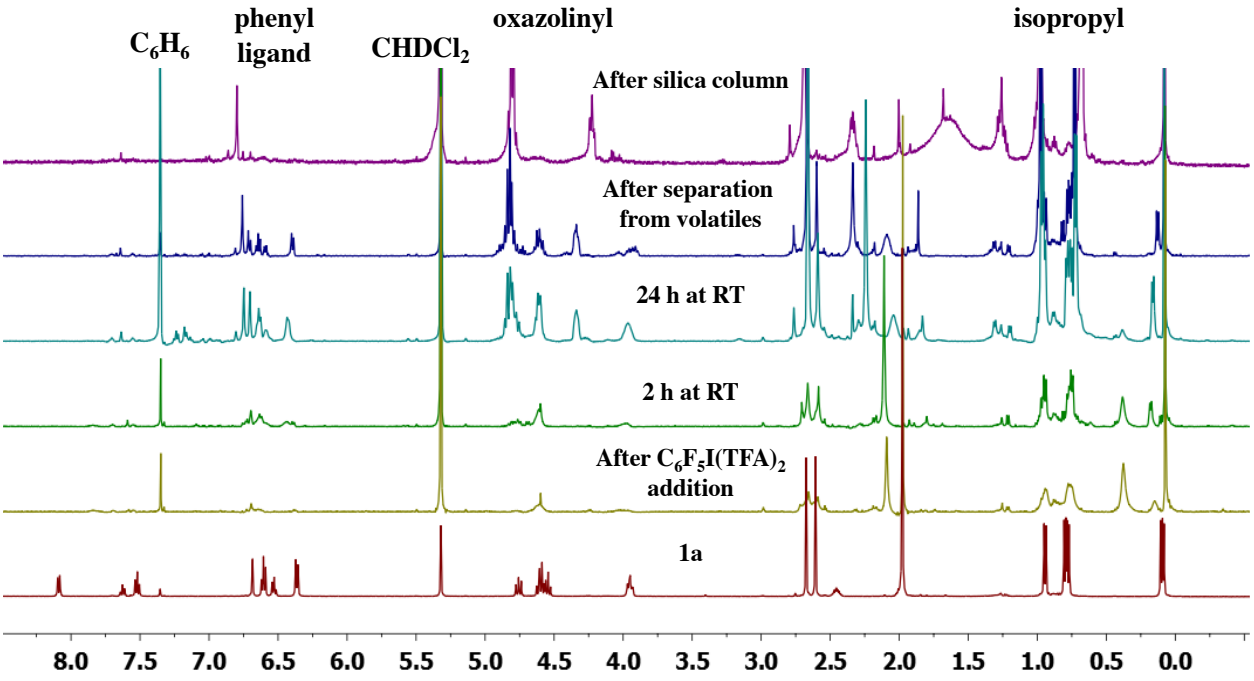

Figure 5.4. ^{1}H NMR spectral data collected over the course of the reaction of **1a** with 1 equiv. of $C_6F_5I(TFA)_2$ at room temperature in CD_2Cl_2. The shift in signals for **3a** in the top spectrum may be a result of a reaction while on the silica gel or in the presence of oxygen and/or water.

Reaction of 1a with PhI(OAc)$_2$. A Teflon-stoppered NMR tube was charged with **1a** (5.4 mg, 0.0082 mmol), $PhI(OAc)_2$ (2.7 mg, 0.0083 mmol), and 450 µL CD_2Cl_2. The orange colored solution was heated at 60 °C for 72 h and then at 100 °C for 24 h. The volatiles were transferred to a separate Teflon-stoppered NMR tube and analyzed by ^{1}H NMR spectroscopy and GC/MS. The nonvolatile residue was dissolved in CD_2Cl_2 and analyzed by ^{1}H NMR spectroscopy. See Figure 5.5 for ^{1}H NMR data acquired during and after the reaction.

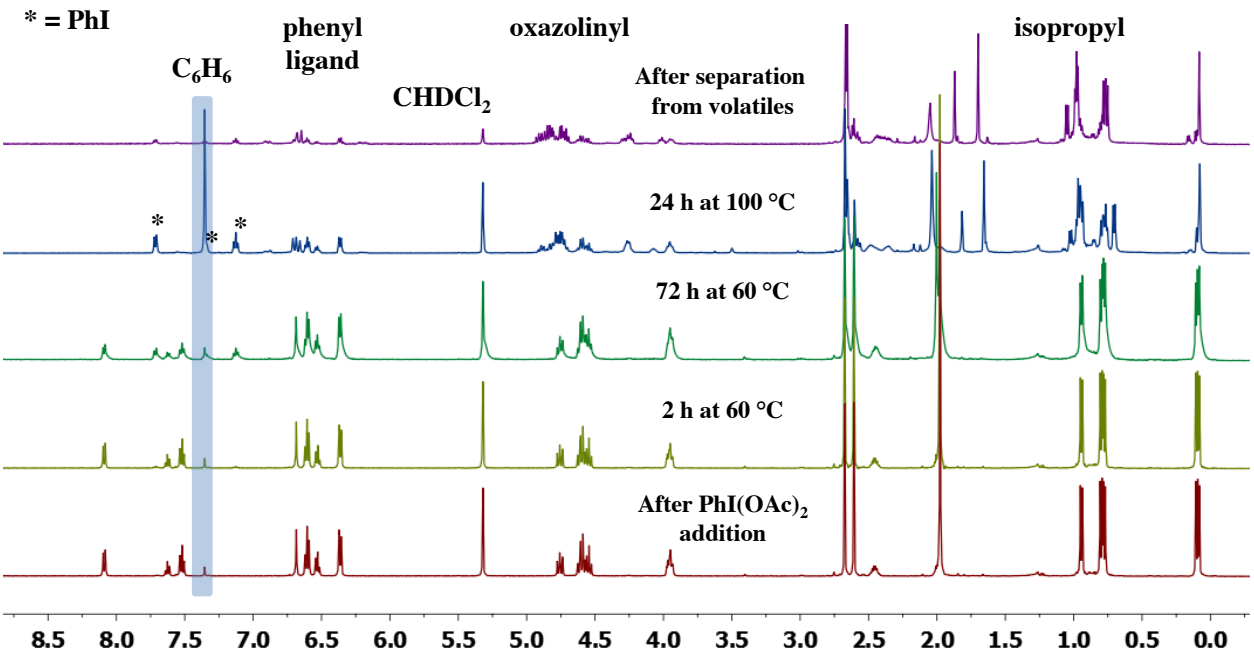

Figure 5.5. ^{1}H NMR spectral data collected over the course of the reaction of **1a** with $PhI(OAc)_2$ at 60-100 °C in CD_2Cl_2.

Reaction of 1a with PhIO. A Teflon-stoppered NMR tube was charged with **1a** (6.4 mg, 0.0097 mmol), PhIO (2.4 mg, 0.011 mmol), and 450 µL CD_2Cl_2. The bright orange colored solution was heated overnight at 60 °C. The volatiles were transferred to a separate Teflon-stoppered NMR tube and analyzed by ^{1}H NMR spectroscopy and GC/MS. The nonvolatile residue was dissolved in CD_2Cl_2 and analyzed by ^{1}H NMR spectroscopy, which showed the formation of multiple Ir containing products.

Reactions with CO

(*dm*Phebox)Ir(CO)(OAc)(Ph) (*trans*-4b). A Teflon-stoppered reaction vessel was charged with **1b** (22 mg, 0.035 mmol), 5 mL of benzene, and CO was bubbled through the solution. Immediately the orange colored solution became pale yellow in color. After stirring for 5 min at room temperature, the volatiles were removed *in vacuo* to give a yellow powder. Yield: 19.4 mg, 84%. X-ray quality crystals of ***trans*-4b** were obtained from concentrated toluene solution

layered with pentane at -35 °C. ^{1}H NMR (C_6D_6, 500 MHz): δ 7.08 (d, 2H, 2-Ph), 7.15 (t, 2H, 3-Ph), 7.01 (t, 1H, 4-Ph), 6.56 (s, 1H, ^{dm}Phebox-aryl), 3.66 (d, 2H, $^1J_{HH'}$ = 8.4 Hz, OCH_2), 3.40 (d, 2H, $^1J_{HH'}$ = 8.4 Hz, OCH_2), 2.68 (s, 3H, OAc), 2.50 (s, 6H, Phebox-CH_3), 1.28 (s, 6H, CH_3), 1.03 (s, 6H, CH_3). IR (KBr): 2033 cm^{-1} (CO).

(^{dm}Phebox)Ir(CO)(OAc)(Ph) (*cis*-4b). Complex ***trans*-4b** was dissolved in 6 mL of benzene and heated at 60 °C overnight, resulting in formation of ***cis*-4b**. X-ray quality crystals of ***cis*-4b** were grown at room temperature from a $CDCl_3$ solution layered with pentane. ^{1}H NMR (C_6D_6, 500 MHz): δ 7.26 (d, 2H, 2-Ph), 6.91 (t, 2H, 3-Ph), 6.82 (t, 1H, 4-Ph), 6.51 (s, 1H, ^{dm}Phebox-aryl), 3.71 (d, 2H, $^1J_{HH'}$ = 8.4 Hz, OCH_2), 3.47 (d, 2H, $^1J_{HH'}$ = 8.4 Hz, OCH_2), 2.41 (s, 6H, Phebox-CH_3), 2.11 (OAc), 1.29 (s, 6H, CH_3), 0.94 (s, 6H, CH_3). IR (KBr): 2023 cm^{-1} (CO).

(^{dm}Phebox)Ir(^{13}CO)(OAc)(Ph) (*trans*-4b). A Teflon-stoppered reaction vessel was charged with **1b** (27 mg, 0.042 mmol) and 5 mL of benzene. The solution was degassed using 3 freeze-pump-thaw cycles and then the vessel was charged with an atm of ^{13}CO. After stirring for 5 min the volatiles were removed *in vacuo* to give a yellow powder. Yield: 22 mg, 79%. ^{1}H NMR ($CDCl_3$, 500 MHz): δ 7.36 (s, 1H, ^{dm}Phebox-aryl), 7.00 (d, 2H, 2-Ph), 6.85 (t, 1H, 4-Ph), 6.81 (t, 2H, 3-Ph), 4.55 (d, 2H, $^1J_{HH'}$ = 8.4 Hz, OCH_2), 4.30 (d, 2H, $^1J_{HH'}$ = 8.4 Hz, OCH_2), 2.61 (s, 6H, Phebox-CH_3), 2.36 (s, 3H, OAc), 1.47 (s, 6H, CH_3), 1.13 (s, 6H, CH_3). ^{13}C NMR ($CDCl_3$, 500 MHz): δ 177.74 (OAc), 176.27, 170.42, 169.09 (CO), 145.45 (d, $^2J_{CC}$ = 38.7 Hz), 141.99, 134.51, 127.39, 126.42, 125.95, 123.18, 82.08 ($OCH_2C(CH_3)_2$), 66.23 ($OCH_2C(CH_3)_2$), 27.89 (CH_3), 26.08 (CH_3), 23.42 (OAc), 18.92 (Phebox-CH_3).

(^{dm}Phebox)Ir(^{13}CO)(OAc)(Ph) (*trans*-4b). Allowing a $CDCl_3$ solution (400 μL) of ***trans*-4b** to sit at room temperature for 48 h resulted in the formation of ***cis*-4b** as a yellow solid. ^{1}H NMR ($CDCl_3$, 500 MHz): δ 6.71 (m, 3H, phenyl and ^{dm}Phebox-aryl), 6.59 (m, 3H, phenyl and

^{dm}Phebox-aryl), 4.45 (d, 2H, $^{1}J_{HH'}$ = 8.4 Hz, OCH_2), 4.28 (d, 2H, $^{1}J_{HH'}$ = 8.4 Hz, OCH_2), 2.50 (s, 6H, Phebox-CH_3), 1.75 (s, 3H, OAc), 1.28 (s, 6H, CH_3), 1.10 (s, 6H, CH_3). ^{13}C NMR ($CDCl_3$, 500 MHz): δ 191.36, 182.54 (CO), 179.81, 177.70, 177.67, 176.58, 141.11, 139.55, 129.02, 127.08, 126.23, 122.26, 81.04 ($OCH_2C(CH_3)_2$), 66.51 ($OCH_2C(CH_3)_2$), 28.04 (CH_3), 27.24 (CH_3), 22.58 (OAc), 18.94 (Phebox-CH_3).

Thermolysis of *cis*-4b in benzene-d_6. A sealable NMR tube was charged with ***cis*-4b** (10.7 mg, 0.0163 mmol) and 500 μL benzene-d_6 and then the solution was degassed using three freeze-pump-thaw cycles. After the tube was flame sealed, the reaction was heated at 150 °C for 72 h and at 200 °C for 24 h. In the ^{1}H NMR spectrum at the end of the reaction ***cis*-4b**, ***trans*-4b**, and **1b** were present in a 2:1:1 ratio.

Synthesis of 1b-d_5 from 1b. A resealable NMR tube was charged with **1b** (6.2 mg, 0.0099 mmol) and 450 μL of benzene-d_6. Dioxane (1 μL, 0.0098 mmol) was added as an internal standard and then the solution was degassed by three freeze-pump-thaw cycles and flame-sealed. After heating at 150 °C for 24 h the yield of **1b-d_5** was determined to be 98% (integration of ^{dm}Phebox-aryl proton against dioxane).

Synthesis of 1b from 5b. A sealable NMR tube was charged with **5b** (2.8 mg, 0.0051 mmol) and 500 μL of benzene. The solution was degassed using three freeze-pump-thaw cycles and then flame sealed. The reaction was heated at 200 °C for 24 h. The tube was opened on the bench and the solution was transferred to a resealable NMR tube. The volatiles were removed *in vacuo* and an internal standard, 1,3,5-trimethoxybenzene (2 mg, 0.012 mmol) was added. The solid was rinsed into the tube using $CDCl_3$. The yield was determined to be 76% and was obtained by integration of the ^{dm}Phebox-aryl proton against the aryl protons of the internal standard.

Details of Solid State Structure Determination of *trans*-4b.

A colorless prism, measuring 0.14 x 0.08 x 0.02 mm^3 was mounted on a glass capillary with oil. Data was collected at -173 °C on a Bruker APEX II single crystal X-ray diffractometer, Mo-radiation. Crystal-to-detector distance was 40 mm and exposure time was 20 seconds per frame for all sets. The scan width was 0.5^o. Data collection was 98.9% complete to 25^o in ϑ. A total of 24300 (merged) reflections were collected covering the indices, h = -10 to 11, k = -11 to 11, l = -25 to 25. 6584 reflections were symmetry independent and the R_{int} = 0.0665 indicated that the data was good (average quality 0.07). Indexing and unit cell refinement indicated a triclinic lattice. The space group was found to be P $\bar{1}$ (No.2). The data was integrated and scaled using SAINT, SADABS within the APEX2 software package by Bruker.[13]

Solution by direct methods (SHELXS, SIR97[14]) produced a complete heavy atom phasing model consistent with the proposed structure. The structure was completed by difference Fourier synthesis with SHELXL97.[15,16] Scattering factors are from Waasmair and Kirfel.[17] Hydrogen atoms were placed in geometrically idealised positions and constrained to ride on their parent atoms with C---H distances in the range 0.95-1.00 Angstrom. Isotropic thermal parameters U_{eq} were fixed such that they were $1.2U_{eq}$ of their parent atom Ueq for CH's and $1.5U_{eq}$ of their parent atom U_{eq} in case of methyl groups. All non-hydrogen atoms were refined anisotropically by full-matrix least-squares. The crystals appeared twinned (180 degree rotation about (0 0 1), but because the overlap was almost complete, twinning was sufficiently addressed during refinement. Integration with two cell settings did not improve on this. Two disordered toluene solvent molecules were found in the unit cell which required some restraints in for the thermal parameters.

Table 5.1. Crystal data and structure refinement for ***trans*-4b**.

Empirical formula	$C_{34}\ H_{39}\ Ir\ N_2\ O_5$	
Formula weight	747.87	
Temperature	100(2) K	
Wavelength	0.71073 Å	
Crystal system	Triclinic	
Space group	P -1	
Unit cell dimensions	a = 8.5830(6) Å	α = 84.907(2)°.
	b = 8.9720(6) Å	β = 84.788(2)°.
	c = 20.1360(13) Å	γ = 78.480(2)°.
Volume	1509.12(18) $Å^3$	
Z	2	
Density (calculated)	1.646 Mg/m^3	
Absorption coefficient	4.468 mm^{-1}	
F(000)	748	
Crystal size	0.14 x 0.08 x 0.02 mm^3	
Theta range for data collection	2.04 to 27.15°.	
Index ranges	-10<=h<=11, -11<=k<=11, -25<=l<=25	
Reflections collected	24300	
Independent reflections	6584 [R(int) = 0.0665]	
Completeness to theta = 25.00°	98.9 %	
Max. and min. transmission	0.9159 and 0.5735	
Refinement method	Full-matrix least-squares on F^2	
Data / restraints / parameters	6584 / 90 / 428	
Goodness-of-fit on F^2	1.131	
Final R indices [I>2sigma(I)]	R1 = 0.0536, wR2 = 0.1138	
R indices (all data)	R1 = 0.0678, wR2 = 0.1198	
Largest diff. peak and hole	3.444 and -3.410 $e.Å^{-3}$	

Details of Solid State Structure Determination of *cis*-4b.

A yellow prism, measuring 0.30 x 0.10 x 0.09 mm^3 was mounted on a glass capillary with oil. Data was collected at -173 °C on a Bruker APEX II single crystal X-ray diffractometer, Mo-radiation. Crystal-to-detector distance was 40 mm and exposure time was 10 seconds per frame for all sets. The scan width was 0.5^o. Data collection was 99.8% complete to 25^o in ϑ. A total of 65456 (merged) reflections were collected covering the indices, h = -12 to 12, k = -16 to 16, l = -19 to 19. 7329 reflections were symmetry independent and the R_{int} = 0.0314 indicated that the data was good (average quality 0.07). Indexing and unit cell refinement indicated a

triclinic lattice. The space group was found to be P $\bar{1}$ (No.2). The data was integrated and scaled using SAINT, SADABS within the APEX2 software package by Bruker.[14]

Solution by direct methods (SHELXS, SIR97[15]) produced a complete heavy atom phasing model consistent with the proposed structure. The structure was completed by difference Fourier synthesis with SHELXL97.[16,17] Scattering factors are from Waasmair and Kirfel.[18] Hydrogen atoms were placed in geometrically idealized positions and constrained to ride on their parent atoms with C---H distances in the range 0.95-1.00 Angstrom. Isotropic thermal parameters U_{eq} were fixed such that they were $1.2U_{eq}$ of their parent atom Ueq for CH's and $1.5U_{eq}$ of their parent atom U_{eq} in case of methyl groups. All non-hydrogen atoms were refined anisotropically by full-matrix least-squares.

Table 5.2. Crystal data and structure refinement for ***cis*-4b**.

Empirical formula	$C_{28}\ H_{32}\ Cl_3\ Ir\ N_2\ O_5$	
Formula weight	775.11	
Temperature	100(2) K	
Wavelength	0.71073 Å	
Crystal system	Triclinic	
Space group	$P\ \bar{1}$	
Unit cell dimensions	a = 9.0373(6) Å	α = 75.140(3)°.
	b = 12.2563(8) Å	β = 79.093(3)°.
	c = 14.4831(10) Å	γ = 72.410(2)°.
Volume	1467.15(17) $Å^3$	
Z	2	
Density (calculated)	1.755 Mg/m^3	
Absorption coefficient	4.864 mm^{-1}	
F(000)	764	
Crystal size	0.30 x 0.10 x 0.09 mm^3	
Theta range for data collection	1.78 to 28.44°.	
Index ranges	-12<=h<=12, -16<=k<=16, -19<=l<=19	
Reflections collected	65456	
Independent reflections	7329 [R(int) = 0.0314]	
Completeness to theta = 25.00°	99.8 %	
Max. and min. transmission	0.6687 and 0.3232	
Refinement method	Full-matrix least-squares on F^2	
Data / restraints / parameters	7329 / 0 / 359	
Goodness-of-fit on F^2	1.052	
Final R indices [I>2sigma(I)]	R1 = 0.0242, wR2 = 0.0606	
R indices (all data)	R1 = 0.0278, wR2 = 0.0626	
Largest diff. peak and hole	1.782 and -1.500 $e.Å^{-3}$	

Notes to Chapter 5

1. Weissermel, K.; Hans-Jurgen, A. *Industrial Organic Chemistry*; Weinheim: Wiley-VCH, 2003; pp 349-367.

2. (a) Emmert, M. H.; Gary, J. B.; Villalobos, J. M.; Sanford, M. S. *Angew*. *Chem*. *Int*. *Ed*. **2010**, *49*, 5884. (b) Emmert, M. H.; Cook, A. K.; Xie, Y. J.; Sanford, M. S. *Angew*. *Chem*. *Int*. *Ed*. **2011**, *50*, 9409.

3. (a) Hartwig, J. F. *Chem*. *Soc*. *Rev*. **2011**, *40*, 1992. (b) Hartwig, J. F. *Acc*. *Chem*. *Res*. **2012**, *45*, 864.

4. (a) Wojcicki, A. *Adv*. *Organomet*. *Chem*. **1973**, *11*, 87. (b) Calderazzo, F. *Angew*. *Chem*. *Int*. *Ed*. *Engl*. **1977**, *16*, 299. (c) Kuhlman, E. J. Alexander, J. J. *Coord*. *Chem*. *Rev*. **1980**, *33*, 195.

5. (a) Anderson, G. K.; Lumetta, G. *Organometallics* **1985**, *4*, 1542. (b) Fryzuk, M. D.; MacNeil, P. A.; Rettig, S. J. *J*. *Organomet*. *Chem*. **1987**, *332*, 345. (c) Carmona, E.; Paneque,, M.; Poveda, M. L. *Polyhedron* **1989**, *8*, 285. (d) Dupont, J.; Pfeffer, M. J. *Chem*. *Soc*. *Dalton Trans*. **1990**, 3193. (e) Hartwig, J. F.; Bergman, R. G.; Andersen, R. A. *J*. *Am*. *Chem*. *Soc*. **1991**, *113*, 6499.

6. Cleary, B. P.; Eisenberg, R. *J*. *Am*. *Chem*. *Soc*. **1995**, *117*, 3510.

7. Li, L.; Jiao, Y.; Brennessel, W. W.; Jones, W. D. *Organometallics* **2010**, *29*, 4593.

8. Davies, D. L.; Al-Duaij, O.; Fawcett, J.; Singh, K. *Organometallics* **2010**, *29*, 1413.

9. Allen, K. E.; Heinekey, D. M.; Goldman, A. S.; Goldberg, K. I. *Organometallics* **2013**, *32*, 1579.

10. The substituents of the Phebox ligand were not chosen for any particular reason.

11. Ito, J.; Kaneda, T.; Nishiyama, H. *Organometallics* **2012**, *31*, 4442.

12. Ghosh, R.; Emge, T. J.; Krogh-Jespersen, K.; Goldman, A. S. *J*. *Am*. *Chem*. *Soc*. **2008**, *130*, 11317.

13. Bruker (**2007**) APEX2 (Version 2.1-4), SAINT (version 7.34A), SADABS (version 2007/4), BrukerAXS Inc, Madison, Wisconsin, USA.

14. (a) Altomare, A.; Burla, C.; Camalli, M.; Cascarano, L.; Giacovazzo, C.; Guagliardi, A.; Moliterni, A. G. G.; Polidori, G.; Spagna, R. *J*. *Appl*. *Cryst*. **1999**, *32***,** 115. (b) Altomare, A.; Cascarano, G.; Giacovazzo, C.; Guagliardi, A. *J*. *Appl*. *Cryst*. **1993**, *26*, 343.

15. Sheldrick GM. **(1997)** SHELXL-97, Program for the Refinement of Crystal Structures. University of Göttingen, Germany.

16. Mackay, S.; Edwards, C.; Henderson, A.; Gilmore, C.; Stewart, N.; Shankland, K.; Donald, A. *MaXus: a computer program for the solution and refinement of crystal structures from diffraction data*. University of Glasgow, Scotland, **1997**.

17. Waasmaier, D.; Kirfel, A. *Acta Crystallogr*. A. **1995**, *51*, 416.

Chapter 6: Synthesis of (^{tBu}NOCON)Rh^{III} and Ir^{III} Complexes and C-H Bond Activation of Arenes and Alkanes

Introduction

The selective transformation of alkanes into functionalized products could lead to greater utilization of the molecules as a source for value added chemicals. Current industrial methods for the functionalization of C-H bonds involve high temperatures and are not always selective for the desired product.[1] In order to transform alkanes into value-added chemicals, an initial C-H activation step is required to enter the catalytic cycle. Cleavage of sp^2 and activated sp^3 C-H bonds via an internal base deprotonation or concerted metalation deprotonation (CMD) mechanism has been reported in Pd arene functionalization systems.[2] This particular C-H activation mechanism involving Ir and Rh has been less widely reported. Davies and Jones independently proposed that directed C-H activation of arenes by $[Cp^*IrCl]_2$ in the presence NaOAc proceeds via an acetate assisted CMD mechanism.[3] Until recently the only proposed example of intermolecular sp^3 C-H cleavage via a CMD mechanism was published by Periana and coworkers.[4] In this study, (NNC^{tBu})Ir^{III}(TFA)$_2$(C_2H_4) (NNC^{tBu} = 6-phenyl-4,4′-di-*tert*-butyl-2,2′-bipyridine), was found to be a catalyst for the conversion methane to methyl trifluoroacetate. Computational work on this system suggested that a CMD mechanism was possible for the C-H activation step.[4]

Recently we found that (^{dm}Phebox)Ir(OAc)$_2$(OH_2) can promote alkane dehydrogenation.[5] Activation of C-H bonds in this system is proposed to occur at the Ir^{III} center through a CMD mechanism. In contrast to the (PCP)Ir^{I} complexes that promote alkane dehydrogenation,[6] our system was not inhibited by nitrogen, alkene, or water, which was attributed to the higher stability of the Ir^{III} center in contrast to Ir^{I}. Regeneration of the Ir bisacetate complex from the

product of dehydrogenation, (^{dm}Phebox)Ir(OAc)H was possible using oxygen and acetic acid at room temperature and completed the proposed catalytic cycle. Unfortunately, the (^{dm}Phebox)Ir system was not stable in the presence of oxygen at temperatures above 100 °C and suggested that a more robust pincer ligand may be necessary to achieve catalysis. Synthesis of the NOCON (NOCON = 1,3-bis(2-pyridyloxy)benzene) pincer ligand has been reported, but it has not been utilized in the exploration of Rh^{III} or Ir^{III} complexes for C-H functionalization. The oxygen linkages present in the pincer ligand and substitution of the oxazoline rings for pyridine should provide greater stability in the presence of oxygen. In order to explore a wider range of M^{III} (M = Rh, Ir) pincer complexes for alkane dehydrogenation we pursued the synthesis, characterization and reactivity exploration of the anionic NOCON and ^{tBu}NOCON ligands.

Results and Discussion

The synthesis of the target complex (NOCON)$RhCl_2(OH_2)$ (**1a**) has been previously described.[7] Complex **1a** was insoluble in benzene, CH_2Cl_2, and THF and only exhibited low solubility in CH_3OH and DMSO. Attempts to generate (NOCON)$Rh(OAc)_2(OH_2)$ (**2a**) from the reaction of **1a** and 2 equiv. of AgOAc in CD_3OD at 60 °C for 48 h were unsuccessful and the starting material, **1a**, was recovered from the reaction (eq. 6.1). When the reactants were heated at 60 °C for an additional 24 h (72 h total) conversion of **1a** to unidentifiable products occurred. In order to probe **2a** for C-H activation without isolating the complex, H/D exchange reactions were performed using **1a** and 10 equiv. of AgOAc in order to try to form **2a** *in situ*. The H/D exchange reactions were conducted using benzene (10 equiv.) and CD_3COOD, D_2O, and CD_3OD (1000 equiv.) and were heated at 80 °C for 24 h. Under these conditions deuterium incorporation into benzene was not observed by GC/MS. The formation of insoluble solids was observed in all cases. While these reactions were conducted in dilute benzene solutions, another method could

be to conduct the H/D exchange reactions in concentrated benzene solutions with added deuterium source. Unfortunately, the insolubility of **1a** in benzene made it difficult to perform the H/D exchange reactions in concentrated benzene solutions.

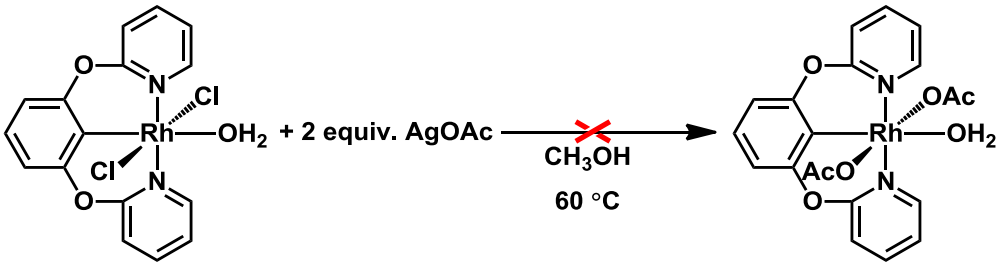

1a **2a** (6.1)

The Ir^{III} analogue of **1a**, (NOCON)$IrCl_2(OH_2)$ (**3a**), has not been previously reported. Several different Ir starting materials were used in efforts to obtain **3a**. A mixture of NOCON and $IrCl_3 \cdot H_2O$ in ethanol was found to be unreactive after heating at reflux for 4 days (Scheme 6.1). When the NOCON ligand was mixed with $[Ir(COD)Cl]_2$ in toluene-d_8 at 100-150 °C for 4 days broad signals were observed in the ^{1}H NMR spectra corresponding to NOCON ligand and a new minor species. A dark colored solid was also present in the reaction. At the end of 4 days the presence of at least three different products was observed in the ^{1}H NMR spectrum. In the olefin region of the spectrum two signals integrating in a 1:1 ratio were observed at 3.43 and 4.79 ppm, indicative of a new Ir-COD complex. Free COD and $[Ir(COD)Cl]_2$ were not observed at any point during the reaction. A small signal was observed upfield at -22.67 ppm suggesting that one of the products may be an Ir-hydride species. Upon further heating the reaction mixture generated more insoluble and unidentifiable products.

Scheme 6.1

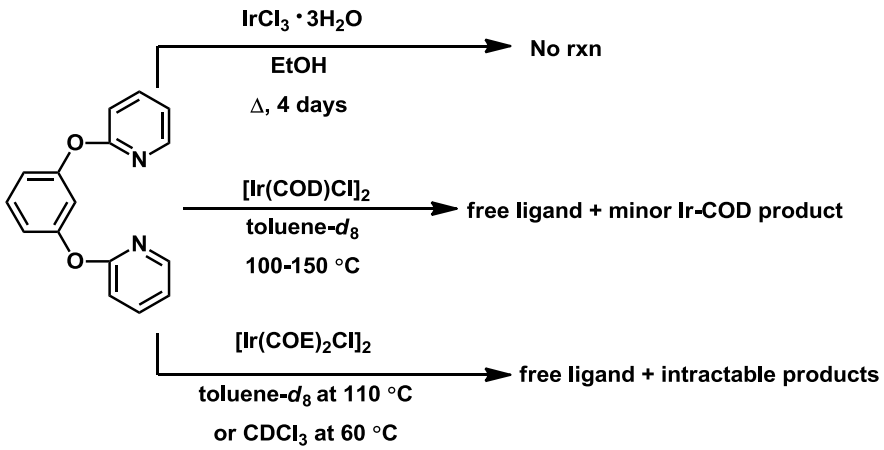

When mixtures of NOCON and $[Ir(COE)_2Cl]_2$ in toluene-d_8 were heated at 110 °C, the formation of a brown solid was observed over the course of 72 h (Scheme 6.1). This solid was only soluble in DMSO. A similar product was also obtained when the reaction was performed in $CDCl_3$ at 60 °C. The low solubility of the solids obtained from these metalation attempts suggested that metalation of the pincer ligand via C-H activation may have occurred in the 4- and 6-positions of the aryl backbone by different Ir centers to generate an insoluble oligomeric species.

Examples of cyclometalation of pincer ligand backbones in the 4- and 6-positions has been reported previously using Ir and Pd precursors.[8] The reaction of $[Ir(COD)Cl]_2$ with (C_{NHC}–N–C_{NHC}) (C_{NHC}–N–C_{NHC} = 2,6-bis(imidazol-2-ylidene)pyridine) in THF at -78 °C resulted in the formation of a cyclometalated Ir^{III} complex and not the expected (C_{NHC}–N–C_{NHC})$Ir^{I}Cl$ species (Scheme 6.2).[8a] Substitution in the 4- and 6- positions of the (C_{NHC}–N–C_{NHC}) ligand precursor backbone permitted metalation in the 2- position of the pincer ligand. It is reasonable to suggest that metalation in the 4- and 6- positions of the NOCON ligand may be occurring and prevented

coordination of the ligand via C-H activation at the 2-position. With this in mind and considering the low solubility observed for **1a** the *tert*-butyl substituted ligand, ^{tBu}NOCON (^{tBu}NOCON = 4,6-di-*tert*-butyl-(1,3-bis(2-pyridyloxy)benzene)), was explored for the formation of Ir^{III} and Rh^{III} complexes for C-H activation.

Scheme 6.2[8a]

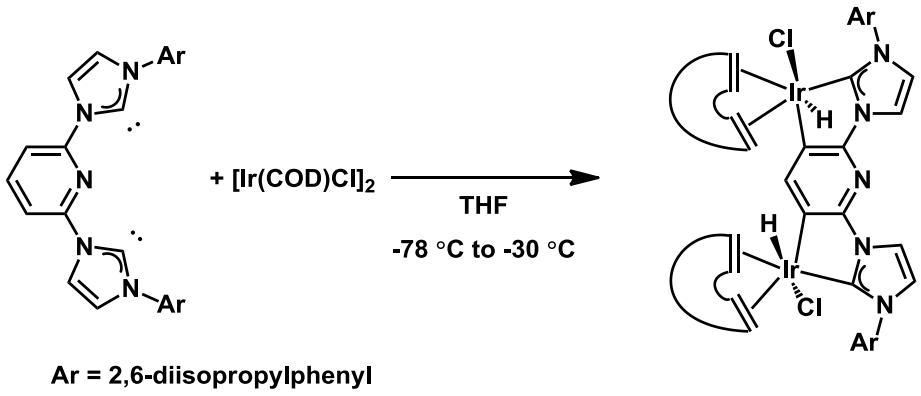

The neat reaction of 4,6-di-*tert*-butylresorcinol and 2.5 equiv. of 2-bromopyridine in the presence of 2 equiv. of K_2CO_3 yielded ^{tBu}NOCON in low yields.[9] Separation of the target ligand from the byproducts of the reaction proved difficult. Multiple attempts to purify crude ^{tBu}NOCON via column chromatography and recrystallization did not lead to pure material. Instead metalation of the crude ligand with Rh was attempted. The reaction of ^{tBu}NOCON with $RhCl_3 \cdot H_2O$ in CH_3OH in the presence of either $NaHCO_3$ (2 equiv.) or Cs_2CO_3 (1 equiv.) at 80 °C resulted in formation of the new compound, (^{tBu}NOCON)$RhCl_2(OH_2)$ (**1b**), after 3 h (eq. 6.2). Longer reaction times, such as 12 h, led to decomposition of **1b** to free ligand and Rh black. In the ^{1}H NMR spectrum of **1b**, coordination at the desired position of ^{tBu}NOCON was confirmed by the disappearance of the singlet at 7.54 ppm, which corresponded to the proton in the 2-position of the aryl backbone. Additionally, the doublet consistent with the *ortho* protons of the

pyridine rings was observed at 8.68 ppm, which is downfield of shift observed in free ligand at 8.12 ppm. The downfield shift observed for the *ortho* protons is consistent with coordination of ^{tBu}NOCON.

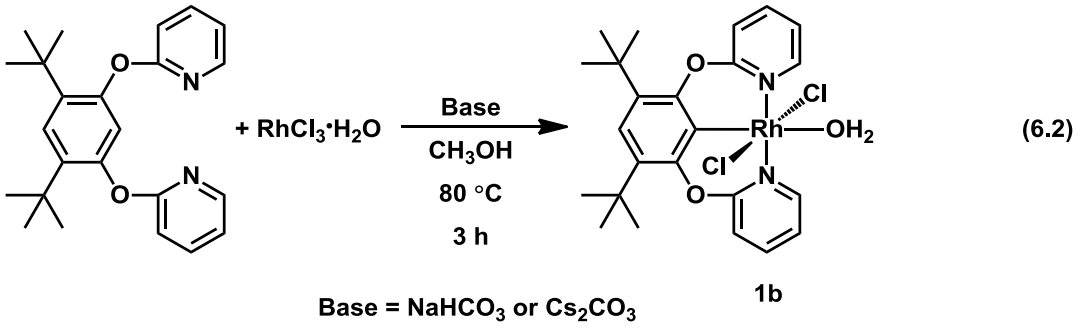

Complex (^{tBu}NOCON)Rh(OAc)$_2$(OH$_2$) (**2b**) was obtained by heating **1b** in the presence of 6 equiv. of AgOAc in CH_2Cl_2 at 80 °C overnight. The presence of the two acetate ligands was confirmed using ^{1}H NMR spectroscopy. A singlet integrating to six protons at 1.63 ppm was diagnostic of the OAc ligands and the expected signals for the bound pincer ligand were also observed. Complex **2b** was obtained as a light yellow solid in low yields, 11%, after purification by column chromatography. When a benzene solution of **2b** was heated at 100 °C for 5 days a new product, (^{tBu}NOCON)Rh(OAc)Ph (**4b**) was obtained (eq. 6.3). In the ^{1}H NMR spectrum of **4b** three multiplets at 6.77, 6.68, and 6.58 ppm corresponded to the bound phenyl ring and a singlet at 2.03 ppm integrating to three protons supported the presence of the remaining acetate ligand. While C-H activation was observed in this reaction, decomposition of **2b** to Rh black was also observed and thus the analogous Ir system was targeted.

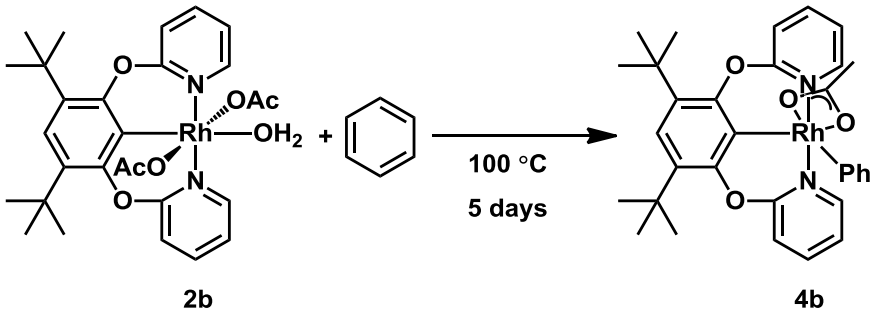

2b 4b (6.3)

The reaction of ^{tBu}NOCON with $IrCl_3 \cdot H_2O$ in CH_3OH resulted in the formation of (^{tBu}NOCON)$IrCl_2(OH_2)$ (**3b**) in 70% isolated yield after 4 h at 100 °C. A doublet in the ^{1}H NMR spectrum at 8.59 ppm corresponded to the two *ortho* protons of the pyridine rings and was indicative of metalation of the ^{tBu}NOCON ligand. This downfield shift from 8.20 ppm in the ^{1}H NMR spectrum of free ligand is consistent with the downfield shift observed upon metalation of ^{tBu}NOCON with $RhCl_3 \cdot H_2O$. Halide abstraction from **3b** using 6 equiv. of AgOAc in CH_2Cl_2 resulted in formation of (^{tBu}NOCON)$Ir(OAc)_2(OH_2)$ (**5b**) in 48% yield after heating at 80 °C for 7 h (eq. 6.4). Complex **5b** was characterized by ^{1}H and ^{13}C NMR spectroscopy, elemental analysis and X-ray crystallography. In the ^{1}H NMR spectrum of **5b** a singlet at 1.69 ppm corresponded to the two acetate ligands and a singlet at 1.50 ppm was observed indicative of the *tert*-butyl signals of the phenyl backbone.

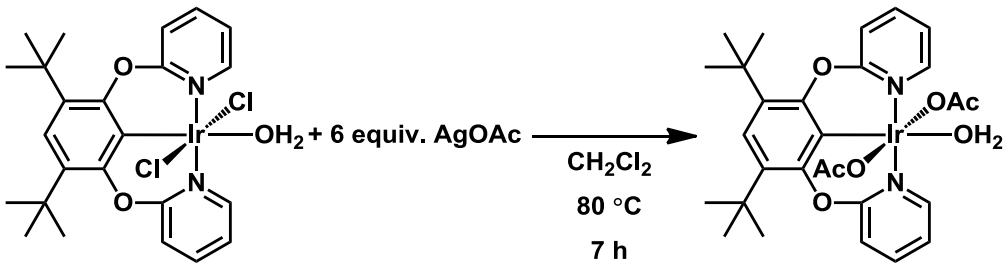

3b 5b (6.4)

The solid state structure of **5b** was determined using X-ray crystallographic analysis (Figure 6.1). The X-ray data revealed an octahedral structure in the solid state. The C(1)-Ir(1)-O(3) and N(2)-Ir(1)-N(1) bond angles are 177.67(8)º and 176.57(8)º. A slight deviation from an octahedral geometry is reflected in the bond angles for N(2)-Ir(1)-O(4) and N(1)-Ir(1)-O(4) which are 84.70(8)º and 96.69(8)º respectively. This is a result of the acetate ligands not residing perfectly in the x,y plane. The water ligand was located *trans* to the phenyl backbone of the ^{tBu}NOCON ligand. The Ir(1)-O(3) bond length, 2.1825(17) Å, is in close agreement to the Ir-OH_2 bond length of 2.206(3) Å previously described for (^{dm}Phebox)Ir(OAc)$_2$(OH_2).[10]

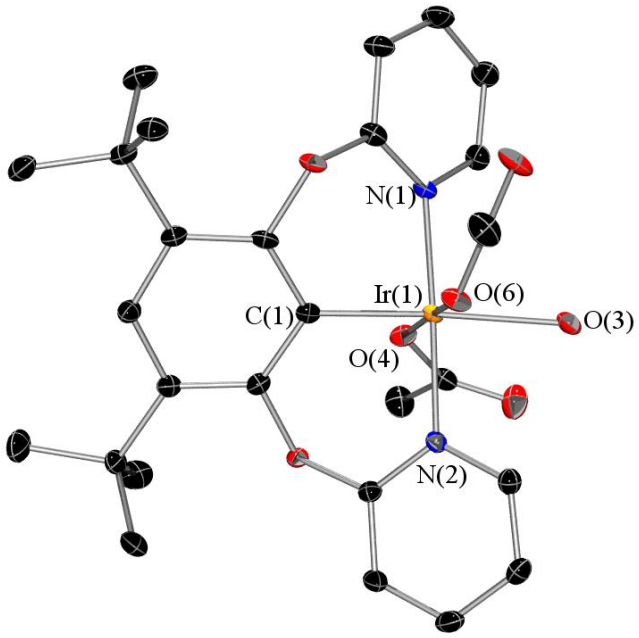

Figure 6.1. ORTEP diagram of (^{tBu}NOCON)Ir(OAc)$_2$(OH_2) (**5b**) (thermal ellipsoids at 50% probably, H atoms omitted for clarity). Selected bond distances (Å) and angles (deg): Ir(1)-C(1) = 1.968(2), Ir(1)-O(3) = 2.1825(17), Ir(1)-N(2) = 2.026(2), Ir(1)-N(1) = 2.029(2), Ir(1)-O(4) = 2.0371(18), Ir(1)-O(6) = 2.0461(19), N(2)-Ir(1)-N(1) = 177.67(8), N(2)-Ir(1)-O(4) = 84.70(8), N(1)-Ir(1)-O(4) = 96.69(8), C(1)-Ir(1)-O(3) = 176.57(8), N(1)-Ir(1)-O(6) = 96.69(8), N(1)-Ir(1)-O(6) = 87.39(8), O(4)-Ir(1)-O(6) = 174.20(6).

Intermolecular cleavage of sp^2 C-H bonds was observed when a benzene solution of **5b** was heated at 120 °C for 45 minutes. This resulted in the formation of the C-H activation product, (^{tBu}NOCON)Ir(OH_2)(OAc)(Ph) (**6b**), in quantitative yield against a hexamethylbenzene internal standard using ^{1}H NMR spectroscopy (eq. 6.5). Complex **6b** was characterized by ^{1}H and ^{13}C NMR spectroscopy and X-ray crystallography. In the ^{1}H NMR spectrum ($CDCl_3$), three signals consistent with a phenyl ligand were clearly observed at 6.69 (t, 1H), 6.60 (t, 2H), and 6.38 (d, 2H) ppm. Five multiplets from 6.93-8.34 ppm were assigned to the aromatic protons of ^{tBu}NOCON and a singlet at 1.44 ppm was assigned to the *tert*-butyl substituents. A singlet at 2.07 ppm integrated to three protons and was consistent with the remaining OAc ligand.

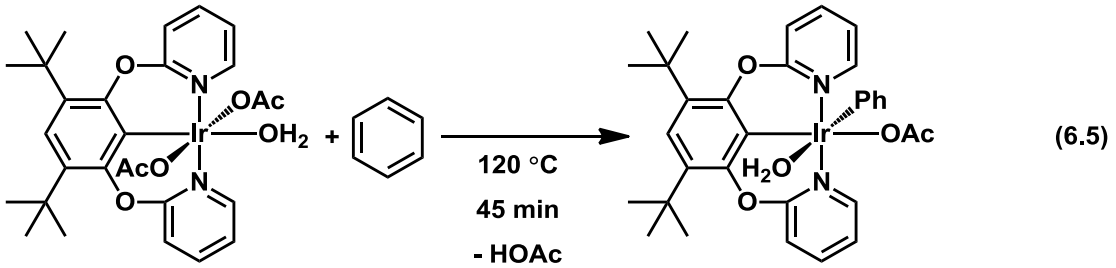

5b **6b** **(6.5)**

The X-ray crystallographic data supported a solid state structure with an octahedral geometry about the metal center (Figure 6.2). The bond angles for N(1)-Ir(1)-N(2) and C(1)-Ir(1)-O(3) are 177.6(5)º and 178.1(3)º, respectively, consistent with an octahedral geometry. The Ir(1)-C(1) bond length, 2.006(6) Å, is in agreement with that described above for **5b** (Ir(1)-C(1) is 1.968(2)) (Figure 6.1). The Ir-OAc, Ir(1)-O(3), bond length was 2.178(9) Å, which is elongated when compared to the Ir-OAc bond lengths of **5b** (2.0371(18) and 2.0461(19) Å). The longer Ir-O bond observed in **6b** is a result of the *trans* effect of the aryl backbone. A water

molecule was located *trans* to the central carbon C(1), of the pincer ligand backbone of **6b**. In the ^{1}H NMR spectrum of **6b**, a signal corresponding to the water ligand was not observed, even in dry solvents. The bond length corresponding to the Ir-OH_2 bond, 2.191(8) Å, was consistent with the Ir-OH_2 bond length, 2.1825(17) Å, determined above for **5b**.

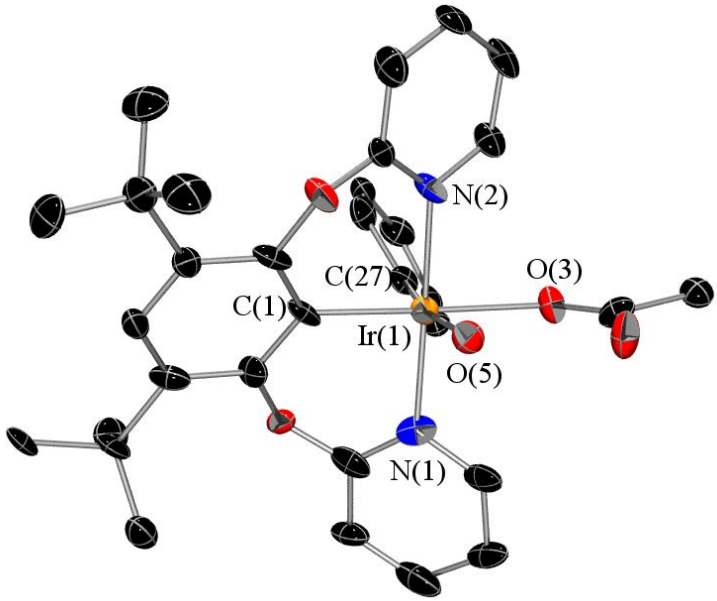

Figure 6.2. ORTEP diagram of (^{tBu}NOCON)Ir(OH_2)(OAc)(Ph) (**6b**) (thermal ellipsoids at 50% probably, H atoms omitted for clarity). Selected bond distances (Å) and angles (deg): Ir(1)-C(1) = 2.006(6), Ir(1)-C(27) = 2.004(11), Ir(1)-O(3) = 2.178(9), Ir(1)-N(1) = 2.030(11), Ir(1)-N(2) = 2.036(10), Ir(1)-O(5) = 2.191(8), N(1)-Ir(1)-N(2) = 177.6(5), C(1)-Ir(1)-O(3) = 178.1(3), C(27)-Ir(1)-O(3) = 83.6(4), N(2)-Ir(1)-O(5) = 85.3(4), O(3)-Ir(1)-O(5) = 88.7(3), C(1)-Ir(1)-C(27) = 94.8(4), C(27)-Ir(1)-O5) = 171.5(4).

When benzene-d_6 was used as a substrate the expected ^{1}H NMR signals for the product **6b-d_5** were observed in solution. The signal corresponding to the remaining acetate ligand at 2.22 ppm was rather broad suggestive of exchange. The addition of 1 equiv. of acetic acid to a benzene solution of isolated **6b** resulted in broadening of the OAc signal by ^{1}H NMR spectroscopy. This result confirmed that at room temperature exchange between the remaining

acetate ligand and the added acetic acid occurs. Similar exchange between acetic acid and an acetate ligand was observed in a related complex, (^{dm}Phebox)Ir(OAc)Ph.[5]

Activation of benzene by the Ir complex **5b** was also observed at lower temperatures, namely 100 °C, however with a longer reaction time of 2.5 h. In comparison to benzene activation with the Rh analogue **2b**, which required 5 days to reach completion, C-H cleavage by **5b** at 100 °C was considerably faster. In the related system, (^{dm}Phebox)M(OAc)$_2$(OH$_2$) (M = Rh, Ir) a similar trend was observed: benzene activation by the Ir^{III} analogue occurred quantitatively after 1.5 h in comparison to the 6 days required for the Rh^{III} complex to perform the same reaction in only modest yields.[5,11]

Along with formation of **6b** a yellow precipitate was also generated during the benzene activation reactions. The yellow solid was only soluble in hot DMSO and attempts to obtain ^{1}H NMR spectroscopic data did not result in any insight into the identity of the solid. It is possible that this yellow material is a result of dimerization of **6b**, which may account for the decreased solubility in all solvents at room temperature. Yields of **6b** were obtained using ^{1}H NMR spectroscopy with various internal standards (hexamethylbenzene, dioxane, and 1,3,5-trimethoxybenzene) and supported quantitative formation of the complex. When activation of benzene-d_6 was performed in the presence of 2 equiv. K_2CO_3 to remove acetic acid at 120 ºC, **6b-*d*$_5$** was also obtained in quantitative yield (99%) along with the appearance of the yellow solid. Complex **6b** was also stable to acetic acid at 120 ºC over the course of several days. The identity of the yellow solid formed during benzene activation has not been determined. It is unclear whether this solid resulted from an impurity in the starting material **5b** or directly from the activation reaction.[12]

Dehydrogenation of alkanes was observed when neat solutions of **5b** were heated at 200 °C (Scheme 6.3). At temperatures lower than 200 °C alkane dehydrogenation by **5b** was not observed. When an *n*-octane solution of **5b** was heated at 200 °C for 5 days, the formation of several octene isomers, *trans*-4-octene, *trans*-3-octene, *trans*-2-octene, *cis*-3-octene, and *cis*-2-octene, was observed by GC analysis. Generation of octene suggested that C-H activation to generate an Ir-alkyl complex had occurred followed by β-hydride elimination. The expected Ir^{III} product of the reaction was (^{tBu}NOCON)Ir(OAc)H (**7b**). When the reaction was monitored by ^{1}H NMR spectroscopy, formation of **7b** was not observed as no hydride signals were observed upfield of the *tert*-butyl singlet of **5b**. In the ^{1}H NMR spectrum (THF-d_8) of the Ir material at the end of the reaction, broad signals were observed in the aromatic and *tert*-butyl regions. Hydride signals were also not observed in the spectrum and Ir black was also present at the end of the reaction. Complex **5b** was found to have increased solubility in cyclooctane (COA) at 200 °C in comparison to *n*-octane. When COA solutions of **5b** were heated at 200 °C for 5 days COE was observed by GC analysis. Double dehydrogenation products, such as COD, were not observed under these conditions. The resulting Ir products from this reaction were also unidentifiable and exhibited broad aromatic signals in the ^{1}H NMR spectrum. Compound **7b** may be unstable at elevated temperatures, which could contribute to the lack of identifiable Ir products from alkane activation.

Scheme 6.3

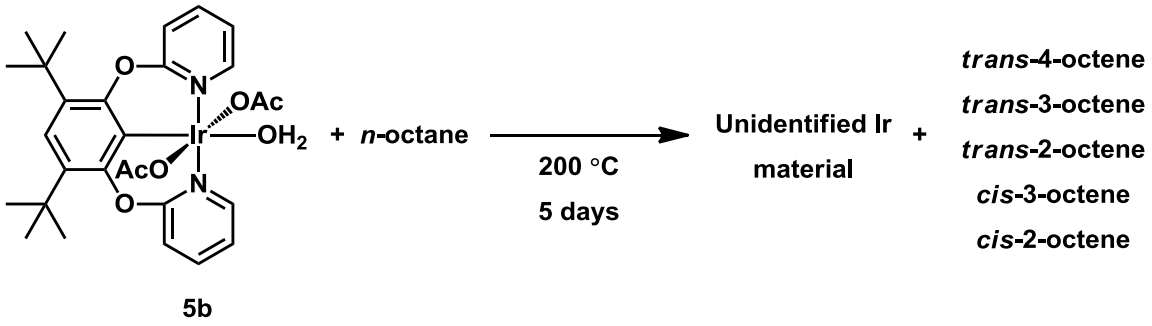

5b

Insertion of small molecules, such as CO, into metal alkyl bonds has been observed in many different systems.[13] There are fewer examples of CO insertion into M-aryl bonds,[14] specifically utilizing Ir complexes.[15] Insertion into Ir-aryl bonds has been explored by Jones and Davies independently as discussed in Chapter 5 (Scheme 6.4). When neutral Cp^*Ir complexes were exposed to CO, insertion into the Ir-aryl bond was observed.[16] No insertion was observed when cationic Cp^*Ir complexes were exposed to an atmosphere of CO.[17] Rather only displacement of acetonitrile and coordination of CO to the Ir^{III} center was observed. In order to better understand what factors contribute to promoting CO insertion into Ir-aryl bond a wider range of complexes must be explored. We were interested in determining if we could achieve benzene functionalization via CO insertion into the Ir-phenyl bonds of **6b**.

Scheme 6.4

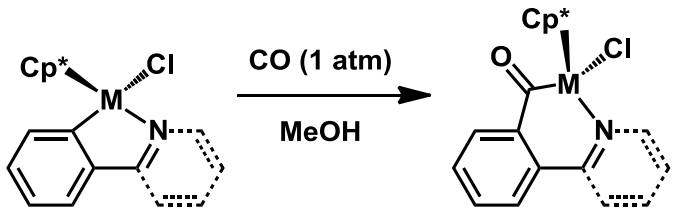

M = Rh, Ir

When CO was bubbled through a benzene-d_6 solution of **6b** the formation of a new compound, (^{tBu}NOCON)Ir(OAc)(CO)Ph (**8b**), was observed after 5 minutes (eq. 6.6). Upon exposure to CO the tan colored solution became colorless almost immediately. In solution, complex **8b** was stable to air over the course of three days. Long term stability to air has not yet been determined. In the ^{1}H NMR spectrum of **8b** three signals were observed at 6.80 (t, 1H), 6.69 (t, 2H), and 6.45 (d, 2H) corresponding to phenyl ligand. These chemical shifts are not significantly different than those observed for the phenyl ligand in complex **6b**. The ^{13}C NMR signal corresponding to the CO ligand was observed at 177.73 ppm supporting coordination of CO to the Ir^{III} center and not insertion. In the IR spectrum of **8b** the CO stretching frequency was determined to be 2057 cm^{-1}. This is indicative of coordinated CO and not insertion. Further studies are needed to explore **8b** for CO insertion at elevated temperatures.

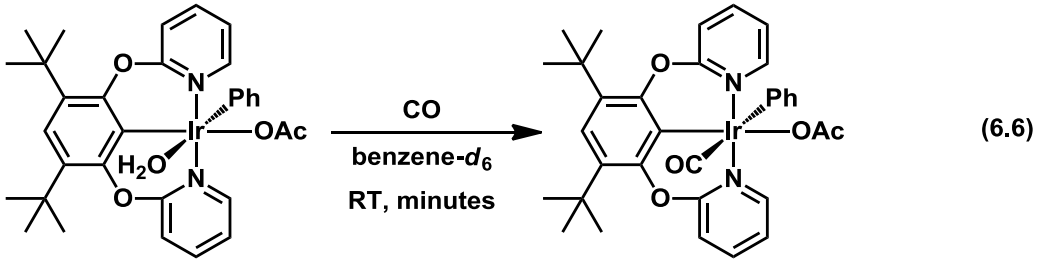

6b 8b (6.6)

Conclusions

Attempts to synthesize (NOCON)$IrCl_2(OH_2)$ using several different Ir starting materials did not result in isolable product. This is most likely a result of cyclometalation of the Ir starting material with the aryl backbone of the pincer ligand. Substitution of the NOCON ligand at the 4- and 6-positions of the aryl ring with *tert*-butyl groups led to C-H activation of the ligand in the desired position using both Rh and Ir materials. A comparison of the reactions of

(^{tBu}NOCON)M(OAc)$_2$(OH$_2$) (M = Rh (**2b**), Ir (**5b**)) with benzene revealed that the Ir analogue activated sp^2 C-H bonds over a shorter period of time. Decomposition was observed during the reaction of the Rh complex **2b** with benzene and demonstrated the enhanced stability of the Ir analogue at elevated temperatures. The greater stability of the Ir analogue allowed for the observation of *n*-octane dehydrogenation at 200 °C. In this reaction decomposition of the **5b** occurred, which may be a result of the decreased solubility of the complex in alkane solvents or a result of the high temperatures required to observe dehydrogenation. This example extends the library of complexes that can promote alkane dehydrogenation utilizing an Ir^{III} center. Based on these results alkane dehydrogenation via an acetate assisted CMD C-H activation mechanism is viable, although pincer ligands with increased rigidity in comparison to NOCON are likely required.

Experimental

General Considerations. Unless specified otherwise, all reactions were carried out under a dry nitrogen atmosphere using standard glovebox, Schlenk, or vacuum-line techniques. *n*-Octane, $\geq$ 98%, and cyclooctane were used as received from Alfa Aesar. All other reagents were used as received from a variety of suppliers. Benzene and pentane were purified by passage through columns of activated alumina and molecular sieves prior to use. Deuterated solvents were purchased from Cambridge Isotope Laboratories. Benzene-d_6, toluene-d_8 and THF-d_8 were dried over sodium/benzophenone, and dichloromethane-d_2 and chloroform-d_1 were dried over CaH_2. NMR spectra were obtained on Bruker AV300 or AV500 MHZ spectrometers with chemical shifts (δ) reported in ppm downfield of tetramethylsilane. Octane and cyclooctadiene dehydrogenation reactions were quantified using Agilent 7890A gas chromatograph with a 30 m x 0.32 mm Agilent GASPRO capillary column. NOCON[7] and (NOCON)RhCl$_2$(OH$_2$) (**1a**)[7] were

prepared using literature procedures. Elemental analyses were performed by Atlantic Microlab Inc. of Norcross, GA.

Synthesis and Characterization of Complexes

^{tBu}NOCON. A sealable ampoule was charged with 4,6-di-*tert*-butylresorcinol (1.0 g, 4.5 mmol), K_2CO_3 (1.56 g, 11.3 mmol), and 2-bromopyridine (1.1 mL, 11.3 mmol) and then flame sealed. The mixture was heated at 190 °C for 15 h and then the ampoule was opened. The crude mixture was extracted three times using Et_2O (5 mL) and washed with a 40% NaOH aqueous solution until precipitation no longer occurred. The organic layer was also washed with 10 mL water and 10 mL brine. Excess 2-bromopyridine was distilled under vacuum, to yield ^{tBu}NOCON as an impure brown solid (776 mg, 46%). The crude product was taken on to obtain pure Rh and Ir complexes. ^{1}H NMR (CD_3OD, 500 MHz): δ 8.12 (d, 2H, 5′), 7.78 (m, 2H, 4′), 7.53 (s, 1H, 4), 7.06 (t, 2H, 3′), 6.93 (d, 2H, 2′), 6.44 (s, 1H, 6), 1.39 (s, 18H, *tBu*). ^{13}C NMR (CD_3OD, 500 MHz): δ 164.90, 152.45, 148.50, 141.55, 138.52, 127.13, 120.09, 117.69, 112.86, 35.72 ($C(CH_3)_3$), 30.81 ($C(CH_3)_3$).

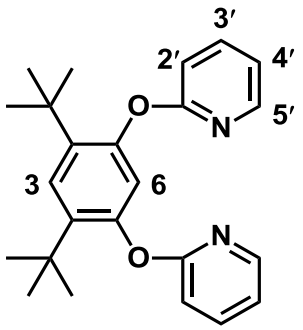

(^{tBu}NOCON)RhCl$_2$(H$_2$O) (1b). A Teflon-sealed reaction vessel was charged with ^{tBu}NOCON (180 mg, 0.48 mmol), $NaHCO_3$ (40 mg, 0.48 mmol), and $RhCl_3 \cdot 3H_2O$ (126 mg, 0.48 mmol). This mixture was suspended in 16 mL of CH_3OH and then heated at 80 °C for 3 h. After cooling to RT, another equivalent of $NaHCO_3$ (40 mg, 0.48 mmol) was added. The reaction mixture was

degassed by three freeze-pump-thaw cycles, and then heated at 80 °C for 3 h. The solution was filtered and a yellow solid was precipitated using pentane. (195 mg, 72%) ^{1}H NMR (CD_3OD, 500 MHz): δ 8.68 (d, 2H, 5′), 8.02 (m, 2H, 4′), 7.37 (d, 2H, 2′), 7.29 (t, 2H, 3′), 7.22 (s, 1H, 3), 1.51 (s, 18H, *tBu*). ^{13}C NMR (CD_3OD, 500 MHz): δ 162.67, 152.14 (d, $^{1}J_{RhC}$ = 2.9 Hz), 152.11, 142.44, 134.55, 129.32, 122.93, 120.19, 115.74, 36.07 ($C(CH_3)_3$), 31.36 ($C(CH_3)_3$).

(^{tBu}NOCON)Rh(OAc)$_2$(H$_2$O) (2b). A Teflon-sealable reaction vessel was charged with **1b** (150 mg, 0.24 mmol), AgOAc (264 mg, 1.59 mmol) and 20 mL of CH_2Cl_2. The reaction mixture was heated at 80 °C overnight. The crude mixture was purified using column chromatography with chloroform/methanol (95:5) used as the eluent, yielding a pale yellow solid after lyophilization from benzene (5.1 mg, 11%). ^{1}H NMR (CD_3OD, 500 MHz): 8.58 (d, 2H, 5′), 8.07 (m, 2H, 4′), 7.44 (d, 2H, 2′), 7.36 (m, 2H, 3′), 7.26 (s, 1H, 3), 1.63 (s, 6H, OAc), 1.53 (s, 18H, *tBu*). ^{13}C NMR (CD_3OD, 500 MHz): δ 182.83 (OAc), 162.77, 151.40, 142.94, 135.21, 132.39, 129.89, 123.01, 116.32, 115.82, 36.04 ($C(CH_3)_3$), 31.30 ($C(CH_3)_3$), 23.15 (OAc).

(^{tBu}NOCON)Rh(OAc)(Ph) (4b). A resealable NMR tube was charged with **2b** (2.5 mg, 0.0041 mmol) and 350 μL of a 2M dioxane-d_8 in benzene solution. The reaction was heated at 100 °C for 5 days and then the volatiles were removed *in vacuo*, to yield **4b** as a yellow colored solid. ^{1}H NMR ($CDCl_3$): δ 8.24 (d, 2H,5′), 7.73 (m, 2H, 4′), 7.16 (s, 1H, 3), 7.14 (d, 2H, 2′), 6.97 (t, 2H, 3′), 6.77 (t, 1H,4-Ph), 6.68 (t, 2H, 3-Ph), 6.59 (d, 2H, 2-Ph), 2.03 (s, 3H, OAc), 1.46 (s, 18H, *tBu*).

(^{tBu}NOCON)IrCl$_2$(H$_2$O) (3b). A resealable reaction vessel was charged with ^{tBu}NOCON (80 mg, 0.21 mmol), $IrCl_3 \cdot 3H_2O$ (75 mg, 0.21 mmol) and 6.4 mL of methanol. The reaction mixture was heated at 100 °C for 4 h and then filtered through a glass fritted filter. After removal of the volatiles *in vacuo* the brown residue was dissolved in minimal benzene. After lyophilization **3b**

was obtained as a brown solid (96 mg, 84% yield). ^{1}H NMR (CD_3OD, 500 MHz): δ 8.60 (d, 2H, 5′), 8.00 (m, 2H, 4′), 7.35 (d, 2H, 2′), 7.24 (t, 2H, 3′), 6.99 (s, 1H, 3), 1.49 (s, 18H, *tBu*). ^{13}C NMR (CD_3OD, 500 MHz): δ 163.54, 154.32, 152.57, 141.70, 133.25, 122.03, 120.35, 115.90, 35.76 ($C(CH_3)_3$), 31.36 ($C(CH_3)_3$).

(^{tBu}NOCON)Ir(OAc)$_2$(H$_2$O) (5b). A Teflon-sealable reaction vessel was charged with **3b** (100 mg, 0.15 mmol), AgOAc (153 mg, 0.91 mmol), and 9 mL of CH_2Cl_2. The mixture was heated at 80 ˚C for 7 h. The crude mixture was purified by column chromatography using dichloromethane/methanol (95:5). After removal of the volatiles in vacuo, the yellow residue was dissolved in benzene and lyophilized. Complex **5b** was obtained as a light yellow solid (78 mg, 48% yield). X-ray quality crystals of **5b** were grown from a CH_2Cl_2 solution layered with pentane at room temperature. ^{1}H NMR (CD_3OD, 500 MHz): δ 8.55 (d, 2H, 5′), 7.98 (m, 2H, 4′), 7.40 (d, 2H, 2′), 7.28 (t, 2H, 3′), 7.05 (s, 1H, 3), 1.68 (s, 6H, OAc), 1.50 (s, 18H, *tBu*). ^{13}C NMR (CD_3OD, 500 MHz): δ 184.10 (OAc), 163.89, 154.68, 152.33, 142.20, 133.78, 122.12, 120.89, 116.30, 115.84, 35.68 ($C(CH_3)_3$), 31.31 ($C(CH_3)_3$), 22.40 (OAc). Anal. Calcd for $C_{28}H_{35}N_2O_7Ir$: C, 47.77; H, 5.01; N, 3.98. Found: C, 47.51; H, 5.06; N, 3.91.

(^{tBu}NOCON)Ir(OAc)(Ph)(H$_2$O) (6b). In a Teflon-stoppered reaction vessel, **4b** (30 mg, 0.042 mmol) was heated at 120 °C in 2 mL of benzene for 45 minutes. After removal of the volatiles in vacuo, the product was lyophilized from benzene yielding a yellow solid (17.1 mg, 70% yield). X-ray quality crystals of **6b** were grown from a CH_2Cl_2 solution layered with pentane at -20 ºC. ^{1}H NMR ($CDCl_3$): δ 8.34 (d, 2H, 5′), 7.73 (m, 2H, 4′), 7.13 (d, 2H, 2′), 7.01 (s, 1H, 3), 6.93 (t, 2H, 3′), 6.69 (t, 1H, 4-Ph), 6.60 (t,2H, 3-Ph), 6.38 (d, 2H, 2-Ph), 2.07 (s, 3H, OAc), 1.44 (s, 18H, *tBu*). ^{13}C NMR (CD_2Cl_2, 500 MHz): δ 160.78, 151.78, 150.40, 139.05, 135.06, 132.16, 128.04, 125.46, 121.60, 119.72, 118.97, 114.54, 106.34, 34.37 ($C(CH_3)_3$), 30.36 ($C(CH_3)_3$).

(^{tBu}NOCON)Ir(OAc)(Ph)(H_2O) (6b-d_5). A resealable NMR tube was charged with **5b** (5.9 mg, 0.0084 mmol) and 400 μL of a 20 mM 1,3,5-trimethoxybenzene in benzene-d_6 solution was added via microsyringe. The reaction was heated at 120 °C for 45 minutes and resulted in **6b-d_5**. Yield: 98% yield determined by integration of ^{tBu}NOCON-aryl-H signal against 1,3,5-trimethoxybenzene internal standard. ^{1}H NMR (C_6D_6, 300 MHz): δ 8.48 (d, 2H, 5′), 7.29 (s, 1H, 3), 6.74 (t, 2H, 4′), 6.62 (d, 2H, 2′), 6.11 (t, 2H, 3′), 2.00 (br s, 6H, OAc and HOAc), 1.53 (s, 18H, *tBu*).

(^{tBu}NOCON)Ir(OAc)(Ph)(CO) (8b). In a 50 mL Schlenk flask, CO was bubbled through a benzene solution (2.4 mL) of **6b** (13 mg, 0.018 mmol). After stirring the mixture at room temperature for 5 minutes, the volatiles were removed *in vacuo* to afford a light brown solid. ^{1}H NMR (CD_2Cl_2, 500 MHz): δ 8.45 (d, 2H, 5′), 7.83 (m, 2H, 4′), 7.26 (d, 2H, 2′), 7.24 (s, 1H,3), 7.14 (t, 2H, 3′), 6.80 (t, 1H,4-Ph), 6.69 (t, 2H, 3-Ph), 6.45 (d, 2H, 2-Ph). ^{13}C NMR (CD_2Cl_2, 500 MHz): δ 177.73 (CO), 174.68 (OAc), 161.12, 152.68, 152.50, 151.28, 141.29, 136.07, 133.85, 128.69, 126.38, 123.50, 121.82, 120.85, 115.40, 105.76, 35.11 (C(CH_3)$_3$), 30.95 (C(CH_3)$_3$), 23.69 (OAc). IR (KBr): 2057 cm^{-1} (CO), 1615 cm^{-1} (OAc).

Details of Solid State Structure Determination of 5b.

A colorless prism, measuring 0.35 x 0.20 x 0.15 mm^3 was mounted on a glass capillary with oil. Data was collected at -173 °C on a Bruker APEX II single crystal X-ray diffractometer, Mo-radiation. Crystal-to-detector distance was 40 mm and exposure time was 2 seconds per frame for all sets. The scan width was 0.5^o. Data collection was 99.8% complete to 25^o in ϑ. A total of 717352 (merged) reflections were collected covering the indices, h = -13 to 13, k = -13 to 13, l = -21 to 20. 7648 reflections were symmetry independent and the R_{int} = 0.0243 indicated that the data was excellent (average quality 0.07). Indexing and unit cell refinement indicated a

triclinic lattice. The space group was found to be P $\bar{1}$ (No.2). The data was integrated and scaled using SAINT, SADABS within the APEX2 software package by Bruker.[18]

Solution by direct methods (SHELXS, SIR97[19]) produced a complete heavy atom phasing model consistent with the proposed structure. The structure was completed by difference Fourier synthesis with SHELXL97.[20,21] Scattering factors are from Waasmair and Kirfel.[22] Hydrogen atoms were placed in geometrically idealized positions and constrained to ride on their parent atoms with C---H distances in the range 0.95-1.00 Angstrom. Isotropic thermal parameters U_{eq} were fixed such that they were $1.2U_{eq}$ of their parent atom Ueq for CH's and $1.5U_{eq}$ of their parent atom U_{eq} in case of methyl groups. All non-hydrogen atoms were refined anisotropically by full-matrix least-squares.

Table 6.1. Crystal data and structure refinement for **5b**.

Empirical formula	$C_{29}\ H_{37}\ Cl_2\ Ir\ N_2\ O_7$	
Formula weight	788.71	
Temperature	100(2) K	
Wavelength	0.71073 Å	
Crystal system	Triclinic	
Space group	P -1	
Unit cell dimensions	a = 9.9847(4) Å	α = 96.259(2)°.
	b = 10.4173(5) Å	β = 102.234(2)°.
	c = 15.7444(8) Å	γ = 101.114(2)°.
Volume	1551.13(12) $Å^3$	
Z	2	
Density (calculated)	1.689 Mg/m^3	
Absorption coefficient	4.523 mm^{-1}	
F(000)	784	
Crystal size	0.35 x 0.20 x 0.15 mm^3	
Theta range for data collection	2.02 to 28.39°.	
Index ranges	-13<=h<=13, -13<=k<=13, -21<=l<=20	
Reflections collected	17352	
Independent reflections	7648 [R(int) = 0.0243]	
Completeness to theta = 25.00°	99.8 %	
Max. and min. transmission	0.5502 and 0.3005	
Refinement method	Full-matrix least-squares on F^2	
Data / restraints / parameters	7648 / 0 / 378	
Goodness-of-fit on F^2	1.045	
Final R indices [I>2sigma(I)]	R1 = 0.0219, wR2 = 0.0517	
R indices (all data)	R1 = 0.0249, wR2 = 0.0530	
Largest diff. peak and hole	1.069 and -1.056 $e.Å^{-3}$	

Details of Solid State Structure Determination of 6b.

A colorless prism, showing signs of decomposition, measuring 0.10 x 0.07 x 0.05 mm^3 was mounted on a glass capillary with oil. Data was collected at -173 °C on a Bruker APEX II single crystal X-ray diffractometer, Mo-radiation. Crystal-to-detector distance was 40 mm and exposure time was 20 seconds per frame for all sets. The scan width was 0.5°. Data collection was 99.2% complete to 25° in ϑ. A total of 173387 (merged) reflections were collected covering the indices, h = -21 to 21, k = -22 to 21, l = -22 to 22. 19543 reflections were symmetry independent and the R_{int} = 0.1685 indicated that the data was of less than average quality (0.07).

Indexing and unit cell refinement indicated a primitive monoclinic lattice. The space group was found to be P $\bar{1}$ (No.2). The data was integrated and scaled using SAINT, SADABS within the APEX2 software package by Bruker.[18]

Solution by direct methods (SHELXS, SIR97[19]) produced a complete heavy atom phasing model consistent with the proposed structure. The structure was completed by difference Fourier synthesis with SHELXL97.[20,21] Scattering factors are from Waasmair and Kirfel.[22] Hydrogen atoms were placed in geometrically idealized positions and constrained to ride on their parent atoms with C---H distances in the range 0.95-1.00 Angstrom. Isotropic thermal parameters U_{eq} were fixed such that they were $1.2U_{eq}$ of their parent atom Ueq for CH's and $1.5U_{eq}$ of their parent atom U_{eq} in case of methyl groups. All non-hydrogen atoms were refined anisotropically by full-matrix least-squares.

Table 6.2. Crystal data and structure refinement for **6b**.

Empirical formula	C_{32} H_{37} Ir N_2 O_5	
Formula weight	721.84	
Temperature	100(2) K	
Wavelength	0.71073 Å	
Crystal system	Triclinic	
Space group	P -1	
Unit cell dimensions	a = 17.188(3) Å	α = 116.971(5)°.
	b = 17.6375(17) Å	β = 99.636(7)°.
	c = 18.3700(18) Å	γ = 91.749(7)°.
Volume	4857.1(11) $Å^3$	
Z	6	
Density (calculated)	1.481 Mg/m^3	
Absorption coefficient	4.162 mm^{-1}	
F(000)	2160	
Crystal size	0.10 x 0.07 x 0.05 mm^3	
Theta range for data collection	1.73 to 26.45°.	
Index ranges	-21<=h<=21, -22<=k<=21, -22<=l<=22	
Reflections collected	173387	
Independent reflections	19543 [R(int) = 0.1685]	
Completeness to theta = 25.00°	99.2 %	
Max. and min. transmission	0.8189 and 0.6810	
Refinement method	Full-matrix least-squares on F^2	
Data / restraints / parameters	19543 / 66 / 1054	
Goodness-of-fit on F^2	0.908	
Final R indices [I>2sigma(I)]	R1 = 0.0775, wR2 = 0.1569	
R indices (all data)	R1 = 0.1809, wR2 = 0.1848	
Largest diff. peak and hole	2.498 and -1.827 $e.Å^{-3}$	

Notes to Chapter 6

---

1. (a) Gesser, H. D.; Hunter, N. R.; Prakash, C. B. *Chem*. *Rev*. **1985**, *85*, 235. (b) *Handbook of Alternative Fuel Technologies*; Lee, S.; Speight, J. G.; Loyalka, S.; CRC Press: Boca Raton, FL, 2007.

2. (a) Davies, D. L.; Donald, S. M. A.; Macgregor, S. A. *J*. *Am*. *Chem*. *Soc*. **2005**, *127*, 13754. (b) Gorelsky, S. I.; Lapointe, D.; Fagnou, K. *J*. *Am*. *Chem*. *Soc*. **2008**, *130*, 10648. (c) Gunay, M. E.; Ilyashenko, G.; Richards, C. J. *Tetrahedron: Asymmetry* **2010**, *21*, 2782. (d) Lapointe, D.; Fagnou, K. *Chem*. *Lett*. **2010**, *39*, 1118, and references within. (e) Li, H.; Li, B.; Shi, Z. *Catal*. *Sci*. *Technol*. **2011**, *1*, 191, and references within.

3. (a) Davies, D. L.; Al-Duaij, O.; Fawcett, J.; Giardiello, M.; Hilton, S. T.; Russell, D. R. *Dalton Trans*. **2003**, 4132. (b) Boutadla, Y.; Al-Duaij, O.; Davies, D. L. Griffith, G. A.; Singh, K. *Organometallics* **2009**, *28*, 433. (c) Li, L.; Brennessel, W. W.; Jones, W. D. *Organometallics* **2009**, *28*, 3492.

4. Young, K. J. H.; Oxgaard, J.; Ess, D. H.; Meier, S. K.; Stewart, T.; Goddard, W. A., III; Periana, R. A. *Chem*. *Commun*. **2009**, 3270.

5. Allen, K. E.; Heinekey, D. M.; Goldman, A. S.; Goldberg, K. I. *Organometallics* **2013**, *32*, 1579.

6. (a) Liu, F.; Pak, E. B.; Singh, B.; Jensen, C. M.; Goldman, A. S. *J*. *Am*. *Chem*. *Soc*. **1999**, *121*, 4086. (b) Adams, J. J.; Arulsamy, N.; Roddick, D. M. *Organometallics* **2012**, *31*, 1439.

7. Raja, M. U.; Ramesh, R.; Ahn, K. H. *Tetrahedron Lett*. **2009**, 7014.

8. (a) Danopoulos, A. A.; Pugh, D.; Wright, J. A. *Angew*. *Chem*. *Int*. *Ed*. **2008**, *47*, 9765. (b) Cardenas, D.; Echavarren, A. M. *Organometallics* **2009**, *18*, 3337.

9. Synthesis of ^{tBu}NOCON was modified from that from the reported procedure for NOCON synthesis: Hartshorn, C. M.; Steel, P. J. *J. Chem. Soc., Dalton Trans*. **1998**, 3927.

10. Ito, J.; Kaneda, T.; Nishiyama, H. *Organometallics* **2012**, *31*, 4442.

11. Ito, J.; Nishiyama, H. *Eur. J. Inorg. Chem*. **2007**, 1114.

12. EA analyses support high purity of **5b**.

13. (a) Wojcicki, A. *Adv. Organomet. Chem*. **1973**, *11*, 87. (b) Calderazzo, F. *Angew. Chem. Int. Ed. Engl*. **1977**, *16*, 299. (c) Kuhlman, E. J. Alexander, J. J. *Coord. Chem. Rev*. **1980**, *33*, 195.

14. (a) Anderson, G. K.; Lumetta, G. *Organometallics* **1985**, *4*, 1542. (b) Fryzuk, M. D.; MacNeil, P. A.; Rettig, S. J. *J. Organomet. Chem*. **1987**, *332*, 345. (c) Carmona, E.; Paneque,, M.; Poveda, M. L. *Polyhedron* **1989**, *8*, 285. (d) Dupont, J.; Pfeffer, M. J. *Chem. Soc. Dalton Trans*. **1990**, 3193. (e) Hartwig, J. F.; Bergman, R. G.; Andersen, R. A. *J. Am. Chem. Soc*. **1991**, *113*, 6499.

15. Cleary, B. P.; Eisenberg, R. *J. Am. Chem. Soc*. **1995**, *117*, 3510.

16. Li, L.; Jiao, Y.; Brennessel, W. W.; Jones, W. D. *Organometallics* **2010**, *29*, 4593.

17. Davies, D. L.; Al-Duaij, O.; Fawcett, J.; Singh, K. *Organometallics* **2010**, *29*, 1413.

18. Bruker (**2007**) APEX2 (Version 2.1-4), SAINT (version 7.34A), SADABS (version 2007/4), BrukerAXS Inc, Madison, Wisconsin, USA.

19. (a) Altomare, A.; Burla, C.; Camalli, M.; Cascarano, L.; Giacovazzo, C.; Guagliardi, A.; Moliterni, A. G. G.; Polidori, G.; Spagna, R. *J. Appl. Cryst*. **1999**, *32***,** 115. (b) Altomare, A.; Cascarano, G.; Giacovazzo, C.; Guagliardi, A. *J. Appl. Cryst*. **1993**, *26*, 343.

20. Sheldrick GM. **(1997)** SHELXL-97, Program for the Refinement of Crystal Structures. University of Göttingen, Germany.

21. Mackay, S.; Edwards, C.; Henderson, A.; Gilmore, C.; Stewart, N.; Shankland, K.; Donald, A. *MaXus: a computer program for the solution and refinement of crystal structures from diffraction data*. University of Glasgow, Scotland, **1997**.

22. Waasmaier, D.; Kirfel, A. *Acta Crystallogr*. A. **1995**, *51*, 416.